

3. Results and Discussion

Results of preparation of *Sāncipāt*, characterization of freshly prepared and old *Sāncipāt*, conservation of *Sāncipāt* manuscript, investigation on the science in *Hengul-Hāitāl* painting tradition, and restoration of heritage woodcarvings with the application of the traditional paints for preserving them in rural set-up in as is where is condition have been described in this chapter together with discussions of the results. The first section of the chapter involves the traditional preparation of *Sāncipāt* and its physicochemical, mechanical, and biochemical properties. Additionally, the structural and morphological features of cellulose and lignin-derived from new and old *Sānci* bark are analyzed, including the impact of zirconium oxychloride-modified cellulose and lignin on these features. By using cellulose and lignin from new *Sānci* bark as a reference and comparing those to the modified ones, it is possible to study the impact of natural degradation on both the structure and conformation of cellulose and lignin. The second section describes the results and discussion of the mechanical and physicochemical experiments on *Sāncipāt* changed after exposure to water and some common conservative chemicals. Based on this, a simplified method of preparation for *Sāncipāt* and a traditional method-based conservation technique for old, dilapidated *Sāncipāt* manuscripts have been proposed. In the third section, the results of the investigation on traditional science behind the *Hengul-Hāitāl* painting tradition have been examined, including the paints' ingredients, formulation, application, and effects. The fourth section presents our highly effective restoration technique that has been specifically designed and tested for the restoration of ancient heritage woodcarvings dating back to medieval Assam. Our technique is based on rigorous scientific research and has produced remarkable results. Some historic woodcarvings that had been painted with synthetic paint and either partially damaged or had lost their historic appearance were chosen for restoration and repainting using *traditional Hengul-Hāitāl painting*.

3.1. Section-1: Structure and properties of *Sāncipāt**

3.1.1. Preparation of *Sāncipāt*

Sāncipāt folios were prepared following the traditional procedure under supervision of the practicing expert of the tradition as mentioned in the section 1.2.4.1. The raw *Sānci* bark peeled from a 25-year-old *Sānci* tree was approximately 6 mm thick which reduced

to 2.3 mm in the final *Sāncipāt*. The freshly prepared *Sāncipāt* was found to be physically strong, smooth, and glazing.

3.1.2. Physicochemical measurements at various stages of preparation of *Sāncipāt*

In each step of preparation of *Sāncipāt* from a raw *Sānci* bark, changes in physical and chemical properties have been analyzed through various techniques.

3.1.2.1. Weight loss during degumming

The weight loss on degumming for different duration of time in presence of 0.1M CuSO_4 is observed. A partial degumming of *Sānci* bark is done without using any base unlike degumming of paper and silk industry. Like in traditional degumming of *Sānci* bark, a cleaned *Sānci* bark strip is dipped in 500 ml tap water containing 0.1M *Tutia* (CuSO_4), 10 seeds of *Konibih* and 30 g of leaves of *Chalkuwari* boiling in a plastic dish and boiled for 20 minutes. The degummed strips were then sundried. For examining weight loss on degumming, a cleaned *Sānci* bark was cut into five rectangular pieces weighing approximately 0.5 g. Then the pieces were dried in hot air oven at 70°C for 2 hours. The pieces were then kept in vacuum desiccator for 7 days and weighted. The weight difference was calculated subtracting final weight of degummed pieces from initial weight of the raw *Sānci* pieces (Figure. 3.1.1 & Table 3.1.1). It is interesting to note a linear relation of percent weight loss, calculated as (final weight of strip/initial weight of strip) \times 100%, with time. The weight loss may be attributed to gradual loss of hemicellulose and lignin of *Sānci* strip during the process.

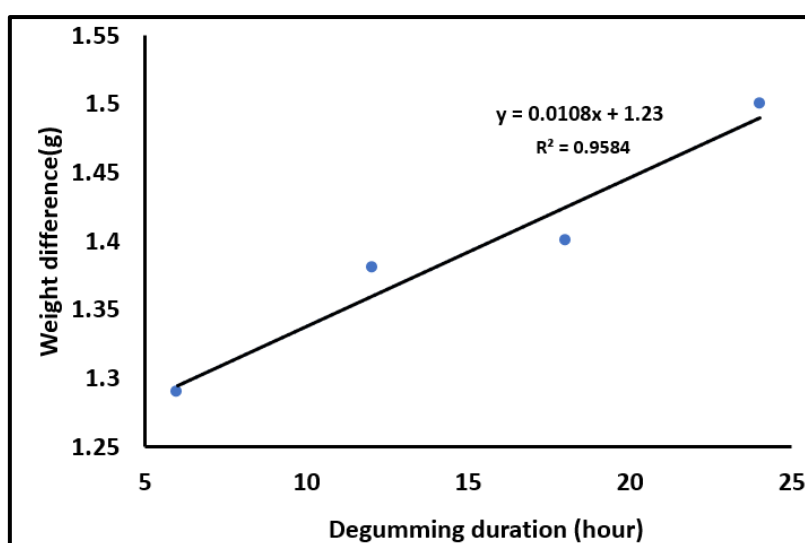


Figure. 3.1.1: Weight loss vs. time of during degumming of cleaned raw *Sānci* strip.

Table 3.1.1: Weight loss degumming of the *Sānci* bark at different time durations of triplicate measurements.

Duration of degumming (hour)	Before degumming		After degumming		Difference weight(g)	Weight loss (%)
	Weight (g)	Average (g)	Weight (g)	Average (g)		
6	3.46	3.89	2.24	2.60	1.29	66.83
	3.95		2.36			
	4.25		3.19			
12	3.76	3.66	2.32	2.28	1.38	62.29
	3.76		2.32			
	3.45		2.20			
18	3.56	3.80	2.15	2.40	1.40	63.15
	3.68		2.18			
	4.15		2.88			
24	4.15	4.07	2.65	2.57	1.50	63.14
	3.97		2.42			
	4.10		2.65			

3.1.2.2. FTIR analysis of *Sāncipat*

FTIR spectra of cleaned raw *Sānci* bark is shown in (Figure. 3.1.2). An intense broad peak at 3381 cm^{-1} can be attributed to the stretching peak of H-bonded -OH group and a smaller peak at 2916 cm^{-1} can be assigned to C-H stretch of lignin [184]. While a small peak at 1743 cm^{-1} can also be attributed to unconjugated ketones of lignin, a major peak at 1626 cm^{-1} can be attributed to absorbed water associated with lignin or cellulose [185]. Medium intensity peaks at 1427 cm^{-1} and 1375 cm^{-1} may be due to C-H asymmetric deformation in $-\text{OCH}_3$, and C-H bending in cellulose and hemicellulose, respectively [185,186]. A small peak at 1159 cm^{-1} can be attributed to C-O-C asymmetric stretching

in cellulose [185]. Other characteristic bands of lignin and cellulose are seen at 1104, and 1064 cm^{-1} , which can be attributed to aromatic C–H in-plane deformation (or C=O stretch) and C–O deformation in secondary alcohols and aliphatic ethers, respectively [185]. The small sharp band at 897 cm^{-1} is probably originated from the β -glucosidic linkages of sugar units in cellulose [187]. A strong peak at 613 cm^{-1} denotes C–OH out-of-plane bending vibration [188]. The FT-IR spectra of the old manuscript folio was also found to be similar to that of the fresh one.

To check the compositional variation of raw *Sānci* after various treatments, FT-IR analysis has been performed for samples of degummed *Sānci* bark and *Sāncipāt* manuscripts of same source (Figure. 3.1.2). It is interesting to note that there was hardly any visible change in the spectra due to treatments except disappearance of a small peak at 1743 cm^{-1} of raw *Sānci* bark on traditional degumming which may be due to dissolution of unconjugated ketones of lignin by the salt. This indicates the traditional degumming method to be less drastic than the common alkaline degumming.

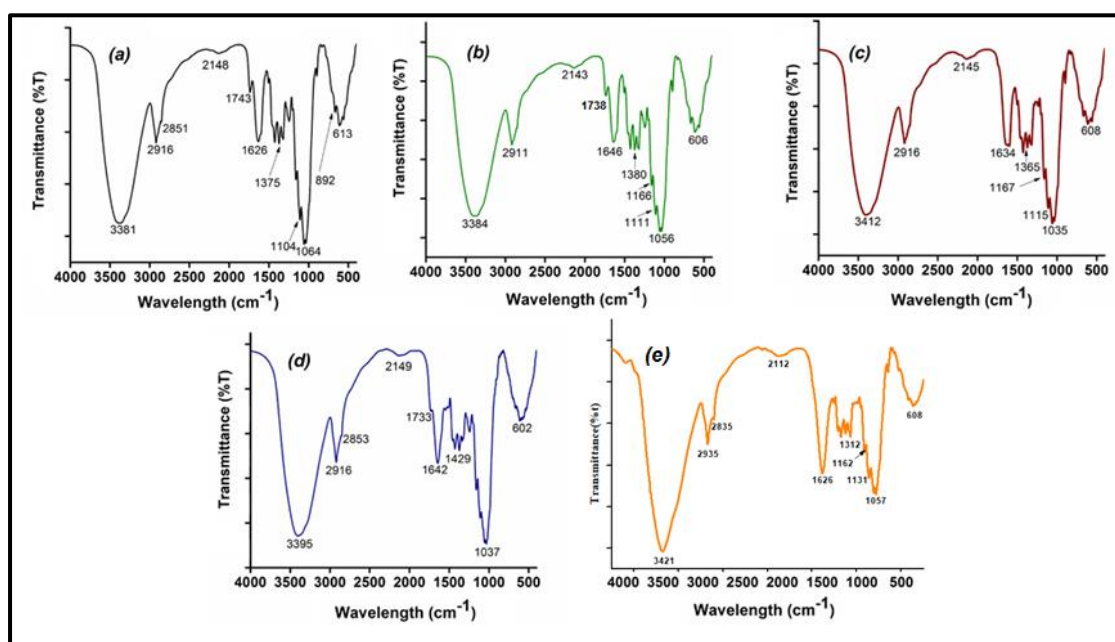


Figure. 3.1.2: FT-IR spectra of (a) raw *Sānci* bark, (b) water-degummed *Sānci* bark, (c) traditionally degummed *Sānci* bark, (d) freshly prepared *Sāncipāt* and (e) old *Sāncipāt*.

FT-IR spectra of raw *Sānci* bark and *Sānci* barks at three stages of preparation indicated presence of lignin, cellulose, and hemicellulose. In traditional method of preparation of *Sāncipāt*, a partial degumming is done retaining the fibrous cellulosic part

in order to retain the basic structure and shape of the bark. As expected, the FT-IR spectra of the old manuscript folio was also found to be like that of the freshly prepared one.

3.1.2.3. Evidence from CHN analysis

The cleaned raw *Sānci* bark to consists of 33.30% carbon and 5.33% hydrogen, respectively, and no nitrogen. Both carbon and hydrogen content decreased after traditional degumming to 31.93% and 5.30%, respectively. Absence of nitrogen is a characteristic of cellulose. The CHN results also indicate that the lignin in *Sānci* bark does not contain nitrogen [189]. A small decrease in carbon and hydrogen is an indicative of loss of lignin during degumming.

3.1.2.4. Evidence from p-XRD analysis

The XRD of freshly prepared *Sāncipāt* and old *Sāncipāt* are shown in Figure. 3.1.3. The XRD pattern indicates both samples to be largely amorphous. However, some peaks appear at 2θ between 10° and 45° for both. Comparing with X-ray diffractograms database (PCPDF-WIN), we suggest *Sāncipāt* to be a native cellulose, $(C_6H_{12}O_6)_x$, system-monoclinic, (PDF no. 030289; ID:03-0289); since characteristic peaks were observed at 14.1° (-1 0 1) and 22.8° (0 0 2) and 41.6° (2 4 0) [190]. Both possess similar XRD pattern with an exception in the range between 21.90° to 22.80° . A broad peak observed in the case of freshly prepared *Sāncipāt* whereas flattened in old *Sāncipāt*. This may be attributed to a slight change in cellulose structure because of difference in degumming during the process of preparation of freshly prepared *Sāncipāt*.

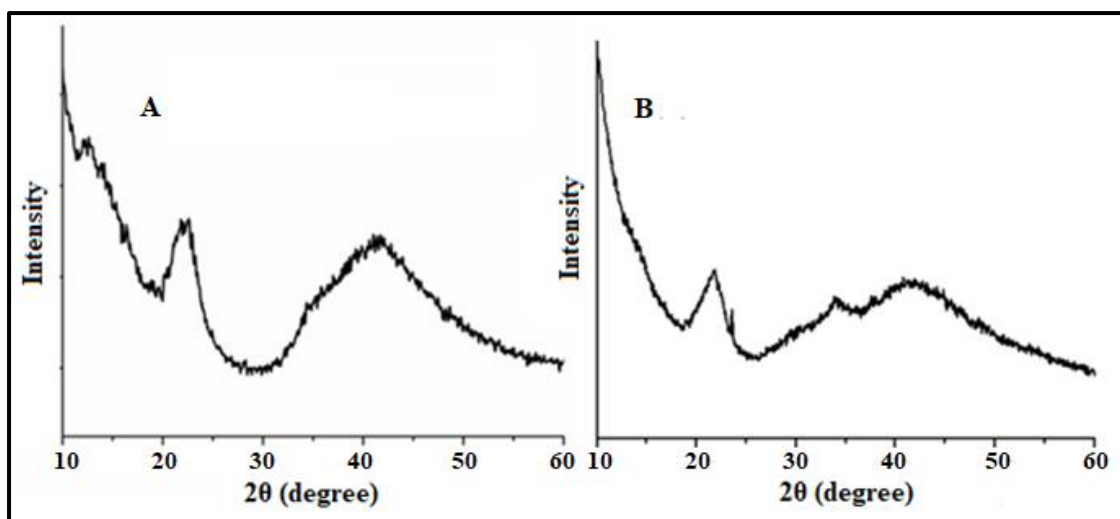


Figure. 3.1.3: XRD patterns of (a) freshly prepared *Sāncipāt* and (b) old *Sāncipāt*.

3.1.2.5. Evidence from Gloss index analysis

The averages of glossiness of inner and outer sides of the folio at three stages of preparation are shown in (Figure. 3.1.4) along with averages of glossiness of three folios of an old manuscript as it was not possible to distinguish the inner and outer sides of the old manuscript. The glossiness of the inner and outer sides of the three stages may be seen in (Figure. 3.1.4). It has been observed that the glossiness of the folio is increased with the angle of measurement as expected. It was interesting to note an increase in the glossiness gradually in each stage of the preparation. The improvement in gloss index from stage 1 to 3 may be attributed to increase in reflection due to filling of the pores and cracks on the surface by the coating of fatty pulse and the coating of *Hāitāl*. However, the glossiness of the damaged old manuscript was somewhat lower than the fresh one which might have decreased over time. The gloss index of both inner and outer sides of freshly prepared *Sāncipāt* were also measured to examine if there was any difference between the two sides (Figure. 3.1.4).

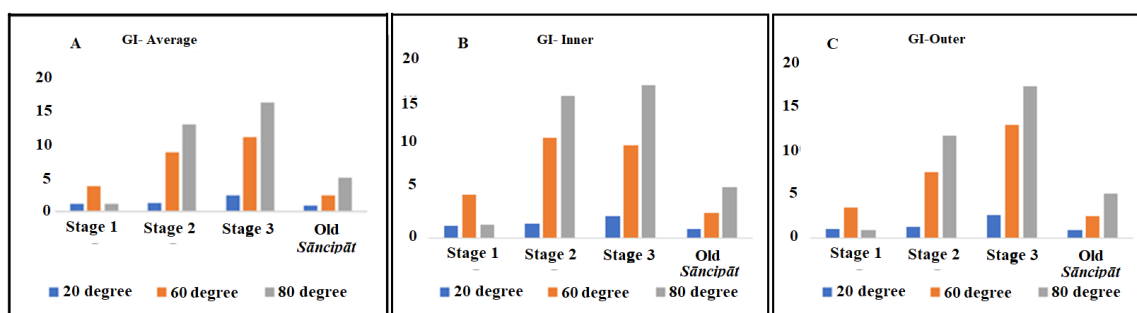


Figure. 3.1.4: Average gloss index (GI) of (A) inner and outer sides of *Sānci* bark at three different stages of preparation: Stage 1 (cleaned raw *Sānci* bark), Stage 2 (fatty pulse treated *Sānci* bark), Stage 3 (freshly prepared *Sāncipāt*) and Old *Sāncipāt* measured at various angles, Gloss index of (B) inner (GI-inner) and (C) outer (GI-outer) sides of *Sānci* bark at three different stages of preparation: Stage 1 (cleaned raw *Sānci* bark), Stage 2 (fatty pulse treated *Sānci* bark), Stage 3 (freshly prepared *Sāncipāt*) and old *Sāncipāt* measured at various angles.

3.1.2.6. Evidence from Mechanical properties

The tensile strength (longitudinal) values of cleaned raw *Sānci* bark, traditionally degummed *Sānci* bark and freshly prepared *Sāncipāt* after drying are shown in Figure. 3.1.5. Elongation at break was same for all three samples and was approximately 7.8%. The ultimate tensile strength of the cleaned raw *Sānci* bark considerably increased from 20 MPa to 48 MPa and 78 MPa in the degummed and freshly prepared *Sāncipāt*, respectively. The Young's modulus (Y/X) calculated from three points on the three curves at (X=3.32, Y=9.97), (X=3.32, Y=28.63) and (X=3.32, Y=48.01) were found to be 3.00, 8.62 and 14.46 for cleaned raw *Sānci* bark, degummed *Sānci* bark and freshly prepared *Sāncipāt*, respectively. Thus, the tensile elasticity of the *Sānci* strip is significantly increased during preparation of *Sāncipāt*. The degumming and application a coating of paste of fatty pulse with stone apple gum have probably contributed to the toughness of *Sāncipāt*.

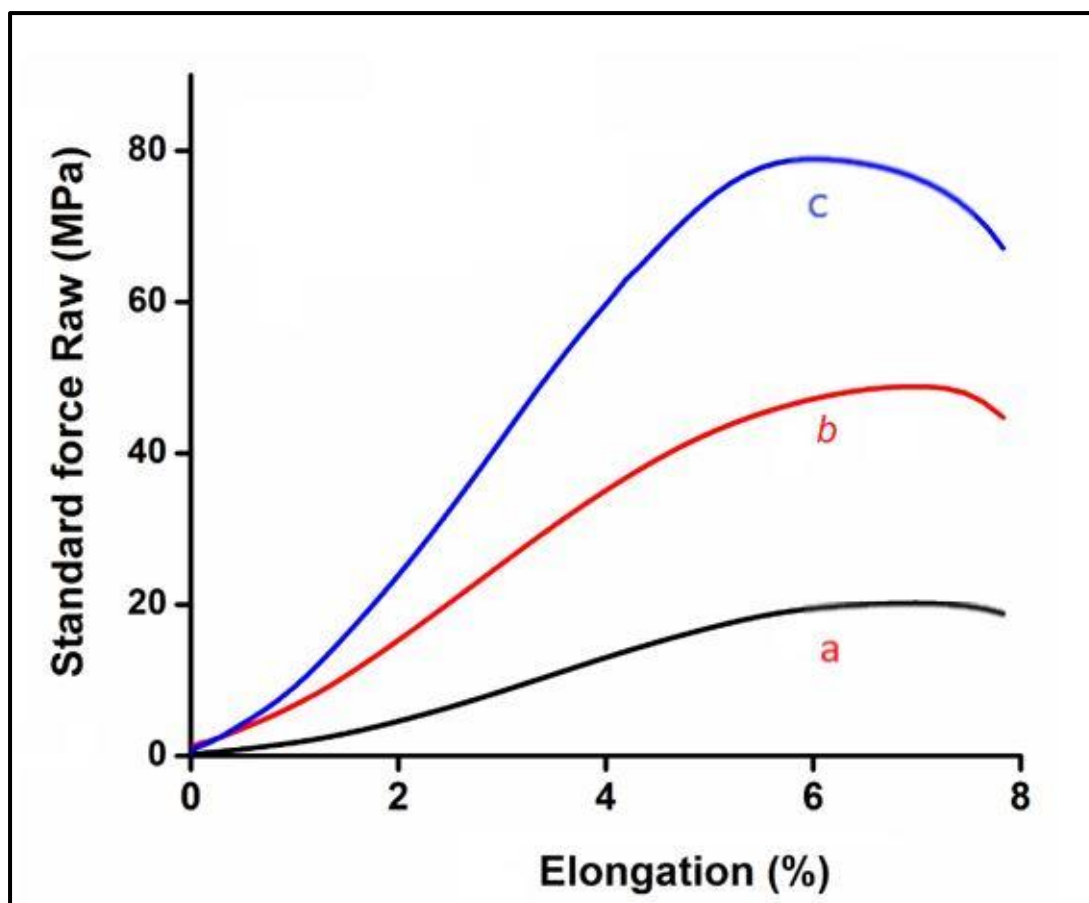


Figure. 3.1.5: Tensile strength of (black, a) cleaned raw *Sānci* bark, (red, b) traditionally degummed *Sānci* bark and (blue, c) freshly prepared *Sāncipāt*.

3.1.2.7. Evidence from image and elemental analysis

SEM shows a marked increase in the fibrous nature of the *Sāncipāt* after the treatment with water and other chemicals (Figure. 3.1.6). EDX analysis shows the presence of C, N and O, and trace amounts of S, K, Ca, Mn, Fe, Cu and As in *Sāncipāt* before treatment which were changed after treatments. Atomic percentages of C, N and O before treatment were 46.69%, 8.16% and 44.06%, respectively; which changed to 48.49%, 12.92% and 37.65% after treatment with water; 50.28%, 10.01% and 38.53% after treatment with cetrimide; 67.01%, 30.70% and 0.33% after treatment with isopropyl alcohol; and 58.47%, 0.80% and 40.50% after treatment with thymol, respectively. There were notable decreases in the atomic percentages of O and N after treatment with isopropyl alcohol and thymol again indicating chemical changes caused by them to *Sāncipāt*. On the other hand, Cu has either disappeared or markedly decreased after the treatments and as disappeared after treatment with thymol indicating removal of the protective metal ions by the chemicals.

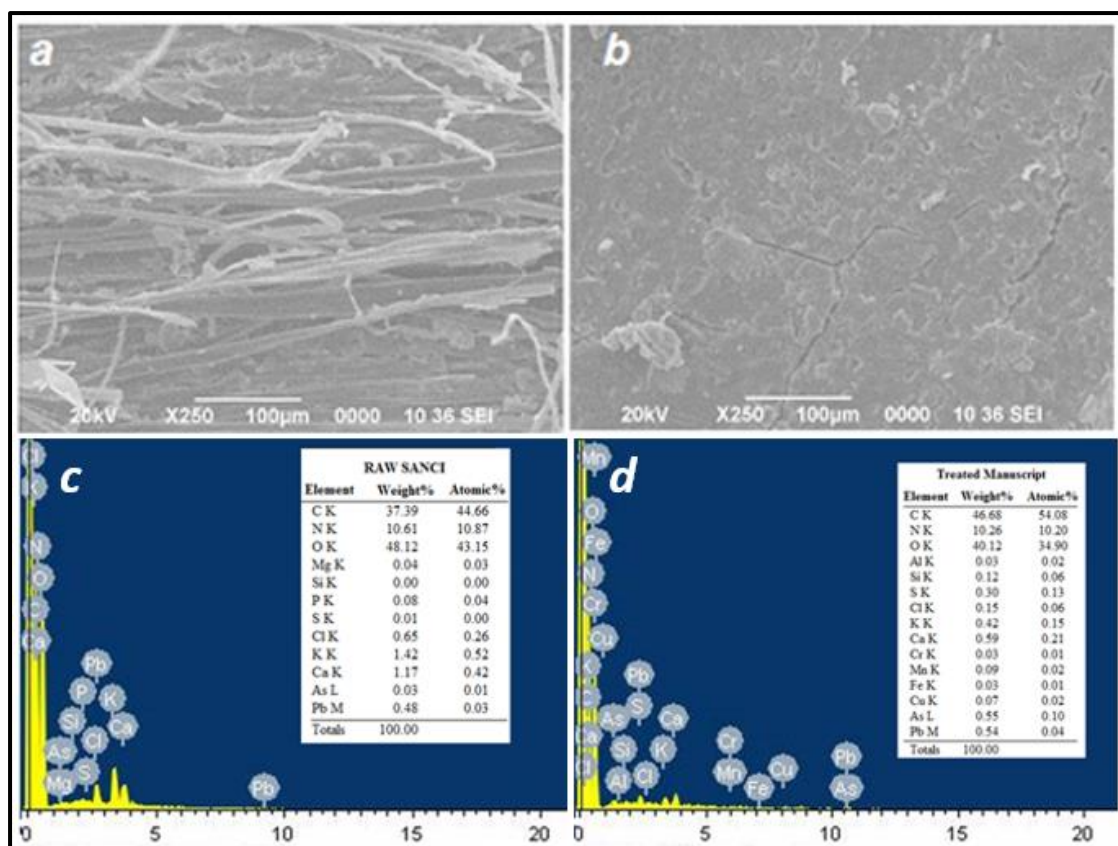


Figure. 3.1.6: SEM images of (a) raw *Sānci* strip and (b) freshly prepared *Sāncipāt* manuscript at resolution of 100 μm and EDXA analysis of (a) raw *Sānci* strip and (b) freshly prepared *Sāncipāt* manuscript at resolution of 100 μm.

3.1.2.8. Microbial Essay

Antifungal activity test [164] was performed on *Sānci* strip at four different stage of the preparation process, viz., cleaned raw *Sānci* bark, degummed *Sānci* bark, *Sānci* bark after application of *Hāitāl* and *Sānci* bark after application of both *Hāitāl* and *Hengul* (Figure. 3.1.7). The *Sānci* manuscript was cut into small pieces having the equal surface area for the experiment. For preparation of potato dextrose broth (PDB) solution, 5g of PDB was dissolved in 50 mL distilled water followed by autoclave at 121°C and 15 pounds for 15 min. Moreover, potato dextrose plates were prepared with PDB and 1.8 g of agar. For antifungal test, three filamentous fungi, viz., *Aspergillus niger*, *Candida albicans* and *Fusarium oxysporum*, were subcultured (Figure. 3.1.8). All the fungal strains were seeded to 50 mL of PDA containing conical flasks and incubated for 7 days at approximately 20°C. For the antifungal test, 100 μL of fungal inoculums were spread carefully in the PDA plates and placed all small pieces of the samples, viz., (1) cleaned raw *Sānci* bark,

(2) degummed *Sānci* bark, (3) *Hāitāl* coated *Sānci* bark and (4) both *Hengul* and *Hāitāl* coated *Sānci* bark,

respectively. All the samples along with controls were incubated in static incubator and their growth was monitored systematically. In this study, water was used as a negative control whereas antimycotic solution from Himedia at 10 μ g/mL were used as a positive control. All the experiments were performed in triplicates.

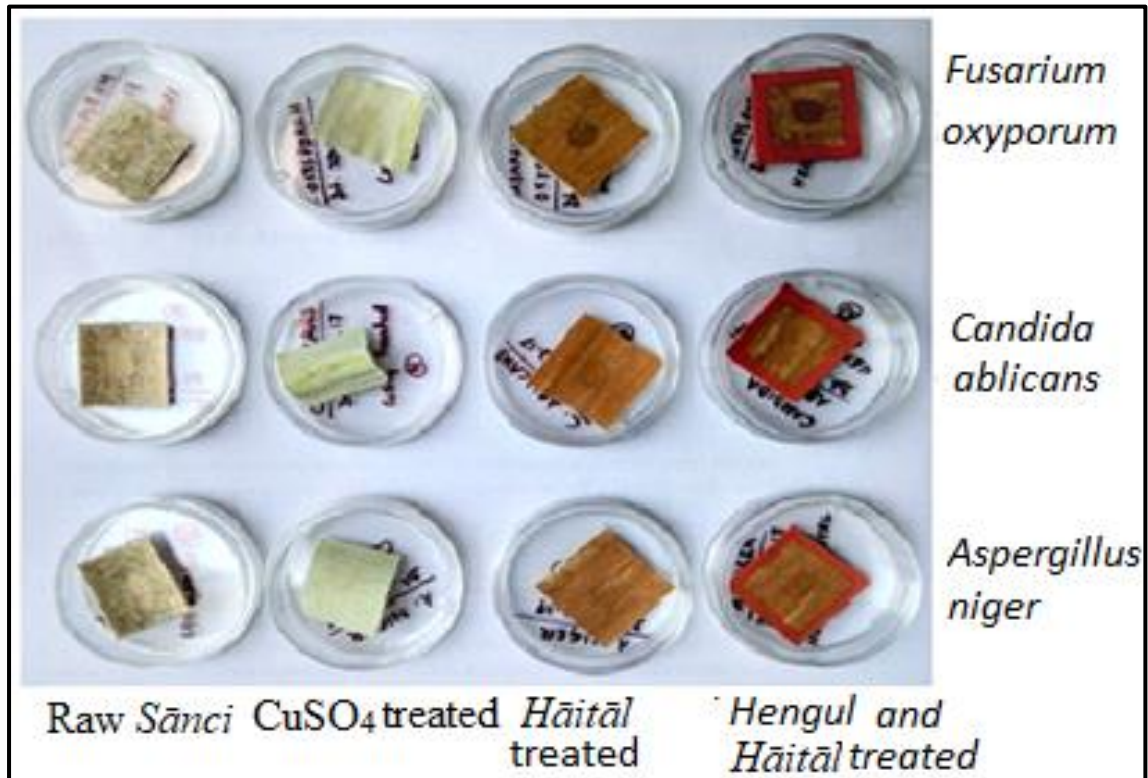


Figure. 3.1.7: Results of antifungal test on samples of cleaned raw *Sānci* bark, degummed *Sānci* bark, *Sānci* bark after application of *Hāitāl* and *Sānci* bark after application of both *Hāitāl* and *Hengul* before (top) and after (bottom) incubation.

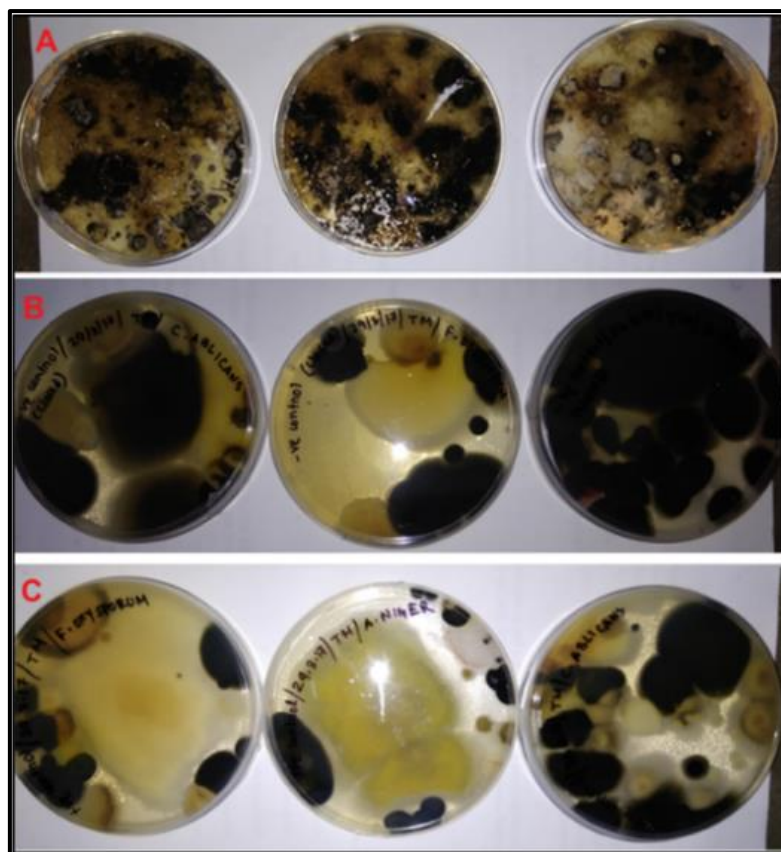


Figure. 3.1.8: Growth of Fungi in (A) open control, (B) negative closed control and (C) positive closed control against the fungi, *Aspergillus Niger*, *Candida albicans* and *Fusarium oxysporum*, respectively.

Table 3.1.2: Comparative observations of the antifungal activity test after 168 h (one week).

Fungus Treated	Control			Types of pretreatments on <i>Sānci</i> sample			
	(+ve Control)	(-ve Control)	Open	Raw <i>Sānci</i>	Degummed with 0.25% CuSO ₄	<i>Hāitāl</i> coated	<i>Hāitāl</i> & <i>Hengul</i> coated
<i>Candida Ablicans</i>	✓	✓	✓	✓	✗	✗	✗
<i>Aspergillus Niger</i>	✓	✓	✓	✓	✗	✗	✗
<i>Fusarium Oxyporum</i>	✓	✓	✓	✓	✗	✗	✗

The growth of the fungi takes place within 48-72h. The observations of antifungal activity in open control, closed negative control and closed positive control were made after 72h. After 2h, it was observed that all three fungi grew equally in the open control. *Aspergillus Niger*, being the most voracious fungus among the three, grew most rapidly in the negative control. On the other hand, *Candida albicans* grew most rapidly in the positive control. The fungal growths on the open positive and negative control have been observed to increase after one week also (Table 3.1.2). The results of antifungal test on samples of cleaned raw *Sānci* bark, degummed *Sānci* bark, *Sānci* bark after application of *Hāitāl* and *Sānci* bark after application of both *Hāitāl* and *Hengul* (Table 3.1.2). There was no fungus growth on any of the samples before incubation. Interestingly, we observed growth of all three fungi only in the petri plates for cleaned raw *Sānci* bark after one week of incubation. But no growth of any of the fungi was observed on the degummed *Sānci* bark, *Sānci* bark after application of *Hāitāl* and *Sānci* bark after application of both *Hāitāl* and *Hengul*. Fungus feed on cellulosic materials and so *Sāncipāt* is likely to be damaged by fungi in a hot and humid climate that exists during most of the year in Assam. On the other hand, the three minerals, viz., *Tutia*, *Hāitāl* and *Hengul*, are also reported to have antifungal properties [18]. The absence of any growth of all three fungi on the samples of degummed *Sānci* bark, *Sānci* bark after application of *Hāitāl* and *Sānci* bark after application of both *Hāitāl* and *Hengul* is expected to be attributed to antifungal properties of CuSO_4 used during degumming of *Sānci* bark and application of coating of *Hāitāl* and *Hengul*. The antifungal property of *Sāncipāt* may be additive, synergistic, or cumulative in nature. Interestingly, the authors have witnessed in various libraries, museums and personal possessions that *Sāncipāt* manuscripts with coating of *Hāitāl* and *Hengul* are never destroyed by insects while those without the coatings are mostly damaged by fungi and insects. It is interesting to note the traditional knowledge of antifungal properties of these minerals and their use for protection of *Sāncipāt* manuscripts from fungus in Assam during the medieval period. This indicates that application of a thin coat of *Hāitāl* on *Sāncipāt* manuscripts on the free spaces of cleaned the cleaned manuscript folios to be a good option for conservation of the manuscripts. A picture of an old *Sāncipāt* damaged by insect and fungus is shown in Figure. 3.1.9. It was found from SEM-EDX results that the As content in this *Sāncipāt* was very low indicative of absence of any protective coating of *Hāitāl* on the folio.

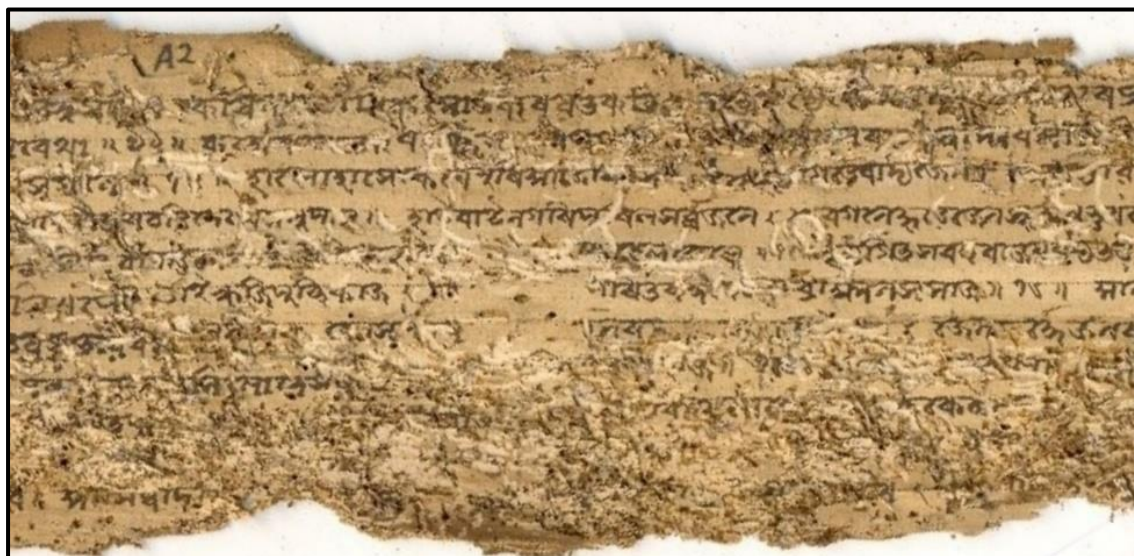


Figure. 3.1.9: Old *Sāncipāt* without *Hengul-Hāitāl* coating and damaged by insect and fungus.

3.1.3. Investigation of different structural and mechanical properties of cellulose and lignin extracted from *Sānci* bark

3.1.3.1. Study on moisture content

As we know, when an object attracts moisture, they undergo chemical, mechanical and biological decomposition reactions, especially the substances containing organic molecules. So, determining the moisture content and maintaining an optimum level is essential with the aim of preserving them. Therefore, it was quantitatively determined in both new and old cellulose (NC, OC) and lignin (NL, OL) by keeping 1g of each in an oven at 105°C for 2 hours until a constant weight was achieved. Moisture (%) = $\frac{W_1 - W_2}{W_1} \times 100$, where W_1 is the weight of the unheated sample and W_2 is the weight of the oven-dried sample, was used to calculate the percentage of moisture. As seen in the Figure. 3.1.10, OC revealed a higher moisture content percentage as compared to NC which might be due to the fact cellulose, being a highly polar molecule due to the –OH groups present in glucose and hydrophilic, tend to interact strongly with water [191]. This leads to a decrease in the mechanical properties, as several hydrogen bonds are lost and disrupted which crosslink the hydroxyl groups on the cellulose chains, making it more easily deformed [192]. Similarly, OL was seen to absorb more moisture compared to NL.

The strong hydrogen bonds present in lignin may be disrupted on interaction with water, resulting in reduced mechanical properties [193].

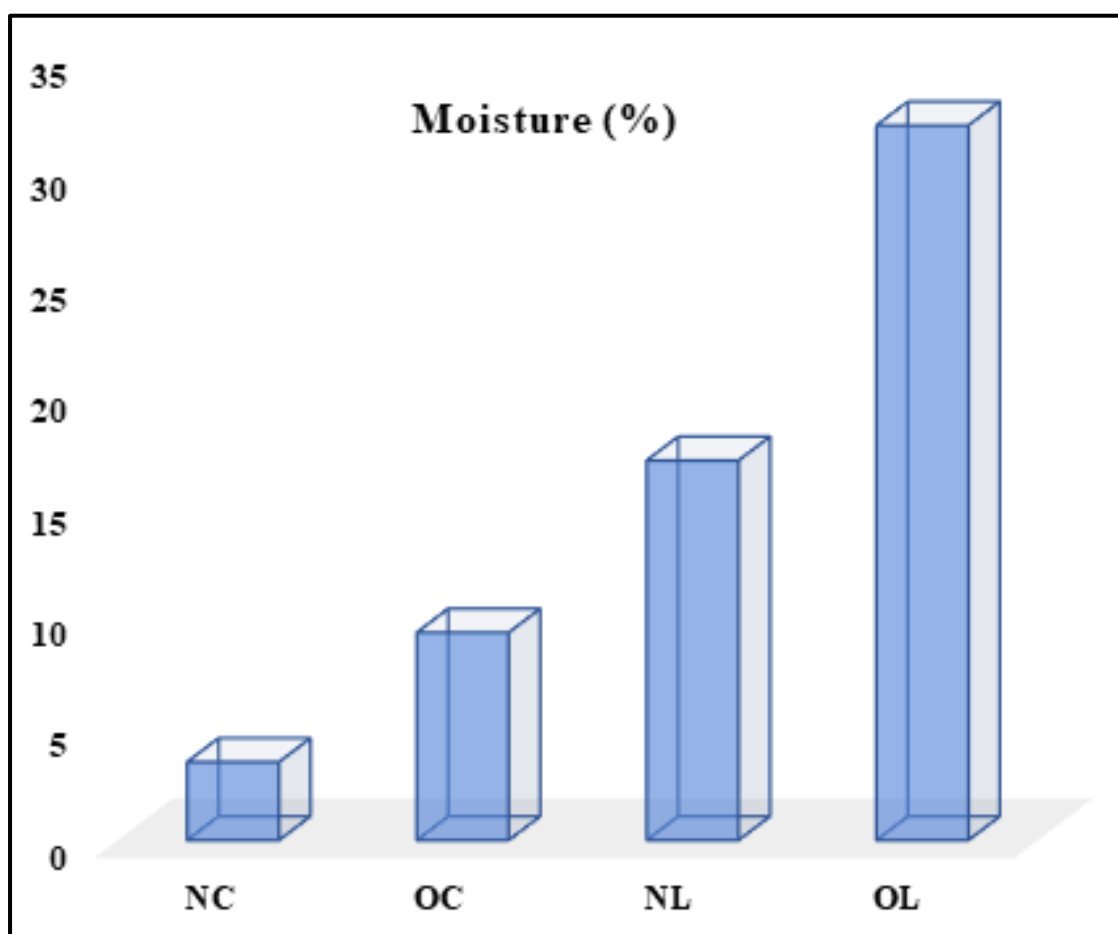


Figure. 3.1.10: Moisture determination of old and new cellulose and lignin.

3.1.3.2. Evidence from UV-visible spectra

The UV-visible spectrum of the cellulose and lignin samples was measured in the wavelength range 200–800 nm as shown in Figure. 3.1.11. The resonance forms of the groups in the cellulose molecule appear to absorb ultraviolet light in the energy range that is primarily between 200 and 300 nm [194]. Hypochromic effect is seen for OC as there is decreased absorption intensity which might be due to distortion of the geometry of the molecules with ageing that results in decreased coplanarity leading to loss of conjugation [195]. While for MC, the induced $ZrO_2 \cdot nH_2O$ might cause distortion of geometry of molecules (amorphous nature of $ZrO_2 \cdot nH_2O$), resulting in poor conjugation or it might limit the resonance which results in decreased absorbance [196].

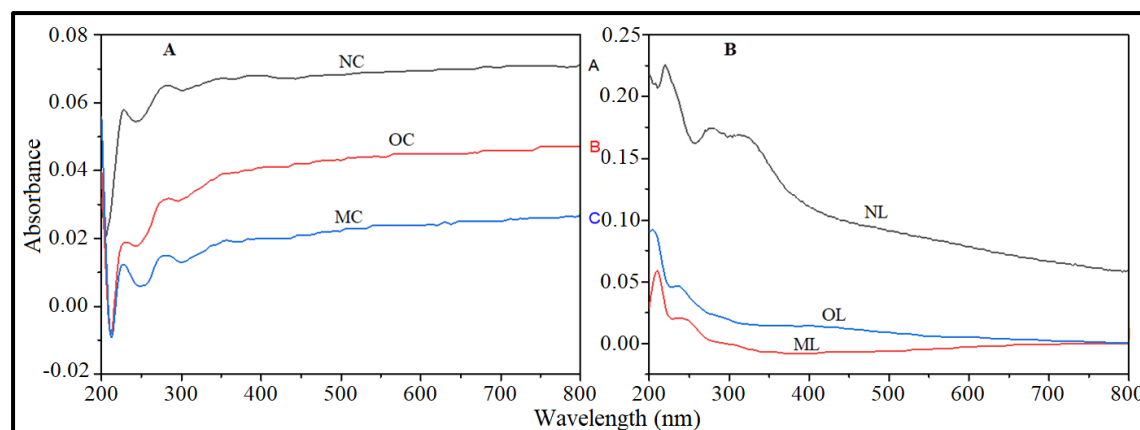


Figure. 3.1.11: UV-visible spectra of A: new cellulose (NC), old cellulose (OC), modified cellulose (MC) and B: new lignin (NL), old lignin (OL), modified lignin (ML).

UV spectroscopy refers to absorption spectroscopy in the UV wavelength region (200–400 nm) which has been used to record the spectrum of lignin as shown in Figure. 3.1.11 [197]. Due to the aromatic nature of lignin, there is a strong absorption in the UV region. The aromatic ring's transition to the $\pi \rightarrow \pi^*$ state causes high absorption in the 200–220 nm region [198]. Absorption peaks of NL near 280–310 nm is due to the phenolic structure (benzene ring) substituted by hydroxyl or methoxyl groups [198]. The absorption band above 300 nm signifies the presence of conjugated structures present with aromatic moieties, while the absorption band in the visible region of wavelength range 400 nm to 600 nm is responsible for the dark brown colour of the extracted lignin [199]. As for cellulose, similar hypochromic effect is also seen for OL as there is decreased absorption intensity which might be due to distortion of the geometry of the molecules with ageing that results in decreased coplanarity leading to loss of conjugation [195]. While for ML, the induced $\text{ZrO}_2 \cdot n\text{H}_2\text{O}$ might cause distortion of geometry of molecules (amorphous nature of $\text{ZrO}_2 \cdot n\text{H}_2\text{O}$), resulting in poor conjugation or it might limit the resonance which results in decreased absorbance [196].

3.1.3.3. Evidence from FTIR spectra

From the FTIR spectra shown in the Figure. 3.1.12A, the broad peak absorption band at 3430 cm^{-1} for NC and 3418 cm^{-1} for OC is assigned to strong hydrogen bonded hydroxyl groups ($-\text{O}-\text{H}$) stretching generally observed in polysaccharides [200]. This peak includes also inter and intra-molecular hydrogen bond in NC and OC. The stretching and deformation vibrations of the C-H group, typically seen in the glucose unit, are attributed

to the bands at 2923 cm^{-1} and 1317 cm^{-1} for NC and 2819 cm^{-1} and 1373 cm^{-1} for OC [201]. The peaks located at around 1633 cm^{-1} for both NC and OC correspond to vibration of water molecules absorbed in cellulose [200], while the amorphous region is represented by the band at about 897 cm^{-1} [200].

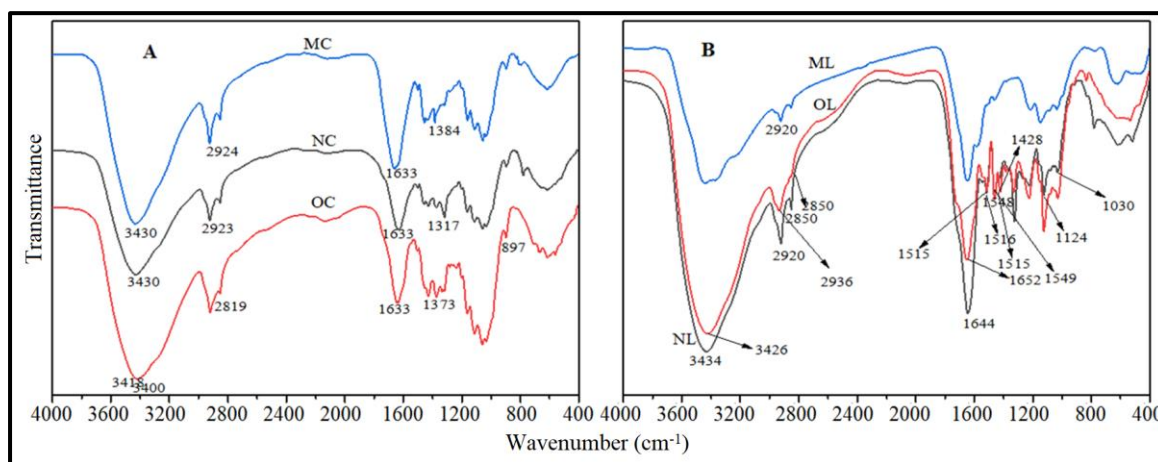


Figure. 3.1.12: FTIR spectra of A: new cellulose (NC), old cellulose (OC), modified cellulose (MC) and B: new lignin (NL), old lignin (OL), modified lignin (ML).

MC showed characteristic bands of cellulose as reported earlier in this work and also agree with the values previously reported in literature [202]. The addition of ZrO_2 nanoparticles to our cellulose sample led to increased intensity of O-H bond in the region around 3430 cm^{-1} [203]. This might be due to sorption of H_2O molecules on Sānci Cell/ ZrO_2 surface. A slightly broader and stronger peak at around 3400 cm^{-1} can be observed in case of OC which might be due to O-H in H_2O as reported previously meaning the OC sample had absorbed more moisture from the atmosphere.

The first peak at 3434 cm^{-1} for NL and 3426 cm^{-1} for OL can be attributed to the OH stretching vibration of the hydroxyl group, according to the FTIR spectra in Figure. 3.1.12B [204]. Due to C-H stretching in the methyl and methylene group, the absorbance at 2920 cm^{-1} for NL and 2936 cm^{-1} for OL is caused [205]. At 2850 cm^{-1} for both NL and OL, a symmetric stretch for CH_3 of the methoxyl group was visible [204]. Ketone and carboxyl groups exhibit a peak at 1644 cm^{-1} for NL and 1652 cm^{-1} for OL, which is attributed to carbonyl stretching.

The peak at 1548 cm^{-1} , 1516 cm^{-1} , 1431 cm^{-1} for NL and 1549 cm^{-1} , 1515 cm^{-1} , 1423 cm^{-1} for OL is equivalent to vibrations of aromatic skeletal, while both NL and OL

observed the β -O-4 ether bond band at 1124 cm^{-1} [204]. As seen in the cases of both the lignin and the primary alcohol, aromatic CH in plane deformation, guaiacyl type, and C-O stretching may be the causes of a small peak at around 1030 cm^{-1} [204]. The aromatic and aliphatic hydroxyl groups in the lignin samples were stretched O-H, which produced a strong and broad absorption band between 3600 and 3200 cm^{-1} [205].

The modification also showed an increase in the hydrophilic nature of the lignin because the ratio of the C-H stretching band intensity (2920 cm^{-1}) is lower in the spectrum of the Sănci Lig/ZrO₂.nH₂O material than that observed for the pure lignin. Moreover, the FTIR spectra of NL and OL samples almost overlap meaning the structural and chemical composition of both the samples are almost identical. This is because lignin has a complicated structure that makes it challenging to break down. Ether linkages and carbon-carbon bonds, which hold the lignin units together, are compelling and stable bonds.

3.1.3.4. Evidence from TGA-DTG spectra

Thermogravimetric spectra of all cellulose and lignin are shown in the Figure. 3.1.13. The two weight loss stages of thermal decomposition of the cellulose fibers correspond to the slow pyrolysis and fast pyrolysis stages. Weight loss was connected to the volatilization and vaporization of absorbed water molecules as well as the removal of moisture content at the early and slow pyrolysis stage of the curve between 30°C and 160°C for NC, 30°C to 180°C for OC, and 30°C to 190°C for MC. Fast pyrolysis occurred between 265°C to 360°C for NC, 256°C to 380°C for OC and 250°C to 390°C for MC as shown by the broad peaks on the DTG curves. Due to the cellulose's decomposition and dehydration, the weight loss occurred relatively quickly. Because of oxidative thermal degradation, and depolymerization of the cellulose chain, cellulose was almost completely burned during this stage. Nearly all of the cellulose was pyrolyzed at temperatures above 400°C , leaving only a minimal amount of solid residue. Maximum degradation occurred at 317°C for NC, 338°C for OC and 320°C for MC as shown in the DTG curves.

Between the different samples of cellulose, MC and OC underwent the maximum weight loss in the first stage due to removal of moisture. This might be since after modification, there is an increase in the hydrophilic character of the fibers while for OC, it might be due to prolonged exposure to the atmosphere over a very long period of time. The highest weight loss was seen in cellulose (old), which may be related to lower intermolecular van der Waals forces and hydrogen bonding, although a similar thermal

degradation and a corresponding percentage weight loss were observed in cellulose samples [206].

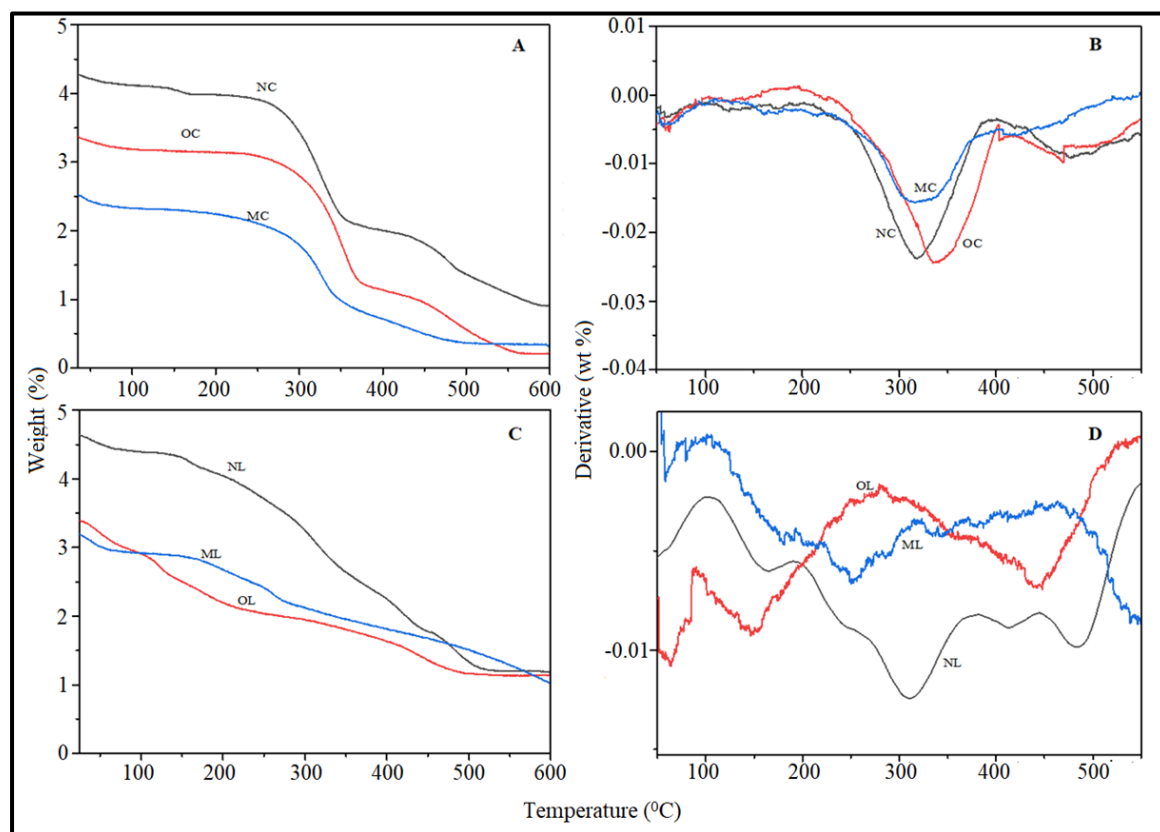


Figure. 3.1.13. TG patterns of A: old cellulose (OC), new cellulose (NC), modified cellulose (MC); DTG patterns of B: old cellulose (OC), new cellulose (NC), modified cellulose; C: old lignin (OL), new lignin (NL), modified lignin (ML); D: old lignin (OL), new lignin (NL), modified lignin (ML).

Compared to cellulose, lignin decomposes more slowly and over a wider temperature range because of its complex structure and composition. This is because different oxygen functional groups from lignin's structure have different thermal stabilities and scission occurs at various temperatures [207]. As seen up to 120 °C for NL, 110 °C for OL, and 130 °C for ML, free and bound water evaporated, which resulted in the lignin samples losing weight. For NL, OL, and ML, the moisture removal or drying stage is defined as a weight loss of approximately 0.3%, 1%, and 0.4%, respectively. Disappearance of side chains, releasing volatiles like CH₄, CO, CO₂, etc., is the cause of the shoulder-like peaks in the lignin samples on the DTG curve temperature ranges between 120–200 °C. The DTG curve's broad peaks show that the lignin samples quickly degraded through pyrolysis in the temperature range of 220 °C - 515 °C for NL, 200 °C -

510°C for OL, and 230°C - 600°C for ML. The primary pyrolysis stage is considered to have occurred at this point because the lignin sample had lost most of its initial weight.

The interunit linkages are broken down during the pyrolytic degradation process which release vaporization of monomeric phenols and their derivatives. Maximum degradation occurred at 310°C for NL, 400°C for OL, and 560°C for ML as shown in the DTG figures which show wide and flat peaks. Between the different samples of lignin, OL underwent the maximum weight loss in the first stage due to removal of moisture. It might be due to the prolonged exposure to the atmosphere over a lengthy period of time. Although all the lignin samples had a similar course of thermal degradation and corresponding percentage weight loss, the DTG of OL was higher than NL, and modified lignin had the highest DTG of all the lignin samples. It is thermally more stable because the DTG value is higher. OL may have higher thermal stability than NL because it contains more C-C linkages and aromatic moieties, which are very stable and require a higher temperature to fragment. While, for modified lignin, it is thermally the most stable which might be due to ZrO₂, a derivative of zirconium oxychloride, that is induced in the modified lignin which exhibits excellent thermal stability and also may be due to the cleavage of the aryl-ether linkages resulting in stable intermediate products [208].

3.1.3.5. Evidence from DSC spectra

Thermal stability studies of cellulose and lignin through DSC are shown in the Figure. 3.1.14. The heat of reaction is measured in between 0^oC to 300^oC. At 60 °C to 100 °C for NC, 50 °C to 80 °C for OC, and 65 °C to 120 °C for MC, the first endotherm of cellulose began. It is believed that these endotherm transitional ranges correspond to an amorphous component that led to the rearrangement of the molecular chains, according to Nandanwar et al, (2016) [204]. This small change in enthalpy may also be caused by the desorption of moisture as water trapped in the polysaccharide structure is released. The second endothermic transition, which corresponds to the cellulose crystallite portion, was visible for NC, OC, and MC between 180°C and 200°C, whereas it was visible for MC between 200°C and 210°C. This endothermic transition was attributed to the onset of cellulose thermal degradation, which includes molecular chain rearrangement, glycosidic bond cleavage, intermolecular cross-linking, and finally cellulose depolymerization, involving the dissolution of intramolecular interactions [206].

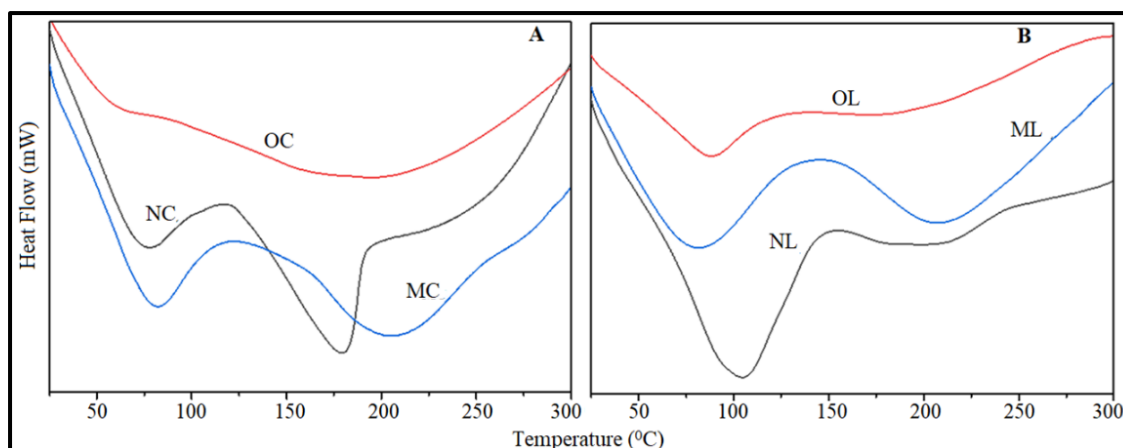


Figure. 3.1.14: DSC spectra of A: old cellulose (OC), new cellulose (NC), modified cellulose (MC); B: old lignin (OL), new lignin (NL), modified lignin (ML).

A very large and broad peak was observed for the endothermic transition in case of OC due to moisture loss in our sample along with the fact that OC having a lower mechanical strength, contains more amorphous regions. So, it consists of a range of interactions and thereby soften gradually. The second endothermic peak for modified cellulose slightly shifted to higher temperature side which may be due to the presence of zirconium oxide nanoparticles [205]. DSC is regarded as a top-notch thermo-analytical technique for determining the glass transition temperature (T_g) of amorphous polymers like lignin. The DSC heating curve shows a slight change in baseline rather than a sharp peak during this process because the glass transition of lignin is not a known phase [205]. As a result, the small variations on the DSC baseline at 140°C, 130°C, and 110°C were identified as the T_g for NL, OL, and ML, respectively. The lower T_g value of OL suggests that its main chain is more pliable and less rigid, which allows for rotation at lower temperatures. Due to its less compact nature, it may also imply that OL has fewer intermolecular interactions. This structural characteristic of OL also suggests that it has the additional ability to create the monomers are physically linked together. Below the glass transition temperature (T_g), the polymer becomes glassy and above which it becomes rubbery (soft) and dimensional stability is lost.

After modification, the lignin sample showed the lowest T_g value which can be related to a more flexible chain structure, lower intermolecular forces of interactions and enhanced presence of cross linking between the monomers. Identifying the T_g of polymers is often used for better conceiving the potential applications of such polymers, and thus it represents a key step in commercial polymer research and development. The

sharp endothermic peaks at 220°C, 225°C and 235°C on the DSC curves are the melting points of NL, OL and ML respectively. The melting points of NL and OL are very close to each other which might be due to its complex composition and structure as well as higher crosslinking [209]. Modified lignin, having the highest melting temperature of them all, is deemed to have higher thermal stability and the side chains will not fragment easily to release volatiles.

3.1.3.6. Evidence from CHN spectra

Table 3.1.3 shows different elemental composition percentage of C, H and N intake in cellulose and lignin samples extracted from *Sānci* bark. The high carbon content is an excellent property as seen in all the cellulose samples due to its properties such as good chemical as well as weathering resistance (C-C main chain linkage does not degrade easily). This might have played a role in maintaining the structural integrity of cellulose. Cellulose samples did not contain nitrogen which might have helped in slowing down the rate of decomposition by fungi, actinomycetes, and bacteria. A slight increase in nitrogen content was also seen after contact with nitrogen containing solvents or chemicals in the lab such as urea in this case which had been used to prepare the zirconium modified cellulose sample.

Table 3.1.3: CHN analysis of cellulose and lignin

Sample	C (%)	H (%)	N (%)
Old Cellulose	37.29	6.12	0.06
New Cellulose	39.5	5.49	0
Modified Cellulose	34.21	5.47	1.78
Old Lignin	31.54	6	2.45
New Lignin	30.99	4.89	2.61
Modified Lignin	29.22	5.21	7.73

For lignin, lower carbon content was seen in the modified sample which might be due to Zr nanoparticles being induced in between the lignin matrix, while nitrogen content also increased after treatment with urea. The origin of nitrogen in lignin samples is from cell proteins. It is believed that the complexity of its bonds, the presence of cross-linkages

in its structure, and the relatively low nitrogen content of lignin all contribute to the slow rate of decomposition of lignin by fungi, actinomycetes, bacteria, etc. [189].

3.1.3.7. Evidence from SEM images

SEM images of all the cellulose and lignin samples are shown in the Figure. 3.1.15. The new cellulose image is quite brighter than that of old one. The lignin samples are look like as cylindrical shape where OL show many open volumes which might be due to the concentration process in lignin extraction. The lignin is extracted with a methodology that heavily affects its structure. Therefore, the morphology of the isolated lignin with respect to the original material may be completely irrelevant. From the Figure. 3.1.15 we observed that a considerable number of fine particles or flakes deposited on the surface of cellulose and lignin fibers heterogeneously which confirms that $ZrO_2.nH_2O$ nanoparticles, roughness on the surface is observed and this heterogeneity may occur due to the lack of agitation.

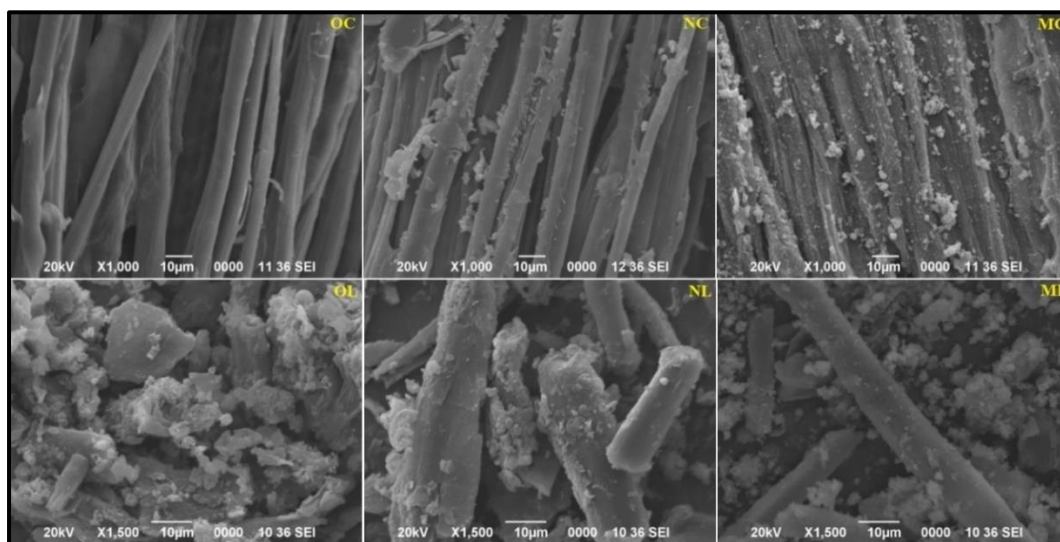


Figure. 3.1.15: SEM images of (OC) old cellulose, (NC) new cellulose, (MC) modified cellulose; (OL) old lignin, (NL) new lignin, and (ML) modified lignin.

3.1.3.8. Evidence from EDXA spectra

From the EDXA spectra (Figure. 3.1.16) it is clearly shown that the amount of carbon content is slightly better in case of both OC and OL in comparison of NC and NL. However, oxygen intake is slightly better in case of both NC and NL. From EDXA spectra, we also confirmed that zirconium oxychloride nanoparticles were successfully induced in MC and ML.

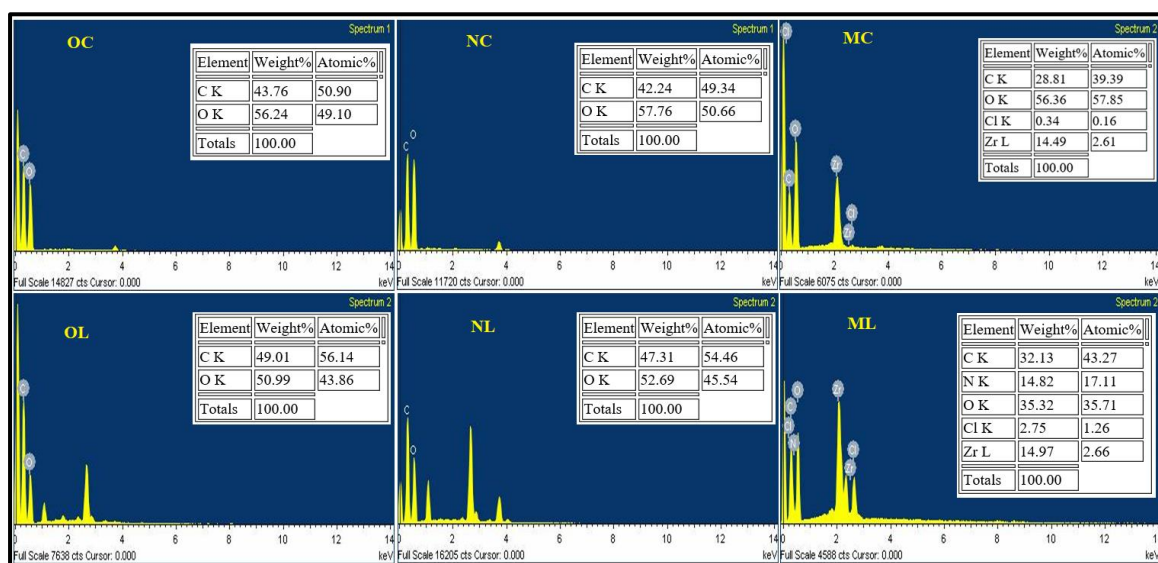


Figure. 3.1.16: EDXA spectra of (OC) old cellulose, (NC) new cellulose, (MC) modified cellulose; (OL) old lignin, (NL) new lignin, and (ML) modified lignin.

3.1.3.9. Evidence from TEM images

As seen from Figure. 3.1.17, $ZrO_2 \cdot nH_2O$ nanoparticles were successfully induced in the cellulose and lignin sample heterogeneously due to different particle size and underwent agglomeration because of its small particle size. On the surface of the cellulose, heterogeneous deposition of $ZrO_2 \cdot nH_2O$ nanoparticles in the size range of 50 to 75 nm in diameter and 40 to 60 nm in diameter was observed on the lignin.

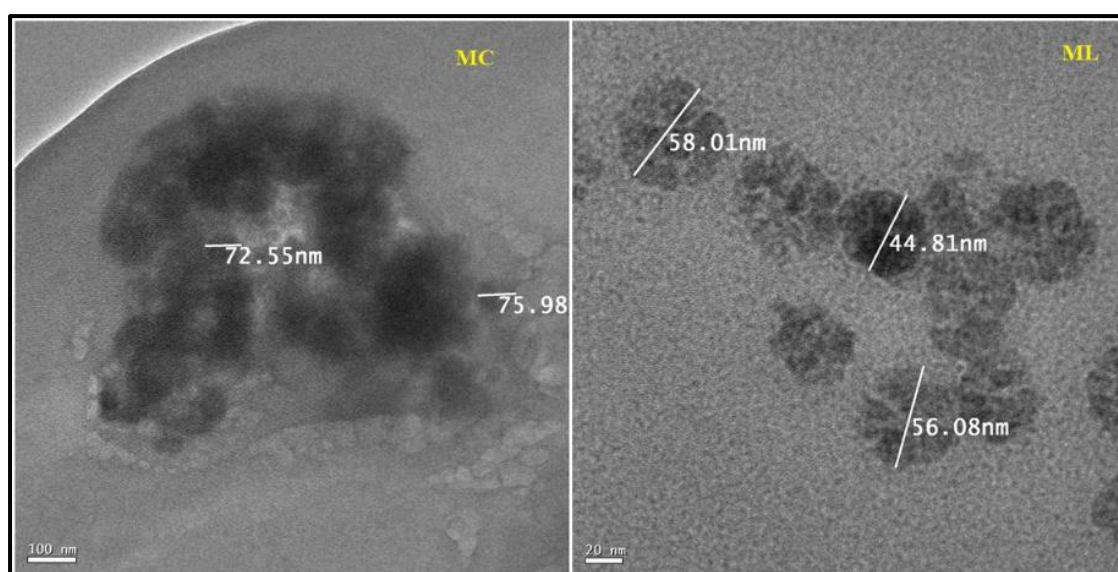


Figure. 3.1.17: TEM image of modified cellulose (MC) and modified lignin (ML).

3.1.3.10. Evidence from p-XRD spectra

All the 2θ values in the p-XRD spectra are obtained from $\text{CuK}\alpha$ radiation with a wavelength of 1.541\AA (λ). The diffraction patterns of cellulose and lignin are shown in Figure. 3.1.18 [210-212]. Peak deconvolution has been performed using the Lorentzian function ranging 2θ from 10° to 40° to determine the relative contributions of each peak to the crystallographic planes of (1-10), (110), (020), etc. [210-214] (Figure. 3.1.18). The p-XRD spectra of NC showed the characteristic peaks of cellulose I_β where the main contributors of intensity to the three diffraction peaks have Miller indices of crystallographic planes (1-10), (110) and (020) at 2θ values of 14.5° , 16.97° and 22.3° , respectively [210,214-216]. Due to the severe peak overlap of several reflections in the region near 34.5° , it was difficult to correctly estimate the (004) signal [215]. Other reflections obtained are not considered as dominant contributors. For OC, peak deconvolution was carried out using the same method as above and characteristic peaks for cellulose I_β are shown. A slight shift in the peaks (by 1°) can be seen in case of OC for some of the crystallographic planes which might be due to the change in lattice parameters (either lattice expansion or contraction) like crystallite size, lattice strain, etc., that can occur with ageing and degradation [217]. The MC patterns are amorphous due to modification of the cellulose with zirconium oxide [166]. The Interplanar spacing (d-spacing) for NC crystallographic planes are calculated from the Bragg equation, $n\lambda = 2d\sin\theta$, as shown in Table 3.1.4 [218].

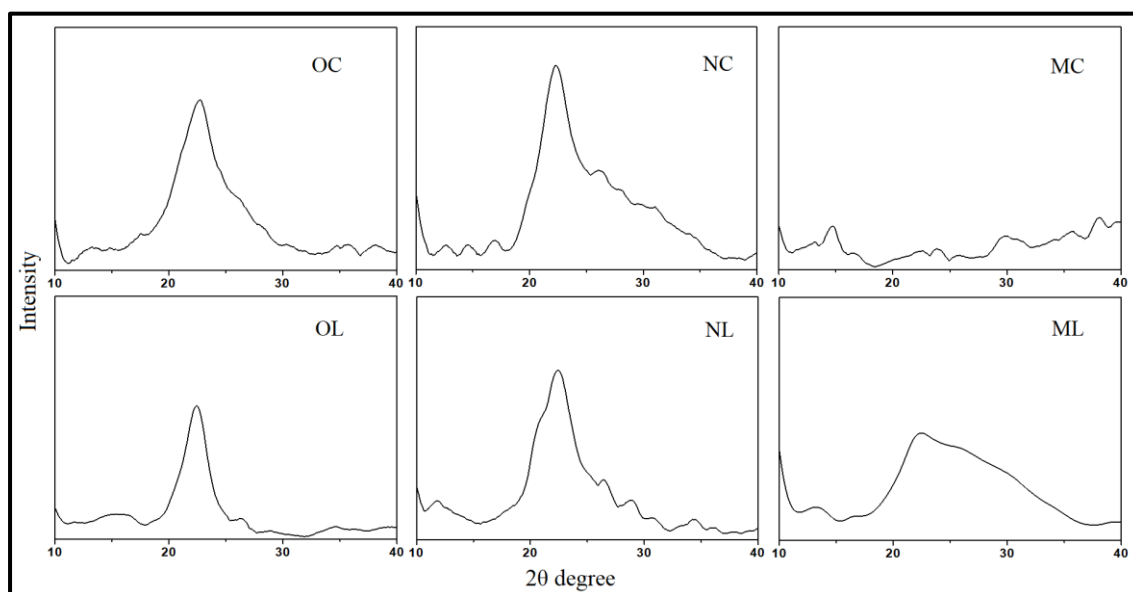


Figure. 3.1.18: p-XRD spectra of (OC) old cellulose, (NC) new cellulose, (MC) modified cellulose; (OL) old lignin, (NL) new lignin, and (ML) modified lignin.

Table 3.1.4: Band position (2θ) and d-spacing of NC

	(1-10)	(110)	(020)
2θ	14.6114	16.9381	22.6564
d (\AA)	3.0543	2.6446	2.0002

The monoclinic and triclinic structure for cellulose structure were determined as per the method developed by Wada et al. 2001. [218]. Discriminant analysis was done according to Samuel et al. 2019 to categorize NC into $I\alpha$ or $I\beta$ predominant form. The function which decides whether it is monoclinic and triclinic structure is $Z = 1693d_1 - 902d_2 - 549$ [216], where $d_1(\text{nm})$ is the d-spacing of the $I\beta$ (1-10) peak and $d_2(\text{nm})$ is the d-spacing of the $I\beta$ (110) peak. $Z > 0$ indicates that the extracted cellulose is rich in the $I\alpha$ form while $Z < 0$ indicates that $I\beta$ is the predominant form in the sample. The Z values of the NC sample obtained were found to be less than zero suggesting that the sample belonged to $I\beta$ form (monoclinic dominant).

For both NL and OL, peak fitting was carried out using Lorentzian function as Lorentzian character was more prominent in hardwood samples (Figure. 3.1.19). After fitting the curves, NL and OL diffraction peaks were located at 2θ of 22.33° [219]. Kubo et al. reported the diffraction angle 2θ of 22.7° for hardwood acetic acid lignin and Ansari and Gaikar 2014 reported 2θ of 22.37° for lignin from sugarcane bagasse [220,221]. Such small differences may be caused by the difference in the lignin type that are obtained from different sources. The ML patterns are amorphous due to modification of the cellulose with zirconium oxide.

3.1.3.11. Evidence from GPC analysis

A popular and widely accepted technique for determining the molecular weights (MW), molecular weight distributions (MWD), and polydispersity indices (PDI) of polymers is gel permeation chromatography (GPC). Samples of lignin were not totally dissolved in tetrahydrofuran (THF) even after stirring and sonication, so the soluble fraction after filtration through Teflon membrane with a pore size $0.45 \mu\text{m}$ was analyzed by GPC [222].

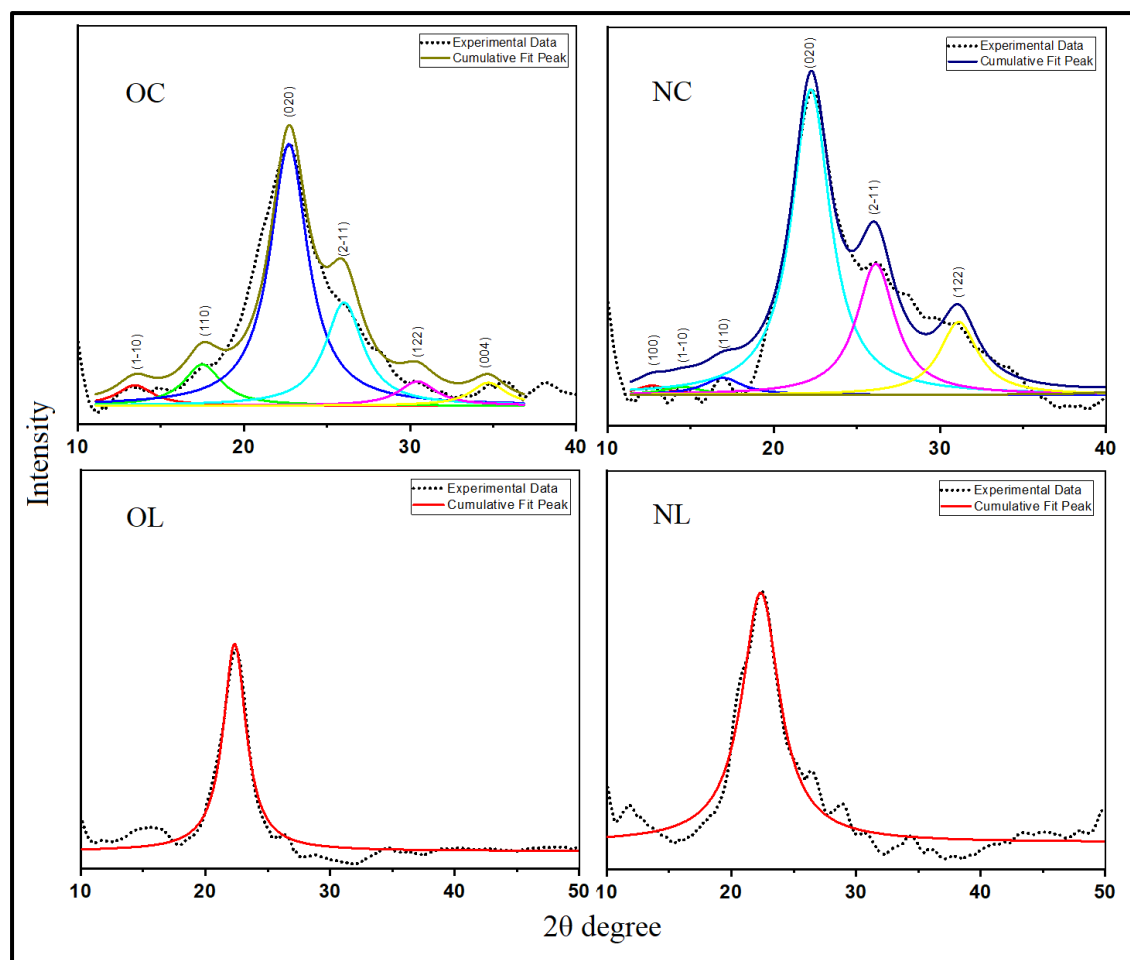


Figure. 3.1.19: X-ray diffraction spectra of (OC) old cellulose, (NC) new cellulose, (OL) old lignin, and (NL) new lignin illustrating peak deconvolution.

Pure cellulose fiber, extracted from *Sānci*, could not be investigated by GPC because they were insoluble in the standard eluent tetrahydrofuran due to its high molecular weight. Table 3.1.5 displays the polydispersity index (PDI) values, number average and weight average molecular weights (M_n and M_w), and molecular weights for the lignin samples. PDI values of all the lignin samples are nearly equivalent to one as expected since lignin is a natural polymer. Slightly higher molecular weight distribution was observed for NL resulting in better mechanical properties [223]. But the difference in molecular weight distribution between NL and OL was not that significant implying that the structural integrity of lignin even after ageing was more or so intact due to its complex structure.

ML was seen to have a lower molecular weight distribution that might be due to chain scission and ring opening caused by the modification, thereby resulting in increased chain mobility and a less compact structure. Since NL sample have been recorded as having slightly higher average molecular weight than that of OL, hence, we may conclude

that the NL has the higher average particle size as higher PDI value also corresponds to a larger size distribution in the particle sample [224].

Table 3.1.5: Molecular weight distribution and polydispersity of lignin samples

Sample	M_n	M_w	Polydispersity
New Lignin	1414	1500	1.06
Old Lignin	1416	1448	1.02
Modified Lignin	1262	1330	1.05

3.1.3.12. Evidence from Dynamic Light Scattering (DLS) analysis

DLS is a useful technique for studying particle size distribution where the light scattered by the particles in suspension fluctuates with time which can be related to the particle diameter [225]. For DLS measurements, lignin samples were dispersed in water for 2 days by sonication. Table 3.1.6 depicts the particle size diameter of lignin samples, including D_{10} (10% of total particle lies below this diameter), D_{50} (50% of total particle lies below this diameter), D_{90} (90% of total particle lies below this diameter), and D_{av} (average diameter of the particle). Figure. 3.1.20 displays the DLS spectra. The average diameter of NL, OL and ML particles was found to be 1.72 μm , 1.24 μm and 4.87 μm respectively. NL was found to have a larger particle size compared to OL as also confirmed by GPC analysis. Decreasing particle size in case of OL might be due to the various degradation processes that take place with time which results in an increase in viscosity and the surface area for more reactions to occur. Decreasing size of particles also leads to lower crystallinity as seen in P-XRD analysis for OL [226]. While modified lignin had the largest particle size among all of them due to zirconium nanoparticles being induced in between the lignin matrix which caused agglomeration, thereby resulting in an increase in the diameter.

Table 3.1.6: Particle sizes of different lignin samples

Sample	Particle diameter	Size range (μm)
New Lignin	D ₁₀	0.43
	D ₅₀	1.31
	D ₉₀	6.08
	D _{average}	1.72
Old Lignin	D ₁₀	0.36
	D ₅₀	1.49
	D ₉₀	6.65
	D _{average}	1.24
Modified Lignin	D ₁₀	1.73
	D ₅₀	4.66
	D ₉₀	13.30
	D _{average}	4.87

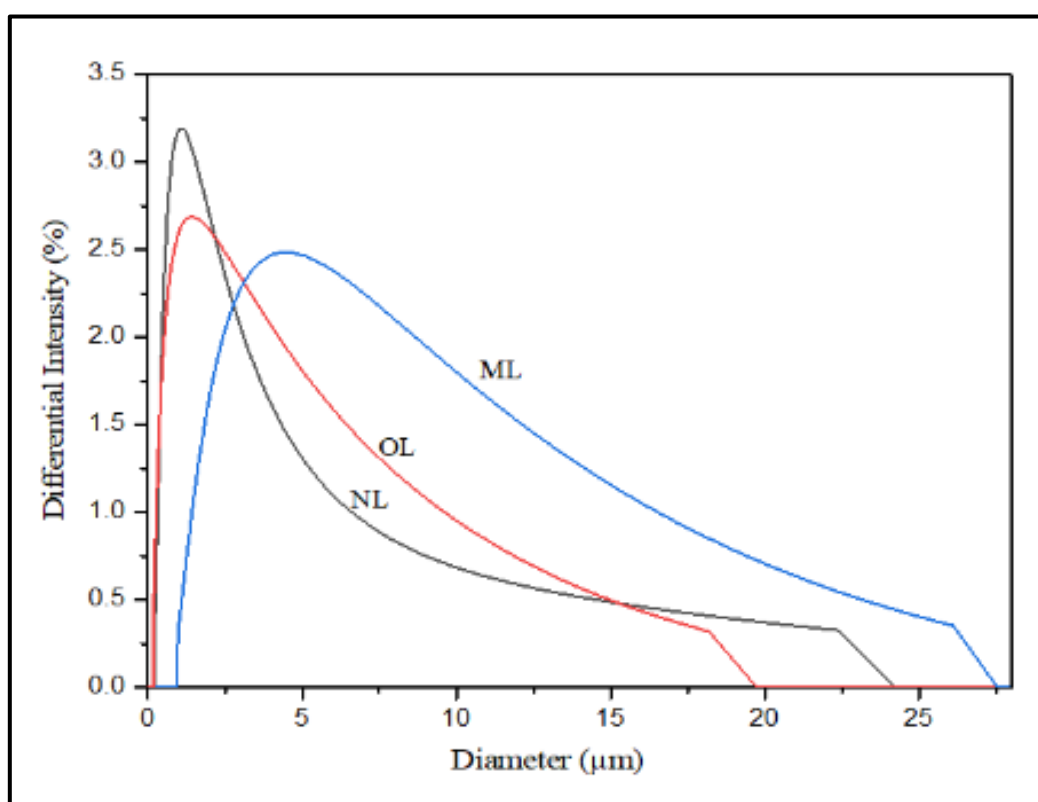


Figure. 3.1.20: DLS size distribution spectra of (OL) old lignin, (NL) new lignin and (ML) modified lignin.

3.1.3.13. Investigation of mechanical properties by UTM

Neat PVA films were used as reference and the tensile strength of the film was found to be 2.24 MPa from UTM measurements. An increase in tensile strength was observed for the PVA-Cellulose and PVA-Lignin composite films as compared to the neat PVA film. This demonstrates that cellulose fibers and PVA, lignin, and PVA are highly compatible. The enhanced tensile strength properties of the PVA-Cellulose and PVA-Lignin composites, compared to neat PVA, and, consequently, the intense reinforcing action of cellulose and lignin, may be explained by strong intermolecular hydrogen bonding between the hydroxyl groups of cellulose, lignin, and the PVA matrix [167]. The results of the mechanical analysis of tensile strengths of different PVA-Cellulose and PVA-Lignin films are summarized in Table 3.1.7 and representative stress-strain curves are shown in the Figure. 3.1.21. A clear decrease in the tensile strength of PVA-OC film was observed which could be correlated with a higher moisture content seen in case of OC. As the strength of the cellulose decreases, the chains loosen and becomes less compact due to poor intermolecular interactions [168]. Also, absorbed water in a polymer behaves like a plasticizer that reduces the entanglement and bonding between molecules, affecting various mechanical properties [170].

Similarly, the tensile strength decreases for PVA-OL film which could again be correlated with a higher moisture content for OL as the intermolecular interactions decreases and chain entanglement lowers, resulting in a flexible structure [168]. However, the decrease in tensile strength was much more prominent in case of the PVA-Cellulose samples as compared to the PVA-Lignin samples. This could be due to the complex and highly branched structure of lignin which contains both aliphatic and aromatic residues that do not degrade easily with ageing [227].

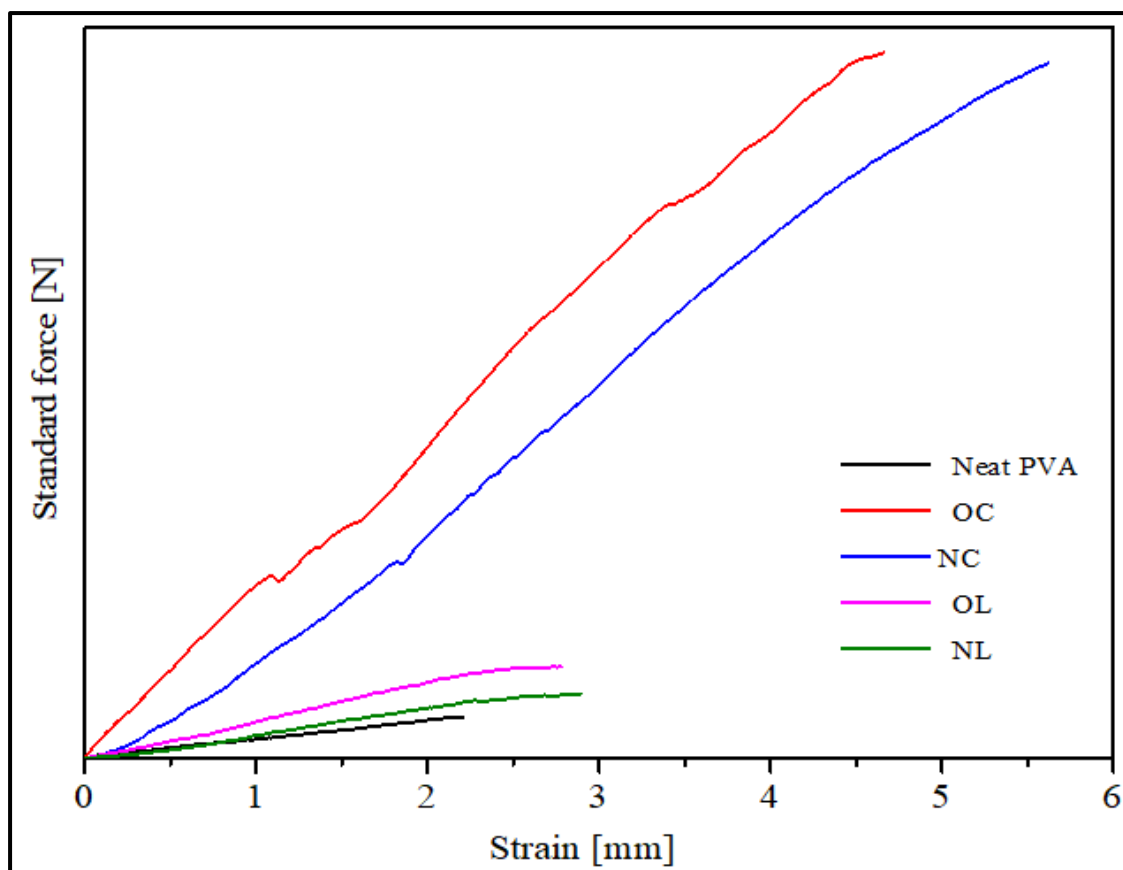


Figure. 3.1.21: Mechanical strength analysis by UTM of neat PVA, (OC) PVA/odd cellulose, (NC) PVA/new cellulose, (OL) PVA/old lignin and (NL) PVA/new lignin film.

Table 3.1.7: Tensile strength of different cellulose and lignin film along with PVA

Sample	Tensile strength (MPa)
Neat PVA	2.24
Old Cellulose	4.66
New Cellulose	5.61
Old Lignin	2.87
New Lignin	3.02

3.1.4. Summary of the section

The present study reveals some interesting traditional knowledges associated with preparation of *Sāncipāt* related to their attractive look, physical properties, composition,

adhesion of the ink on it and longevity of the manuscript in harsh climate. Raw *Sānci* bark consists of native cellulose together with some hemicellulose and lignin devoid of nitrogenous compounds. The traditional degumming process is less drastic than common alkaline degumming which partially removes the unwanted hemicellulose and lignin leaving mostly the fibrous cellulosic part. The amount of carbon and oxygen in freshly prepared *Sāncipāt* is slightly higher than that of raw *Sānci* bark. The smoothness of surface, tensile strength and gloss index are increased during the preparation of *Sāncipāt*. Antimicrobial test shows that raw *Sānci* bark has no antifungal properties but the *Sānci* bark after degumming in the presence of CuSO_4 , and after application of a coating of *Hāitāl* and *Hengul* shows remarkable inhibition towards fungi. The antifungal property of *Sāncipāt* manuscript have been attributed to a synergistic effect of CuSO_4 used during degumming and due to application of *Hāitāl* and *Hengul*. Application of a thin layer of *Hāitāl* and *Hengul* in the empty spaces of cleaned folios can be used as a method of conservation of *Sāncipāt* manuscript to protect them from insect and fungus. Cellulose and lignin were extracted from century old and new *Sānci* bark using alkaline and peroxide treatments for cellulose and acidic treatments them from insect and fungus. Cellulose and lignin were extracted from century old and new *Sānci* bark using alkaline and peroxide treatments for cellulose and acidic treatments for lignin. The cellulose and lignin extracted from new *Sānci* bark were embedded with $\text{ZrO}_2 \cdot n\text{H}_2\text{O}$ nanoparticles using zirconium oxychloride. Old cellulose (OC) and old lignin (OL) were found to show a higher moisture content percentage compared to new cellulose (NC) and new lignin (NL), reducing mechanical properties in both OC and OL. The structural and chemical compositions were nearly identical, indicating only a minor degradation of intricate structure. The complex composition and structure of lignin results in a slower thermal decomposition rate. It can withstand a more comprehensive range of temperatures compared to cellulose because the different oxygen functional groups that make up its structure have different thermal stabilities and scission temperatures. The cellulose samples were found to have a high carbon content, which is an excellent property because of its good chemical and weathering resistance. The carbon content is marginally higher for both OC and OL than for NC and NL. Heterogeneous $\text{ZrO}_2 \cdot n\text{H}_2\text{O}$ nanoparticles deposited on cellulose and lignin.

Better mechanical properties of NC have been observed. A lower level of mechanical strength for OC is seen because of aging and degradation. The amorphous

nature of $ZrO_2 \cdot nH_2O$ may cause the gradual reduction in XRD peak intensity observed for MC and ML. OL particles had the least average diameter among NL, OL, and ML particles. The P-XRD of OL confirmed that as particle size decreases, mechanical strength also decreases. The apparent decrease in tensile strength of PVA-OC and PVA-OL films was noticed. This finding could be related to decrease in mechanical strength and higher moisture content found in OC and OL. Zirconium oxychloride modifications in case of NC and NL should not have a significant impact on the conservation of these manuscripts.

*A paper based on a part of this work has been published in **Current Science** as cover article with a highlight, (Current Science, 123, 1-6, 2022. doi: 10.18520/cs/v123/i11/1359-1364)



3.2. Section-2: Restoration and conservation of *Sāncipāt* manuscripts*

Fresh *Sāncipāt* was prepared using the traditional procedure [15]. However, hot-pressing with a BAJAJ DX2 light-weight 600W dry iron was used for rapid drying and smoothening of the bark after cleaning, after partial degumming and after application of fatty pulse. Haital paint was expertly created by mixing finely-ground Haital, with an average particle size of $6.5\mu\text{m}$ as measured by the Hegman scale, with water and Bael glue. The paint was then skillfully applied to Sanci bark following the application of a fatty pulse. Same procedure was followed for preparation of *Hengul* paint for application on borders of the folios. The *Hāitāl* paint was mixed with traces of *Hengul* in order to match its color with the old *Sāncipāt* for application on free surfaces of old *Sāncipāt* for conservation of *Sāncipāt* manuscripts. Porcelain mortar and pestle were used for grinding pigments. For experiments to analyze effects of solvents and chemicals on *Sāncipāt*, $3.0\text{cm} \times 2.5\text{cm}$ sized pieces of old damaged and freshly prepared *Sāncipāt* were immersed in water, isopropyl alcohol and 5% (w/v) aqueous cetrimide and 5% (w/v) thymol in 1:20 water-ethanol mixture for 2h. Then the pieces were oven dried at 105°C for 2h and kept in desiccator overnight before analysis of physicochemical changes caused by the treatments. The resulting solutions also were analyzed after filtration for detecting any leaching from the pieces. Marked changes were observed in various physicochemical, structural and mechanical properties of old and freshly prepared *Sāncipāt* after the treatment with water and other chemicals, commonly used in cleaning and conservation.

3.2.1. Effects of conservative chemicals on old *Sāncipāt*

3.2.1.1. Evidence from FTIR

Figure. 3.2.1(a) and 3.2.1(b) show almost similar FTIR spectra of old *Sāncipāt* before and after physical cleaning using a rubber eraser. A small peak at 2508cm^{-1} indicates the presence of some acidic compounds in the uncleaned *Sāncipāt* which disappears after cleaning [228]. The major characteristic peaks observed for the cleaned *Sāncipāt* were: an intense broad peak at 3428cm^{-1} due to intermolecular H-bonded -OH group of lignin [184,229], a small sharp peak at 2913cm^{-1} due to N-H stretching of lignin [184,229], a major peak at 1648cm^{-1} due to water associated with lignin and cellulose [184], medium intensity peaks in the range of $1364\text{-}1450\text{cm}^{-1}$ due to C-H asymmetric deformation in –

OCH₃ or C-H bending in cellulose and hemicellulose [188,190], and a medium peak at 1027cm⁻¹ due to lignin [186].

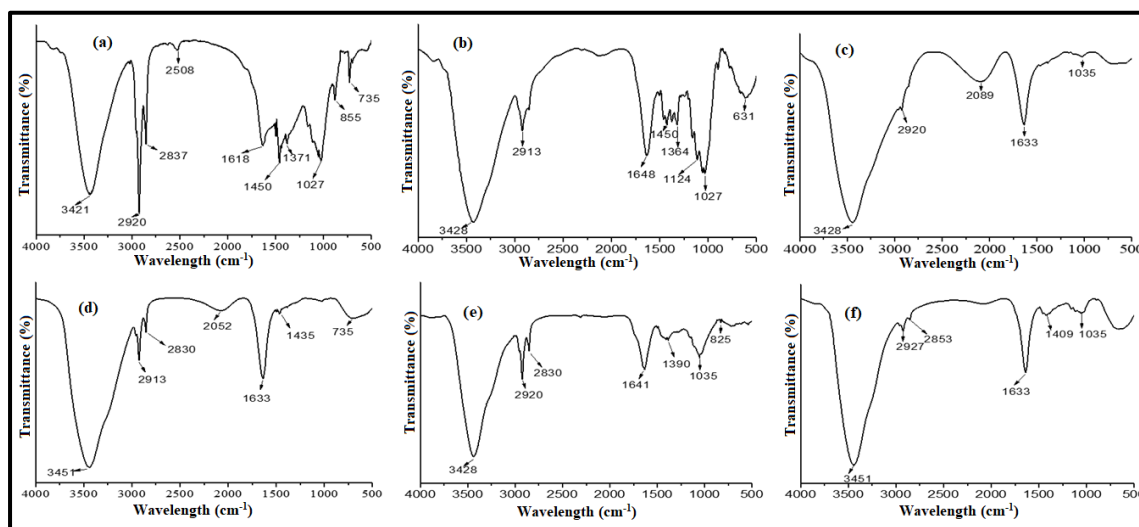


Figure. 3.2.1: FTIR spectra of old *Sāncipāt* (a) before and (b) after cleaning, and (c) after immersing in water, (d) 5% aqueous cetrimide, (e) isopropyl alcohol, and (f) 5% thymol in water-ethanol mixture for 2h.

All these peaks either disappeared or their intensities decreased after treatment with water, isopropyl alcohol, 5% aqueous cetrimide and 5% thymol solution water-ethanol mixture (Figure. 3.2.1(c)-(f)). This indicates that the conservative chemicals may cause some damage to *Sāncipāt* through removal of some lignin and structural changes in cellulose and hemicellulose of *Sāncipāt* as has already been reported for effect of thymol on paper [230].

3.2.1.2. Evidence from XRD

XRD peaks at 17.83⁰(-102), 23.80⁰(-202), 26.05⁰ (030), 29.49⁰(-222), 29.37⁰(-222), 23.68⁰(-202) [JCPDS card no 03-0226] are characteristic of cellulose with monoclinic system [190,231] (Figure. 3.2.2). Similarly, the characteristic peaks at 14.24⁰ (-101), 29.49⁰ (-122), 22.31⁰ (002), 29.37⁰ (-122), 29.47⁰ (-122), 22.08⁰ (002), 14.89⁰ (-101) indicate the presence of native cellulose [JCPDS card no 03-0289]. The thymol-treated sample showed some deficiency of cellulose and lignin compared to that of before and after treatment with distilled water, 5% aqueous cetrimide solution and isopropyl alcohol. XRD evidence of *Hāitāl* and *Tutia* have been seen in the old *Sāncipāt* before and after treatment with the chemicals. The peak of 37.42⁰ (040), 45.35⁰ (-202), 49.69⁰ (-341)

observed before and after immersion in water is due to arsenic sulfide [JCPDS card no 00-044-1419] of *Hāitāl* traditionally applied on *Sāncipāt*. While the peak at 37.42° disappeared after treatment with cetrimide and isopropyl alcohol, all three peaks disappeared after treatment with thymol indicating leaching of the pigment into the solutions. The peak at 29.49° (110) is due to *Tutia* (copper sulphate) [JCPDS card no 00-005-0667] used during partial degumming during preparation of *Sāncipāt*. This peak also has disappeared after thymol treatment indicating a loss due to leaching. We see a characteristic peak in the range of 21.50° to 22.30° before and after treatment with all chemicals which may be attributed to the presence of *Mahī*, the traditional herbal ink which may contain trace amount of hematite($\alpha\text{-Fe}_2\text{O}_3$) [JCPDS card no 33-0664] [56].

The crystallinity of *Sāncipāt*, which was 83% before treatment also considerably decreased after treatment with the chemicals. The crystallinity decreased to 26%, 60%, 14% and 13% after treatment with water, 5% aqueous cetrimide solution, isopropyl alcohol and 5% thymol in water-ethanol mixture, respectively (Figure. 3.2.2). The drastic decrease in crystallinity by isopropyl alcohol and thymol indicate possible structural damages to *Sāncipāt* by these chemicals if used in conservation.

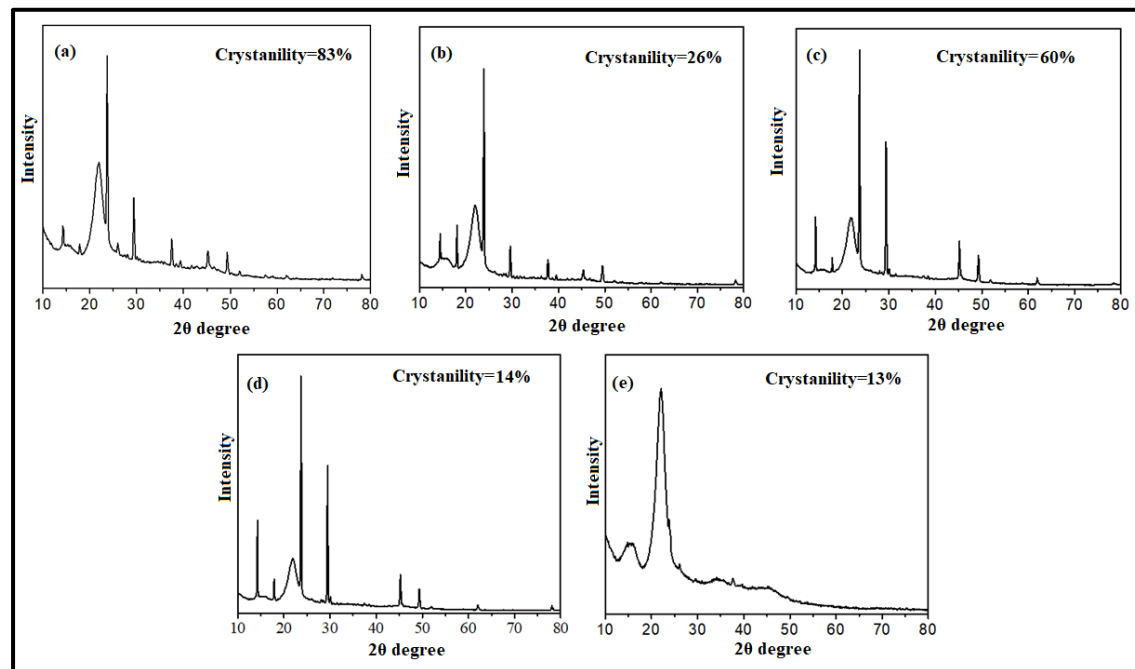


Figure. 3.2.2: XRD patterns of old *Sāncipāt* (a) after cleaning, and (b) after immersing in water, (c) 5% aqueous cetrimide, (d) isopropyl alcohol, and (e) 5% thymol in water-ethanol.

3.2.1.3. Evidence from image and elemental analysis

SEM shows a marked increase in the fibrous nature of the *Sāncipāt* after the treatment with water and other chemicals (Figure. 3.2.3). EDX analysis shows the presence of C, N and O, and trace amounts of S, K, Ca, Mn, Fe, Cu and As in *Sāncipāt* before treatment which were changed after treatments. Atomic percentages of C, N and O before treatment were 46.69%, 8.16% and 44.06%, respectively; which changed to 48.49%, 12.92% and 37.65% after treatment with water; 50.28%, 10.01% and 38.53% after treatment with cetrimide; 67.01%, 30.70% and 0.33% after treatment with isopropyl alcohol; and 58.47%, 0.80% and 40.50% after treatment with thymol, respectively. There were notable decreases in the atomic percentages of O and N after treatment with isopropyl alcohol and thymol again indicating chemical changes caused by them to *Sāncipāt*. On the other hand, Cu has either disappeared or markedly decreased after the treatments and as disappeared after treatment with thymol indicating removal of the protective metal ions by the chemicals.

3.2.1.4. Weight loss after treatment

The weight loss of old *Sāncipāt* upon immersion in water, 5% aqueous cetrimide, isopropyl alcohol and 5% thymol in water-ethanol mixture for 2h was found to be 85%, 28%, 58% and 83%, respectively (Figure. 3.2.4). The marked weight loss after treatment may be attributed to loss of lignin and hemicellulose indicating associated damage the folios.

3.2.1.5. Changes in mechanical properties

The effects of water and the chemicals on mechanical properties of *Sāncipāt* are shown in Figure. 3.2.4. The tensile strength of the *Sāncipāt* before treatment was found to be 3.27MPa which decreased to 3.05MPa, 3.18MPa, 2.64MPa and 3.04MPa after treatment with water, 5% aqueous cetrimide, isopropyl alcohol and 5% thymol in water-ethanol mixture, respectively. On the other hand, the toughness of 0.26MegaJ/m³ of before treatment slightly increased to 0.28MegaJ/m³ after treatment with aqueous cetrimide but decreased to 0.22MegaJ/m³, 0.17MegaJ/m³ and 0.12MegaJ/m³ after treatment with water, isopropyl alcohol and thymol solution. The elongation at break of *Sāncipāt* before treatment was 13.48%, which remained almost same after treatment with water (13.37%) and cetrimide (14.10%) but decreased markedly after treatment with isopropyl alcohol (9.82%) and thymol (7.44%). Thus, isopropyl alcohol and thymol treatment lead low

ductility turning the material brittle and prone to fracture before deforming much under a tensile load [232,233].

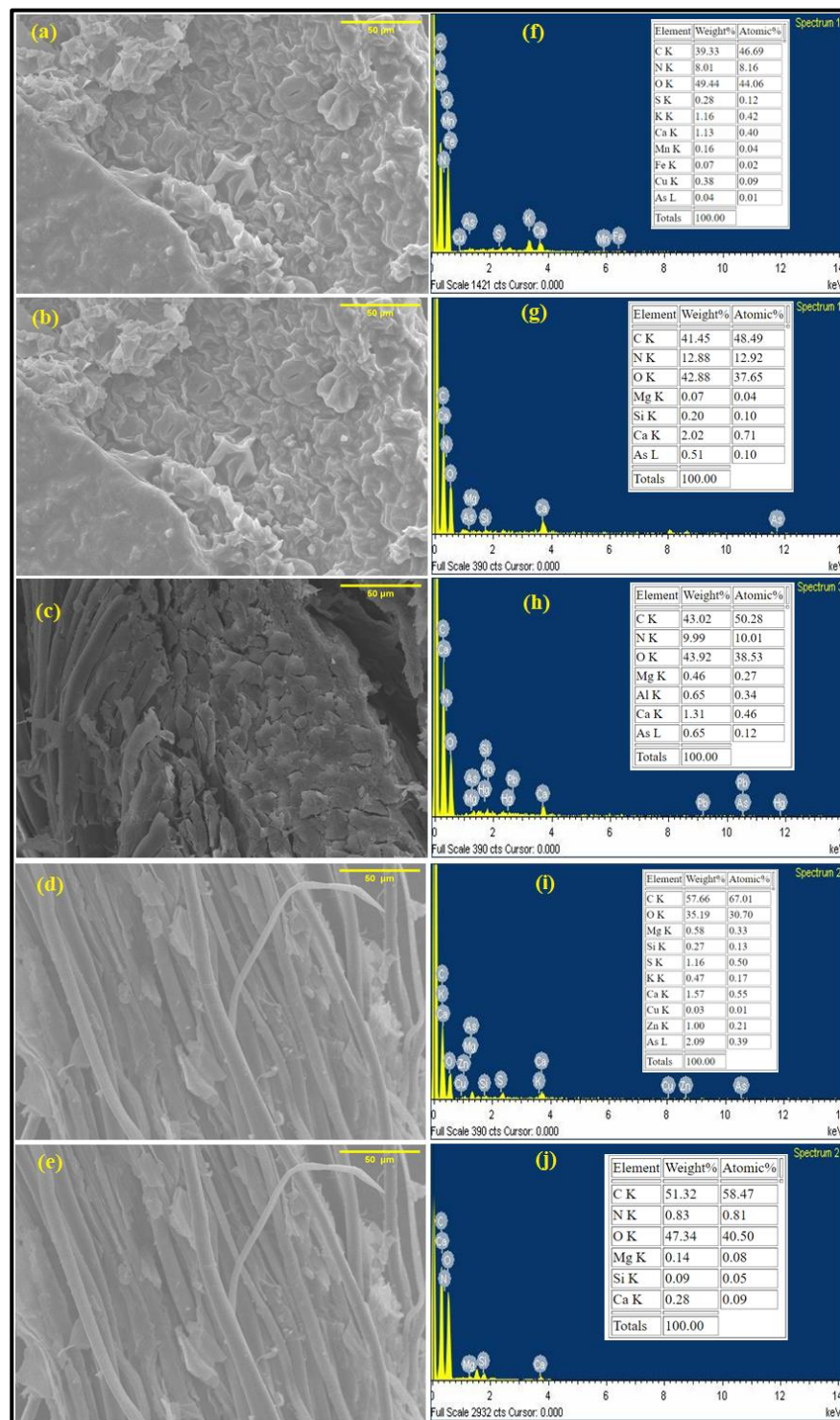


Figure. 3.2.3: SEM images and EDX spectra of old *Sāncipāt* (a, f) after cleaning, and after immersing in (b, g) water, (c, h) 5% aqueous cetrimide, (d, i) isopropyl alcohol, and (e, j) 5% thymol in water-ethanol.

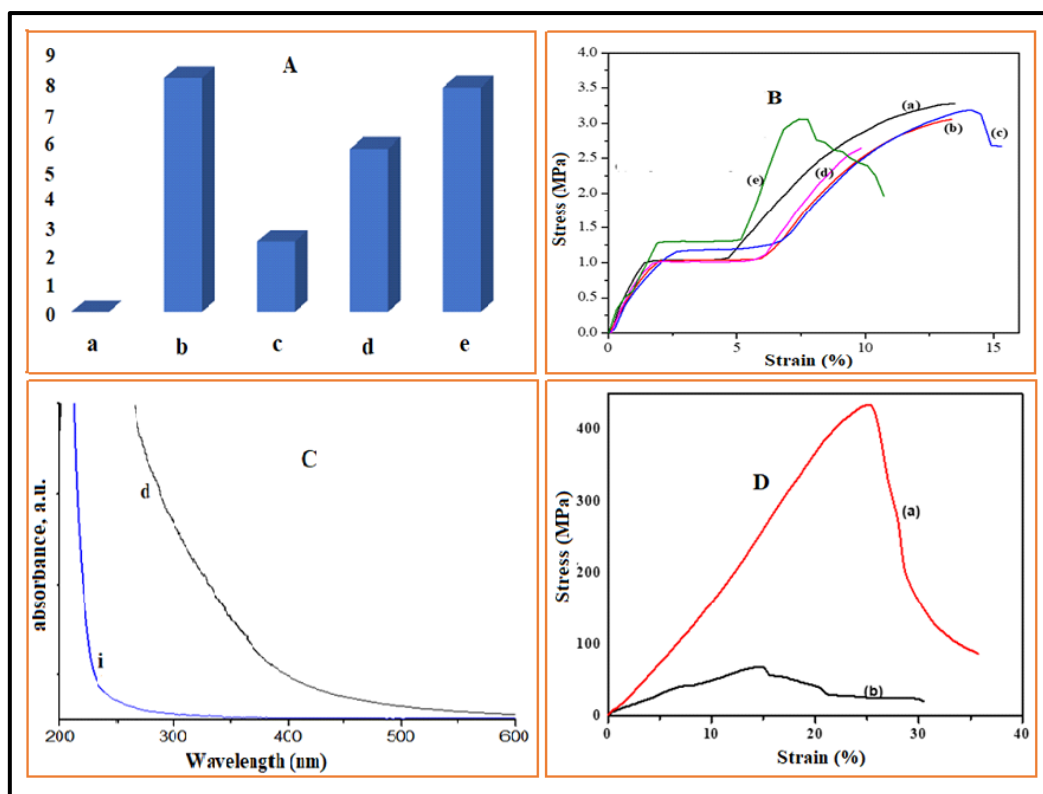


Figure. 3.2.4: A: Percent weight loss of old *Sāncipāt* after soaking for 2h in (a) distilled water, (b) 5% aqueous cetrimide, (c) isopropyl alcohol and (d) 5% thymol in water-ethanol mixture, and B: mechanical strength analysis by UTM of old *Sāncipāt* (a) before and after treatment with (b) distilled water, (c) 5% aqueous cetrimide, (d) isopropyl alcohol and (e) 5% thymol in water ethanol; C: UV-visible spectra of *Sāncipāt* after immersion of with the respective solvents of (d) distilled water, (i) isopropyl alcohol; D: mechanical strength analysis of freshly prepared *Sāncipāt* (a) before and (b) after application of *Lā*-coating.

3.2.1.6. Leaching of material into solvent

Leaching of materials from the *Sāncipāt* into the solvent after immersion of *Sāncipāt* was examined by UV-visible spectroscopy with water and isopropyl alcohol with the pure solvents as references. Cetrimide and thymol were avoided due to their absorbance in the UV region. The observed absorbances above 230nm in the UV region with both solvents, after filtration, indicate leaching of small monomeric fragments of cellulose, hemicellulose or lignin [231] (Figure. 3.2.4).

3.2.1.7. Effect of solvents on Mahī

Mahī, the herbal ink used to write on *Sāncipāt* was prepared in cow urine which is basically aqueous and is hydrophilic and water soluble but insoluble in organic solvents [7,45,55,56]. However, we have seen that the letters written on *Sāncipāt* with *Mahī* to remain intact after immersion in water up to 30 min though the color of the writing base turns darker (Figure. 3.2.5). The chromogenic polyphenolic components and their iron complexes in *Mahī* can bind very well to lignocellulosic *Sāncipāt* and therefore is not affected by water [45,56].

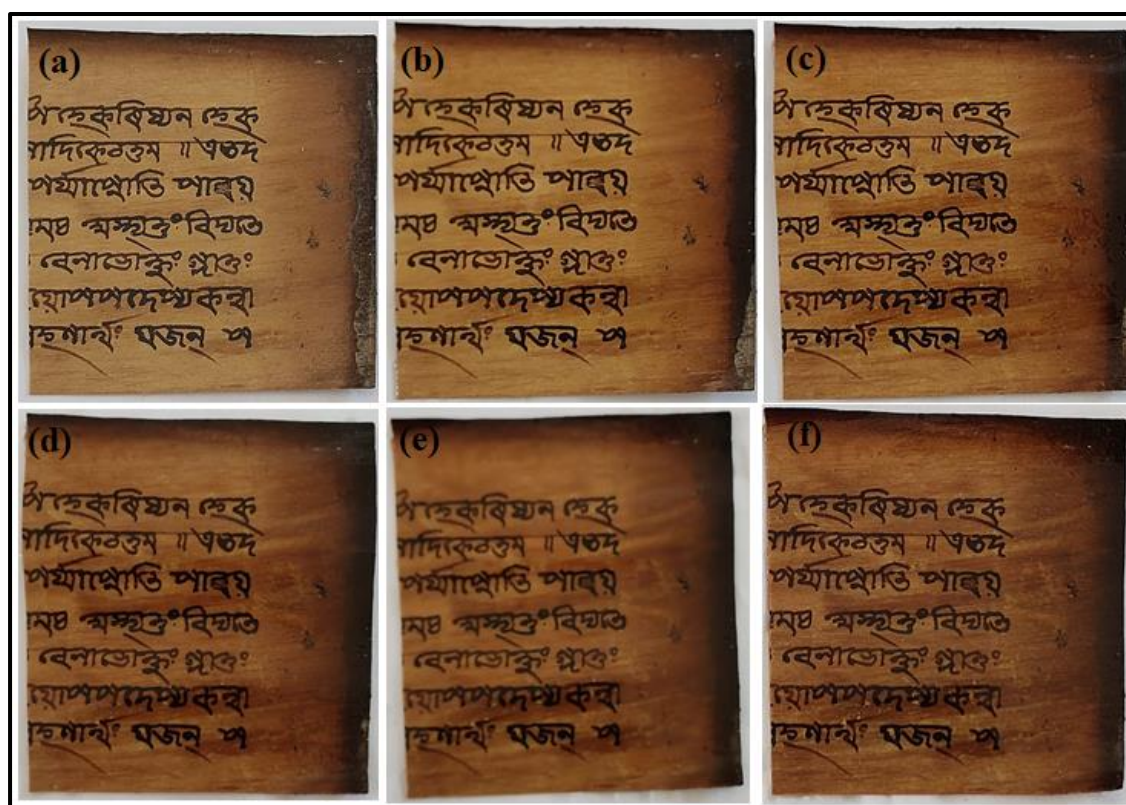


Figure. 3.2.5. Photographs of a piece of *Sāncipāt* written with *Mahī* (a) before and after soaking in water for (b) 1sec, (c) 1min, (d) 5min, (e) 10min and (f) 30min.

3.2.2. Effects of conservative chemicals on fresh *Sāncipāt*

3.2.2.1. Evidence from UV Visible spectra

The absorption of freshly prepared *Sāncipāt* manuscripts immersed in thymol, 5% cetrimide, and isopropyl alcohol and all four of the solutions were examined using a UV-visible spectrophotometer (Figure. 3.2.6). A distinctive peak was visible in all of the solutions between 200 and 600 nm in wavelength. In all of the four solutions, there was a noticeable peak within the 230-320 nm range, indicating that cellulose, hemicellulose,

and lignin may be present [231]. Additionally, we noticed that the distilled water solution immersion with fresh *Sāncipāt* has a relatively weak peak compared to others, which may mean that less cellulose and hemicellulose were lost than in the case of other solutions.

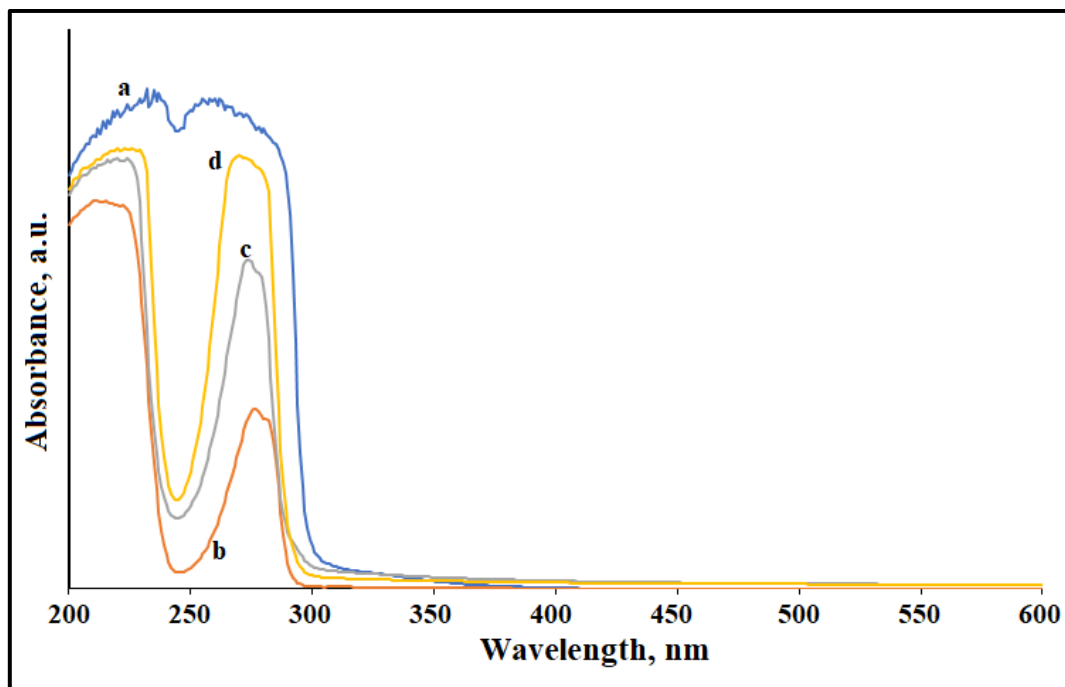


Figure. 3.2.6: UV-visible spectra of (a) distilled water, (b) cetrimide, (c) isopropyl alcohol, and (d) thymol after immersion of *Sāncipāt* with the respective solvents.

3.2.2.2. Evidence from FTIR spectra

From the FTIR spectra shown in the Figure. 3.2.7., the broad peak absorption band at 3430 cm^{-1} for NC and 3418 cm^{-1} for OC is assigned to strong hydrogen bonded hydroxyl groups ($-\text{O}-\text{H}$) stretching generally observed in polysaccharides [184,234]. This peak also includes inter and intra-molecular hydrogen bonds in NC and OC. The stretching and deformation vibrations of the C-H group, typically seen in the glucose unit, are attributed to the bands at 2923 cm^{-1} and 1317 cm^{-1} for NC and 2819 cm^{-1} and 1373 cm^{-1} for OC [184,234]. The peaks located at around 1633 cm^{-1} for both NC and OC correspond to vibration of water molecules absorbed in cellulose, while the amorphous region is represented by the band at about 897 cm^{-1} [184]. The addition of ZrO_2 nanoparticles to our cellulose sample led to increased intensity of O-H bond in the region around 3430 cm^{-1} [186]. This might be due to sorption of H_2O molecules on *Sānci* Cell/ ZrO_2 surface which became more hydrophilic due to polarity of $\text{Zr}-\text{OH}$. Due to C-H stretching in the methyl and methylene group, the absorbance at 2920 cm^{-1} for NL and 2936 cm^{-1} for OL is

caused. At 2850 cm^{-1} for both NL and OL, a symmetric stretch for CH_3 of the methoxyl group was visible [186]. Ketone and carboxyl groups exhibit a peak at 1644 cm^{-1} for NL and 1652 cm^{-1} for OL, which is attributed to carbonyl stretching [184]. The peak at 1548 cm^{-1} , 1516 cm^{-1} , 1431 cm^{-1} for NL and 1549 cm^{-1} , 1515 cm^{-1} , 1423 cm^{-1} for OL is equivalent to vibrations of aromatic skeletal, while both NL and OL observed the β -O-4 ether bond band at 1124 cm^{-1} [184]. The modification also showed an increase in the hydrophilic nature of the lignin because the ratio of the C-H stretching band intensity (2920 cm^{-1}) is lower in the spectrum of the *Sānci* Lig/ $\text{ZrO}_2 \cdot n\text{H}_2\text{O}$ material than that observed for the pure lignin.

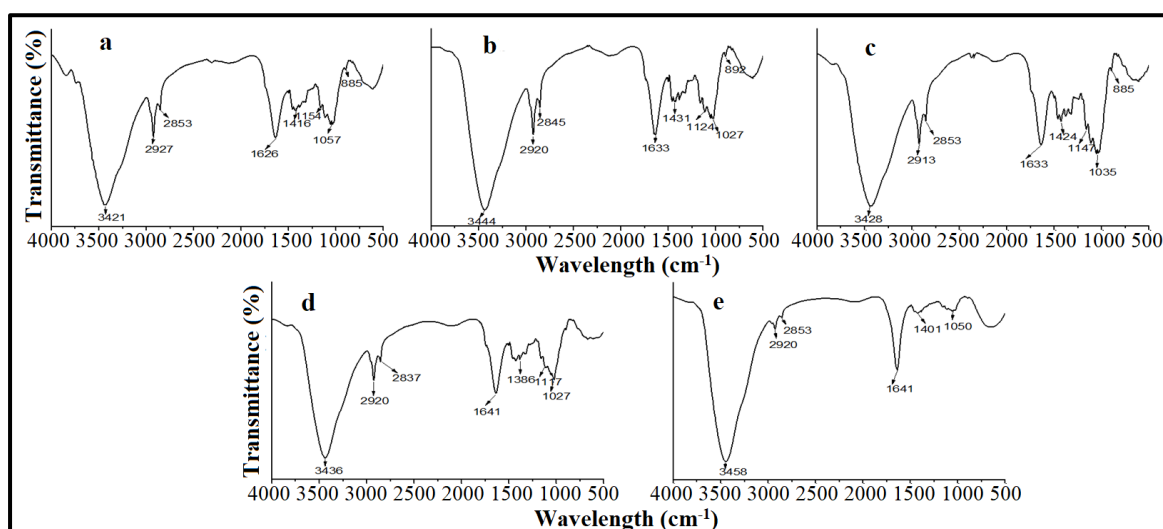


Figure. 3.2.7. FTIR spectra of (a) fresh *Sāncipāt* and after immersing in (b) distil water, (c) 5% aqueous cetrimide, (d) isopropyl alcohol, and (e) 5% thymol in water-ethanol mixture.

3.2.2.3. Evidence from p-XRD spectra

We compared freshly prepared *Sāncipāt* that had been chemically treated versus freshly prepared *Sāncipāt* that had not been treated using a p-XRD analysis (Figure. 3.2.8). The characteristic peaks at 14.24° (-101), 29.49° (-122), 22.31° (002), 29.37° (-122), 29.47° (-122), 22.08° (002), and 14.89° (-101) also denote the presence of native cellulose [JCPDS card no. 03-0289]. The presence of native cellulose was determined by the characteristic peaks of 22.84° (002), 29.35° (-122), 34.06° (310), and 44.36° (302) found in the p-XRD spectra of the freshly prepared *Sāncipāt*, indicating that both lignin and cellulose are present [JCPDS card no. 03-0289]. Fresh *Sāncipāt* treated with cetrimide has

been found to have nearly the same distinctive peak. Several small peaks can be seen in Figure 3.2.8(b), in addition to the peak associated with the lignocellulosic compound, which is most likely the result of the formation of a hydrogen bond [235,236]. This is because cellulose has a strong affinity for the hydroxyl group. Similar peaks have been seen in Figures 3.2.8(b) and 3.2.8(e) due to the hydrolysis of cellulose reacting with the acidic group of the β -1 and 4-glycosidic bonds [235]. In order of increasing crystallinity, freshly prepared *Sāncipāt* that has been treated with thymol (24%), isopropyl alcohol (36%), cetrimide (40%) and distil water (53%). Freshly prepared *Sāncipāt* that has not been treated has a 26% crystallinity. Our understanding of the variation in physicochemical characteristics for both treated and untreated fresh *Sāncipāt* manuscripts comes from the results of p-xrd spectra.

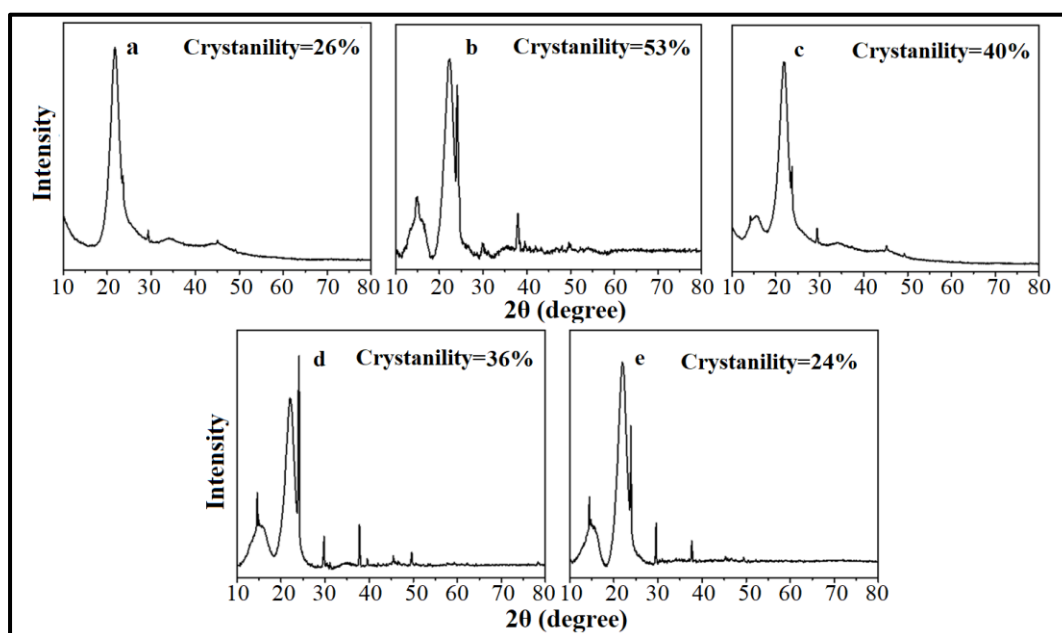


Figure. 3.2.8: XRD patterns of (a) fresh *Sāncipāt* and after immersing in (b) distil water, (c) 5% aqueous cetrimide, (d) isopropyl alcohol, and (e) 5% thymol in water-ethanol mixture.

3.2.2.4. Morphological study

There is no significant change observed in the case of chemically treated freshly prepared *Sāncipāt* in comparison with untreated freshly prepared *Sāncipāt* (Figure. 3.2.9). This shows that neither water nor chemical emersion is required to prepare freshly prepared *Sāncipāt*. The morphological structure of every *Sāncipāt* sample, treated or not, is uniformly smooth.

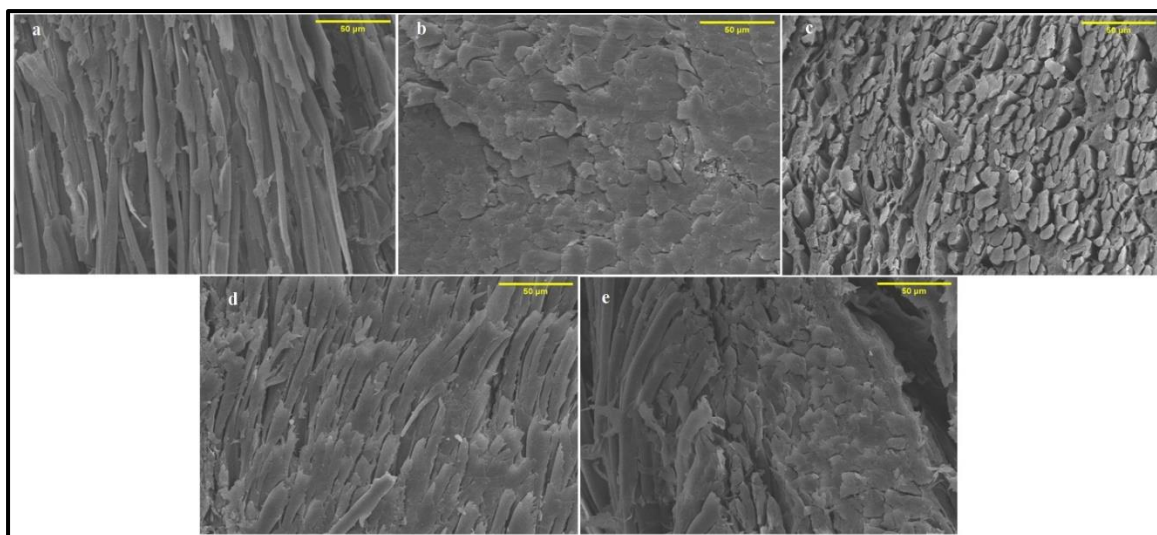


Figure. 3.2.9: SEM image of (a) fresh *Sāncipāt* and after immersing in (b) distil water, (c) 5% aqueous cetrimide, (d) isopropyl alcohol, and (e) 5% thymol in water-ethanol mixture.

3.2.2.5. Elemental analysis

The EDX spectra show the fluctuation of the atomic percentage of C, N, and O amounts in all the treated fresh *Sāncipāt* compared to untreated fresh *Sāncipāt* (Figure. 3.2.10). The highest atomic percentage of carbon is found in the cetrimide-treated *Sāncipāt*. In contrast, the amount of nitrogen is lowest in all other treated *Sāncipāt* except for the thymol-treated ones. Compared to fresh *Sāncipāt* that has not been treated, distil water, and alcohol-treated *Sāncipāt* have higher oxygen values. It is best to avoid using any chemicals to preserve this remarkable writing base because the difference between changing all of the elemental compositions is not very high.

3.2.2.6. Weight loss percentage during degumming

We sought weight loss when treating fresh *Sāncipāt* with different chemicals and solvents (Figure. 3.2.4). For this, all the degummed *Sāncipāt* were oven dried in 105⁰C for 2h. Freshly prepared *Sāncipāt* consumed with distill water results in the highest weight loss percentages. While in the case of cetrimide treated *Sāncipāt*, this amount is slightly higher. Similarly, freshly prepared *Sāncipāt* that has been cetrimide-treated has the lowest weight loss percentage. Weight loss of *Sāncipāt* may indicate the loss of lignin and hemicellulose in freshly prepared manuscripts.

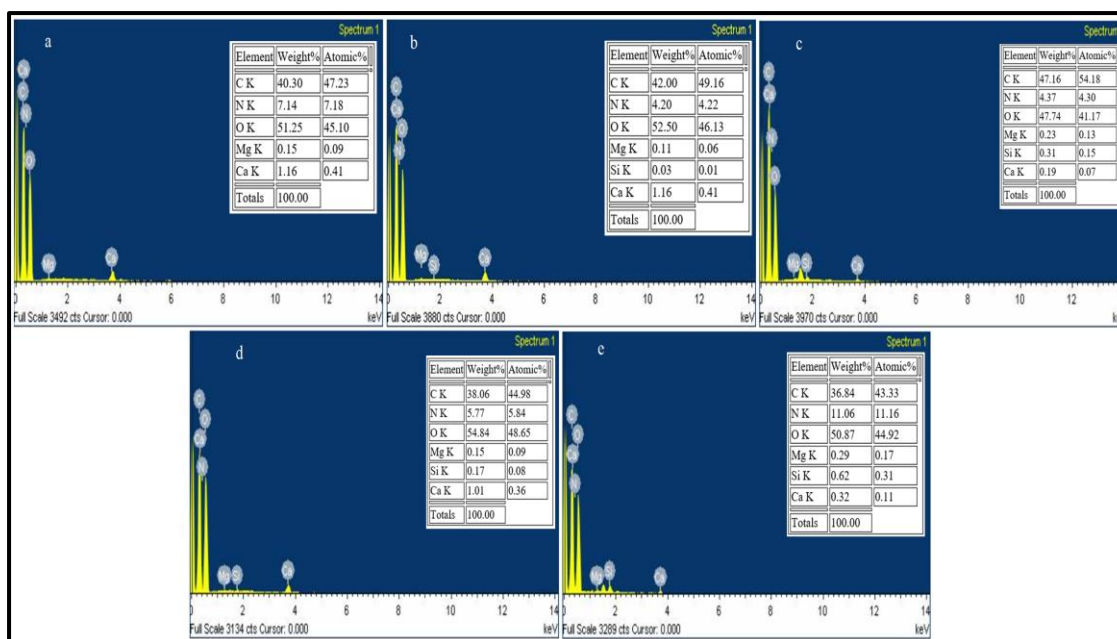


Figure. 3.2.10. EDXA spectra of (a) fresh *Sāncipāt* and after immersing in (b) distil water, (c) 5% aqueous cetrimide, (d) isopropyl alcohol, and (e) 5% thymol in water-ethanol mixture.

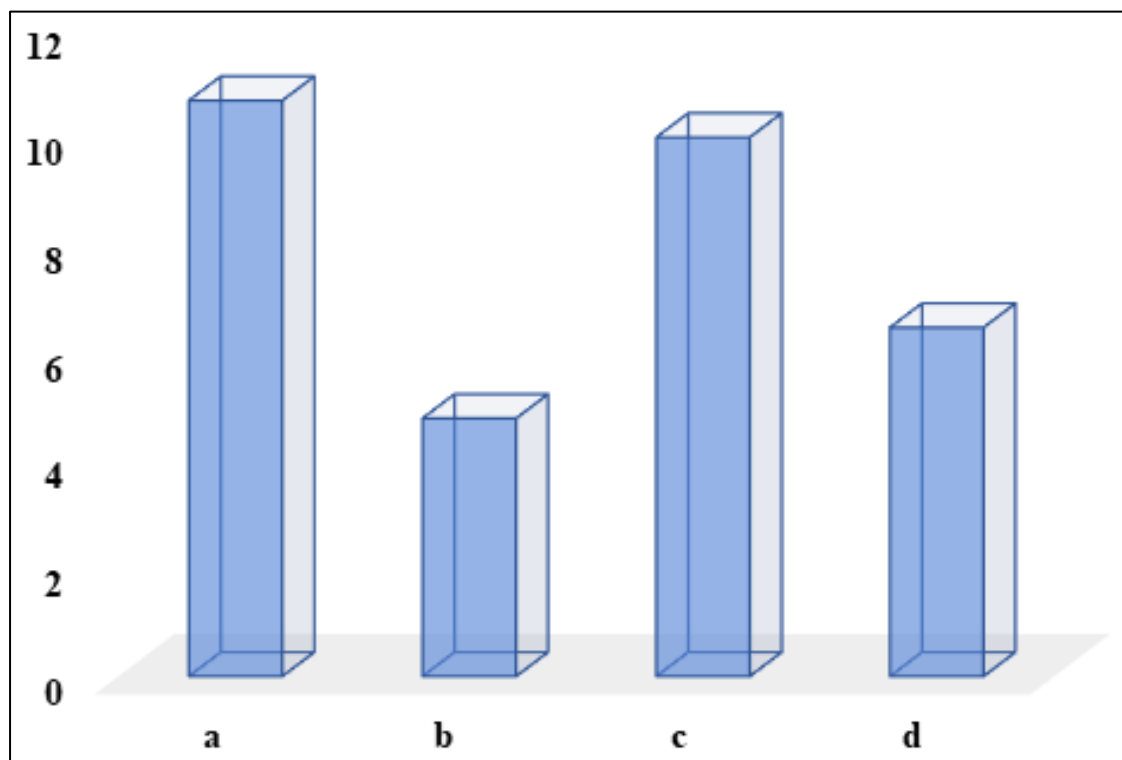


Figure. 3.2.11. Percent weight loss of old *Sāncipāt* after soaking for 2h in (a) distilled water, (b) 5% aqueous cetrimide, (c) isopropyl alcohol and (d) 5% thymol in water-ethanol mixture.

3.2.2.7. Analysis of mechanical properties

The mechanical characteristics of the old treated and untreated *Sāncipāt*, such as tensile strength, toughness, and elongation break, were assessed on universal testing apparatus (Figure. 3.2.12). Similarly, we checked the mechanical strength properties of freshly prepared *Sāncipāt* under the same environment. Untreated, freshly prepared *Sāncipāt* was found to have a toughness of 11.38 Mega J/m³. The tensile strengths of freshly prepared *Sāncipāt* treated with distil water, cetrimide, isopropyl alcohol, and thymol are 5.25 Mega J/m³, 4.78 Mega J/m³, 7.92 Mega J/m³, and 3.79 Mega J/m³, respectively. Freshly prepared *Sāncipāt* that has been thymol-treated is found to have the lowest toughness. The freshly prepared *Sāncipāt* that has not been treated is found to have a tensile strength of 68.34 MPa. In contrast, freshly prepared *Sāncipāt* treated with distil water, cetrimide, isopropyl alcohol, and thymol has a tensile strength of 43.92 MPa, 57.75 MPa, 99.82 MPa, and 72.19 MPa, respectively. The freshly prepared *Sāncipāt* with distil water, cetrimide, isopropyl alcohol, and thymol treatments has an elongation break of 15.20%, compared to the freshly prepared *Sāncipāt* without these treatments, which has an elongation break of 14.88%. The lowest elongation breaks in freshly prepared *Sāncipāt* treated with cetrimide shows low ductility in nature. The tensile strength of freshly prepared *Sāncipāt* treated with isopropyl alcohol, and thymol is higher than that of untreated freshly prepared *Sāncipāt*, but the toughness is significantly reduced.

3.2.3. Conservation based on traditional recipe of *Sāncipāt*

It has been observed from the above observations that the physicochemical and mechanical characteristics of old as well as fresh *Sāncipāt* changes after the application of various common conservative aids, including distill water, cetrimide, isopropyl alcohol, and thymol. Therefore, one needs to explore the remaining options for conservation of *Sāncipāt* manuscript. A method, based on the traditional method of preparation of *Sāncipāt* without using any other conservative chemicals, should be appropriate for restoration and conservation of *Sāncipāt* manuscripts enabling preservation and reading in ordinary hot and humid conditions in villages and monasteries of Assam. The proposed method uses only the fungus and insect-repellant pigments of *Hāitāl* and *Hengul* with *Bael* gum as done traditionally during preparation of *Sāncipāt*. As water is used in preparation of both *Sāncipāt* and *Mahī*, we have chosen to apply *Hāitāl* and *Hengul* with water and *Bael* gum, of course, with subsequent drying of the *Sāncipāt* as quickly as possible. We have also chosen to apply a La-coating on the *Sāncipāt* finally as is done

traditionally during preparation of *Sāncipāt* manuscript. Section 1.2.4.1 of the introduction already makes mention of the suggested approach.

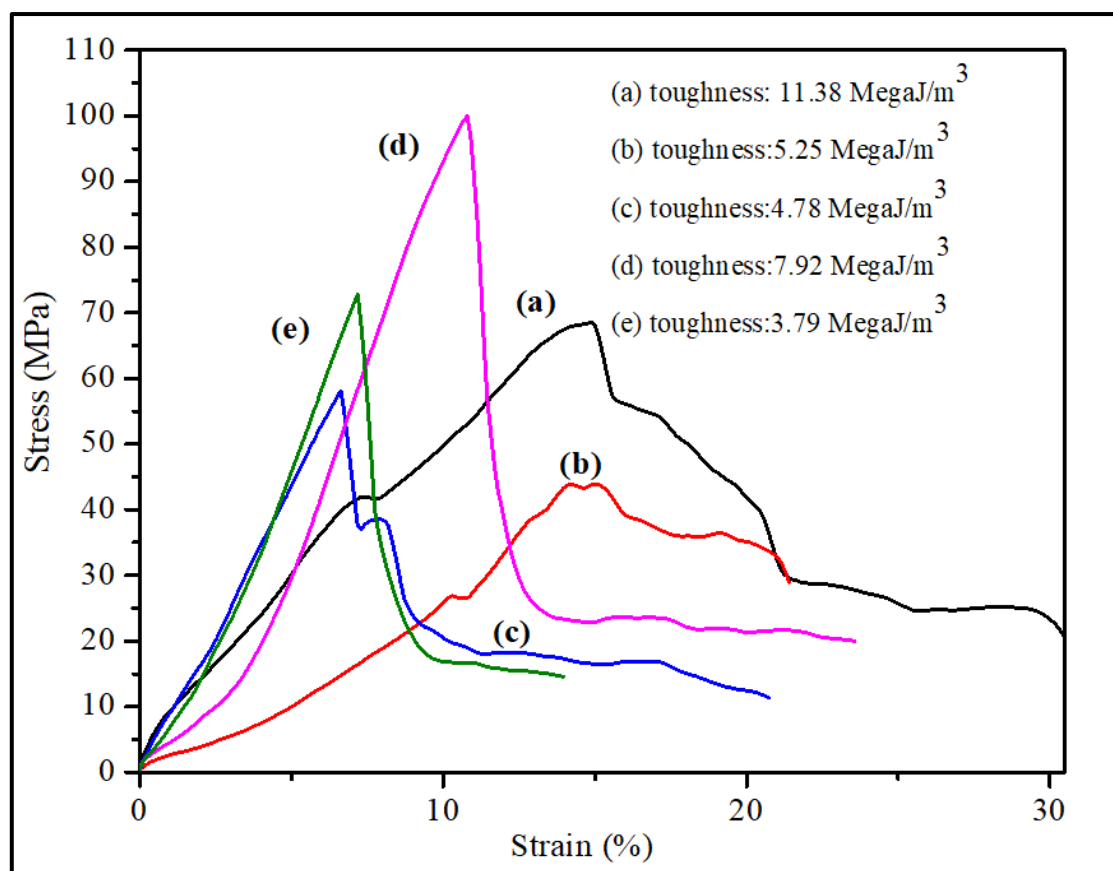


Figure. 3.2.12: Mechanical strength analysis by UTM of old *Sāncipāt* (a) before and after treatment with (b) distilled water, (c) 5% aqueous cetrimide, (d) isopropyl alcohol and (e) 5% thymol in water ethanol.

3.2.3.1 Physical cleaning

The above analysis has shown that isopropyl alcohol, thymol and cetrimide, are not suitable for conservation of *Sāncipāt* manuscripts as they affect physicochemical, structural and mechanical properties of *Sāncipāt*. Excess exposure to water also can damage *Sāncipāt* manuscript. It has been seen that isopropyl alcohol used for cleaning of *Sāncipāt* manuscripts for conservation purpose conserved by National Manuscript Mission and later by others have in fact caused crumbling of folios and spread of black dirt from the edges and the central hole (Nābhi) of the folios (Figure. 3.2.13). So, a mild rubbing of the free spaces of the folios with mild brushing is preferable to cleaning with chemicals.

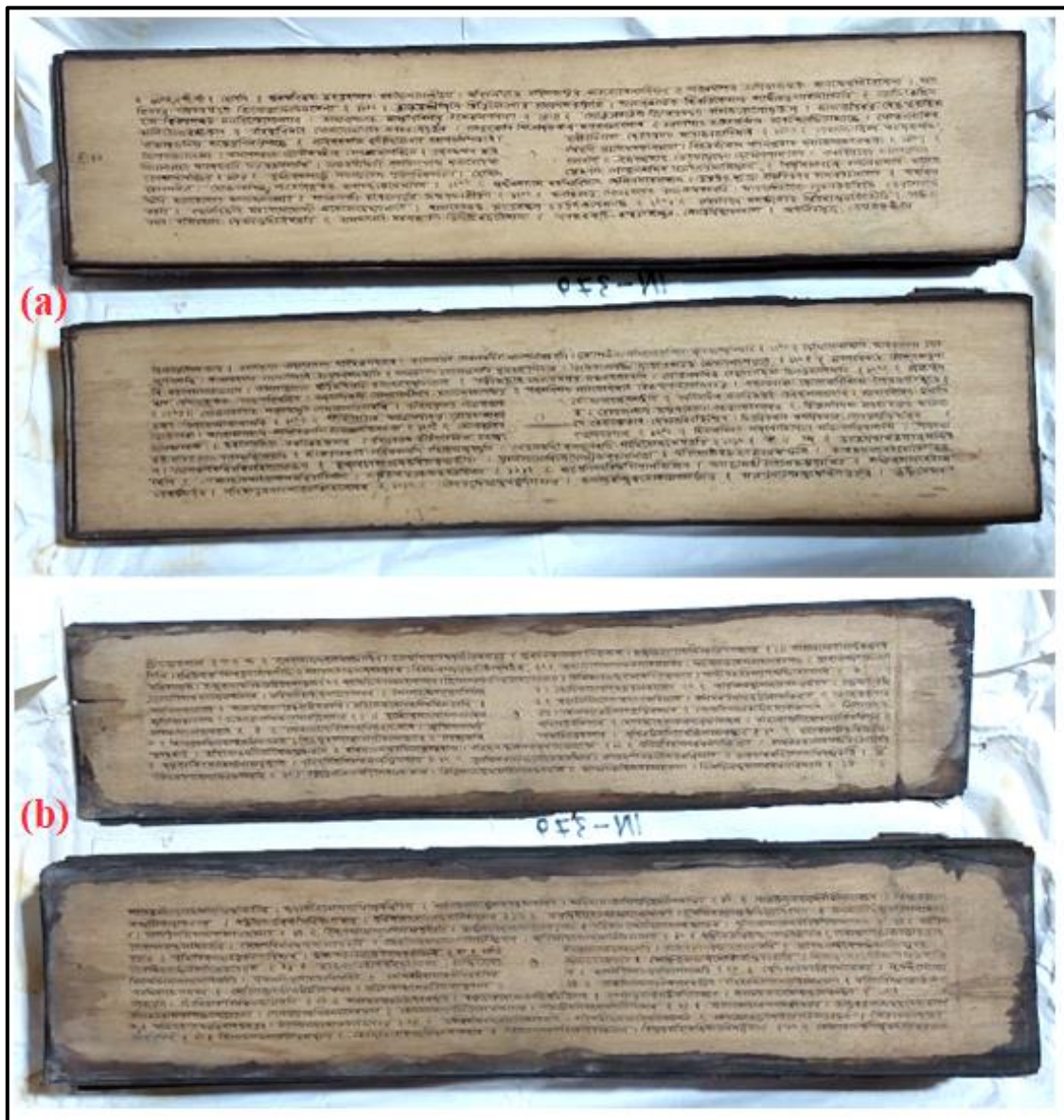


Figure. 3.2.13: *Sāncipāt* folios (a) without cleaning using isopropyl alcohol and *Sāncipāt* folios from the same manuscripts (b) after cleaning using isopropyl alcohol by National Manuscript Mission. The manuscript, *Dasham*, copied in 1801 AD (1723 Saka) and is preserved at home of Mr. Jagot Duwaria, Mohkina village, Majuli, Assam.

3.2.3.2. Mending with freshly prepared *Sāncipāt*

Sāncipāt manuscripts are often seen with some folios repaired at the time of preparation by pasting pieces of *Sāncipāt* (Figure. 1.8). Pasting of freshly prepared *Sāncipāt* for mending of torn or broken folios in this traditional way is preferable over Japanese paper also because the fresh *Sāncipāt* can be made fungus-resistant if degummed in presence of *Tutia* during its preparation [123].

3.2.3.3. Application of Hengul-Hāitāl

Fungal and insect attack on papyrus and paper manuscripts is well known [237,238] but *Sāncipāt* prepared by following complete traditional procedure including application of a thin coating of *Hāitāl* pigment on the folios before writing and thin strips on the borders and around the central hole (*Nābhi*) with *Hengul* pigment (Figure. 1.9) are, in general, not attacked by fungi and insects even for centuries (Figure. 1.6). However, the *Sāncipāt* manuscripts whose folios were not coated with *Hāitāl* during preparation, probably because it was not easily available, are attacked by fungi and insects (Figure .3.2.14). *Hāitāl* and *Hengul* protect *Sāncipāt* from fungi and insects in addition to markedly increasing glossiness of *Sāncipāt* with a golden-yellow look [7,124].



Figure. 3.2.14: A *Sāncipāt* manuscript, Adi Dasham, in traditional wooden box (A), outside the box (B) and opened (C), prepared in 1868 AD (1791 Saka) preserved at Bor Alengi Bogi Ai Satra, Jorhat, Assam, and some damaged manuscripts (D) received from Mr. Rupam Sarma, Tezpur.

Use of *Hāitāl* and *Hengul* in *Sāncipāt* and painting of woodcarvings followed by *Lā-charōwa* was a centuries-long tradition in Assam [15]. Interestingly, application of *Hāitāl* and *Hengul* for conservation of *Sāncipāt* manuscript also might have been an old traditional practice Figure. 3.2.15. A worn-out *Sāncipāt* manuscript, which had not been coated with *Hāitāl* and *Hengul* initially during preparation, was found to be conserved at

a later stage by applying *Hāitāl* in the free spaces and *Hengul* on the borders and around the *Nābhi* of the folios (Figure. 3.2.15).



Figure. 3.2.15: Evidence of the application of *Hengul-Hāitāl* for conservation at a later stage (undated) on a 300-year-old *Sāncipāt* manuscript, *Adikanda Ramayana* of Shri Madhavdev copied by Sri Ramratan Devasarma in 1826 AD is preserved at Kochbihar State Library. The folios were not coated with *Hāitāl-Hengul* initially and have been found to be conserved by applying *Hāitāl-Hengul* later before collection of the manuscript for the library. Kochbehar in Assam before British occupation. Photo credit: Indranil Gayan.

A relevant issue here is whether to use antifungal and insect-repellant *Hāitāl* and *Hengul* in conservation of *Sāncipāt* manuscripts. *Hāitāl* has been being used traditionally for centuries in make-up of dancer in Kathakali dance, a popular classical dance form of India, without any known toxicity. *Hāitāl* has also been being used for lightening of dark skin for centuries and its only prolific use in cosmetics has been reported to pose risk to human health [239]. Vermilion, powdered *Hengul*, also has been being used traditionally by married Hindu women for millennia as *Bindi* without any known toxicity. Thus, *Hāitāl* and *Hengul* can be applied on *Sāncipāt* with careful handling using gloves and masks to avoid a minor health risk for restoration and conservation of *Sāncipāt* manuscripts for preserving them under ordinary conditions where passive environment is impractical. A final traditional *Lā*-coating on the folios also protects the readers from contamination of hands with *Hāitāl* and *Hengul* during handling of the manuscripts (Figure. 1.7).

3.2.3.4. Application of *Lā*-coating

Use of *Lā* was a very old practice in India since the Vedic time [240]. Though *Lā*-coating is somewhat similar to varnishing, in *Lā*-coating only pure herbal *Lā* dissolved in hot spirit is applied on written and/or illustrated *Sāncipāt* as a very thin coating using a white cotton cloth (Figure. 1.9b). A thin *Lā*-coating was found to markedly improve mechanical properties of freshly prepared *Sāncipāt* by increasing tensile strength from 68.34MPa to 434MPa and toughness from 41.89MegaJ/m³ to 11.38MegaJ/m³ (Figure. 3.2.4D). *Lā*-coating being water-resistant also protects the manuscript from humidity in addition to resisting erosion of the inner coating of *Hāitāl* and *Hengul*. *Lā*-coating *Sāncipāt* manuscript helps in retaining its glaze for centuries unlike discoloration observed after lamination (Figure. 1.9). Lamination has been alleged to have discolored and harmed several *Sāncipāt* manuscripts in Assam including a precious century-old, illustrated manuscript, *Adi Dasham*, preserved at Bali Satra in Nagaon, Assam. Thus, application of *Lā*-coating in conserving *Sāncipāt* manuscripts has manifold benefits.

3.2.4. Results of piloting of the proposed method of conservation

The proposed method has been piloted thrice in the form of three week-long workshops during 2021-22 which were participated by a scholar of writing and painting of traditional manuscript of Assam, some practitioners of the traditional art forms involving *Hengul*-*Hāitāl*, and some learners participated in the workshops with the authors. The proposed method has been piloted thrice in the form of three workshops held at Kaliabor College,

Nagaon, Assam during 20-26 February 2021, at Department of Chemical Sciences, Tezpur University during 24-29 November 2021 and at Auniati Satra, Majuli during 9-15 March 2022. A scholar of writing and painting of traditional manuscript of Assam, Dr. Naren Kalita, from Nagaon, some practitioners of the traditional art involving *Hengul-Hāitāl* in some ways, namely, Mr. Niron Kotoki, Mr. Prabin Bora and Mr. Gobinda Borah Ozah, all from Auniati Satra, a vaishnavite monastery in Majuli, Mr. Indranil Gayan and Mr. Chittaranjan Borah from Puranigudam, Nagaon, and some learners participated in the workshops with the authors.

Thirteen old *Sāncipāt* manuscripts have been conserved at the piloting workshops including restoration of some torn and partially damaged folios (Figure. 1.9c, Figure. 3.2.16). The piloting helped us in finer improvement of the method, e.g., in matching the color of *Hāitāl* with the old manuscript color by mixing a little of *Hengul* and *Nīl* (Indigo, Prussian blue herbal pigment used traditionally in combination with *Hengul-Hāitāl*) as can be seen in Figure. 1.9. The improvement in the glossiness of representative folios of three *Sāncipāt* manuscripts before and after complete conservation measured at 20°, 60° and 80° angles at areas newly coated with *Hāitāl* is shown in Figure. 3.2.17. The increase in glossiness after conservation may be attributed to application of *Hāitāl* and *Lā*.



Figure. 3.2.16: Folios of a 2 feet 6 inches long *Sāncipāt* manuscript, probably the longest *Sāncipāt* manuscript, before (a) and after (b) conservation at Auniati Satra, Majuli.

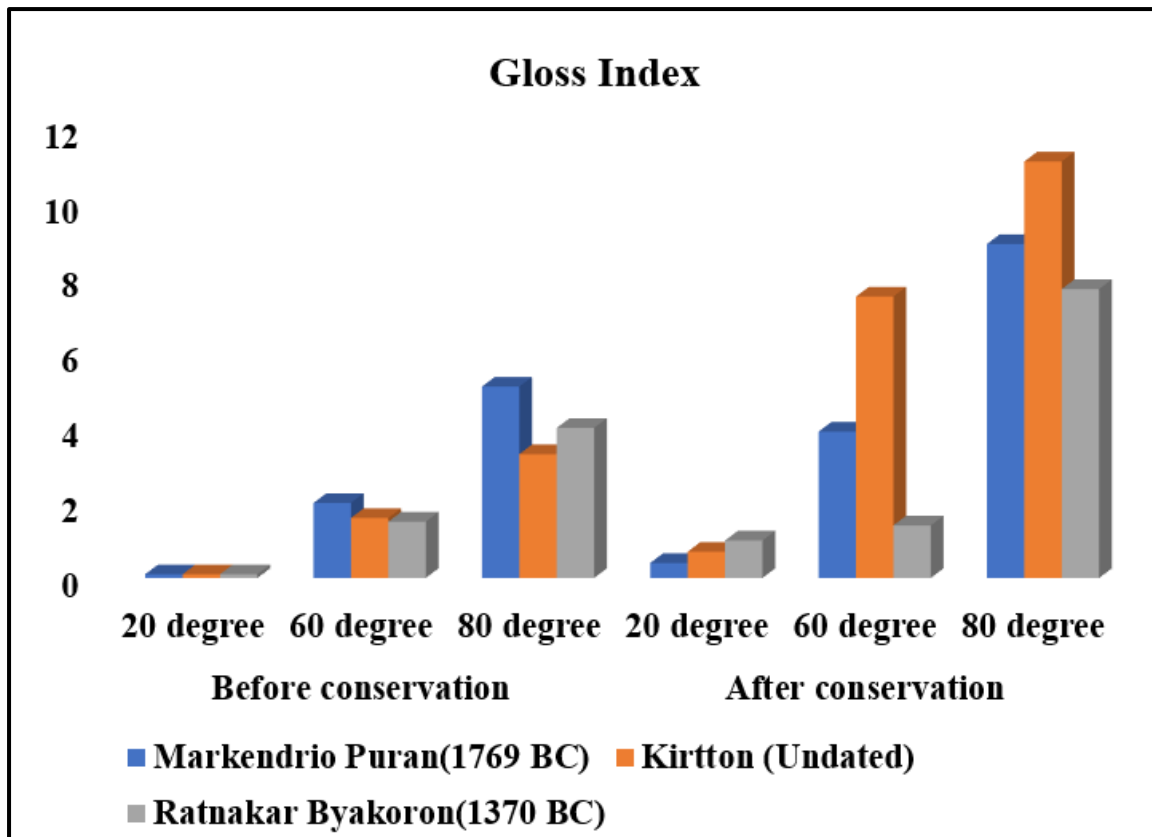


Figure. 3.2.17: Glossiness of representative folios of three *Sāncipāt* manuscripts measured at 20°, 60° and 80° angles before and after complete conservation with *Lā-charowā* at areas newly coated with *Hāitāl*.

3.2.4.1. Comparison of thermal properties

The weight loss percentage during the temperature range of 0-160 °C is almost similar in case of both fresh and *Hengul-Hāitāl* aided *Sāncipāt* (Figure. 3.2.18). However, this weight loss percentages are less in case of *Hengul-Hāitāl* aided fresh *Sāncipāt* in the temperature range between 180-400 °C and 400-550 °C, which indicates that *Hengul-Hāitāl* prolongs the life of existence of fresh *Sāncipāt* (Table 3.2.1).

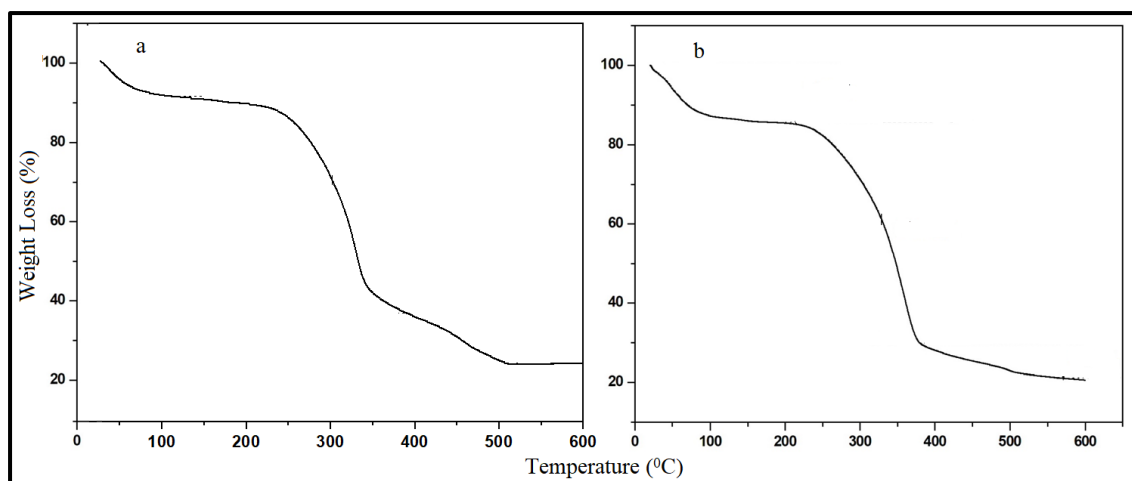


Figure. 3.2.18: TG patterns of fresh *Sāncipāt* and *Hengul-Hāitāl* aided fresh *Sāncipāt*.

3.2.4.2. Comparison of C, H and N proportion

It can be seen from the CHN analyzer that the carbon and hydrogen percentages in case of both fresh *Sāncipāt* and *Hengul-Hāitāl* aided *Sāncipāt* are almost similar. The number percentages of C (31.83), H (5.66) in fresh *Sāncipāt* and C (31.93), H (5.30) in *Hengul-Hāitāl* aided fresh *Sāncipāt*. Nitrogen is absent in both samples. This result indicates the acceptability of *Hengul-Hāitāl* as a conservative aid to prolongs the life of fresh *Sāncipāt*.

Table 3.2.1: Mass loss percentage of the fresh *Sāncipāt* and *Hengul-Hāitāl* aids *Sāncipāt* in thermal analysis

Sample	Mass loss percentage in the temperature range (°C)		
	0-160	180-400	400-550
Fresh <i>Sāncipāt</i>	12.09	63.26	13.28
<i>Hengul-Hāitāl</i> treated <i>Sāncipāt</i>	14.30	55.60	8.77

3.2.5. Summary of the section

This first study on conservation of *Sāncipāt* manuscripts reveals some interesting traditional knowledge which contributed to longevity of the manuscripts. Treatment of old partially damaged *Sāncipāt* with some commonly used solvent and chemicals, viz.,

isopropyl alcohol, thymol and cetrinide, has shown marked changes in physicochemical properties, structure and mechanical strength of lignocellulosic *Sāncipāt*. Even a prolonged exposure to water also causes such changes in *Sāncipāt*. On the other hand, some treatments of *Sānci* bark during the traditional preparation of *Sāncipāt*, viz., partial de-gumming in presence of *Tutia* and application of a thin coating of antifungal and insect repellent *Hāitāl-Hengul* pigments protect the folios from fungi and insects. *Lā-charowā*, a traditional way of varnishing, finally imparts physical strength and water resistance to the folios in addition to protecting the readers from exposure to *Hāitāl* and *Hengul*. *Bael* gum used in mending of *Sāncipāt* does not leave any stain on the folio unlike many other traditional natural gums. Though *Mahī*, a unique traditional herbal ink used in writing *Sāncipāt*, is prepared in water and is as such water soluble, the ink has a strong adhesion on the folio and is hardly affected by water. Preservation of *Sāncipāt* manuscript between two flat wooden plates coated with *Hāitāl* avoids kinking or bending of the folios. A novel method of restoration and conservation of *Sāncipāt* manuscripts, based on the traditional method of their preparation avoiding harmful chemicals and with minimum exposure to water. The method involves mild physical cleaning, mending with freshly prepared *Sāncipāt* using *Beal* gum, application of *Hāitāl-Hengul* with matched color, application of *Lā* and keeping the manuscript between two flat wooden plates coated with *Hāitāl* and rapping with red cotton cloth. Results of piloting of the proposed method of conservation on eleven *Sāncipāt* manuscripts show that the method can be employed to save tens of thousands of precious *Sāncipāt* manuscripts existing in museums, Satras and villages in Assam from natural damage.

In addition of, the present study reveals some interesting effects of the four common conservative chemicals, namely, water, thymol, isopropyl alcohol and cetrinide on fresh *Sāncipāt* also. The UV-visible spectra of water after soaking of fresh *Sāncipāt* has shown a weaker peak compared to other solvents indicating that less cellulose and hemicellulose were leached into water compared to the other solvents. The FTIR spectra of *Sāncipāt* samples recorded after treatment with the solvents suggest that thymol, a commonly used conservative chemical, causes the maximum damage to the *Sāncipāt* among all four solvents which have been studied. Treatment with isopropyl alcohol, and thymol increases the tensile strength of freshly prepared *Sāncipāt* but reduces the toughness. Weight loss of *Sāncipāt* after treatment indicates leaching of lignin and hemicellulose from freshly prepared manuscripts. However, this weight loss decreases after application of *Hengul-Hāitāl* indicating a positive effect of *Hengul-Hāitāl* to the

Sāncipāt. Thus, the present study reveals that treatment of fresh *Sāncipāt* with the common conservative chemicals causes physicochemical and mechanical changes to *Sāncipāt* such as destruction of lignocellulosic properties, fluctuation of crystallinity, weight loss and reduction of toughness.

3.3. Section-3: Traditional Science in pigments and recipe of *Hengul-Hāitāl* painting*

This section of my research focused on the studying of the traditional science involved in the tradition of *Hengul-Hāitāl* painting including analysis of the ingredients, formulations, application, and effects of the paints which is expected to help in developing a suitable method for restoration of such partially damaged heritage woodcarvings reinstating their original look. I also tried to characterize various formulations of the paints including synthetic and natural binder through physicochemical analyses including Hunter color analysis, zeta potential measurements, glossiness, and hiding power measurements.

3.3.1. Physicochemical characterization of the pigments

A physicochemical characterization of the natural pigments used in the study has been presented here.

3.3.1.1. Morphological and elemental analysis

SEM images of *Hengul*, *Hāitāl*, *Nīl* and *Kharimāti* (Figure. 3.3.1) show the morphological structures of the pigments. The particles of *Hengul*, *Hāitāl* and *Nīl* have been found to be distinctly distributed while that of the particles of *Kharimāti* have been found to be spread smoothly and due to its cohesiveness and agglomeration, accurate particle size determination was not possible [241]. This is evidenced by the surface plot of all the samples obtained using image J software. The particles of *Hāitāl* and *Hengul* are spread out almost equally. On the other hand, the size of the particle is the clearest and largest in *Nīl*. Figure. 3.3.1 also includes the histogram of particle size distribution obtained using image J software. The mean length of the particles of *Hāitāl*, *Hengul* and *Nīl* were found to be 12.50 μm , 11.58 μm and 19.26 μm respectively.

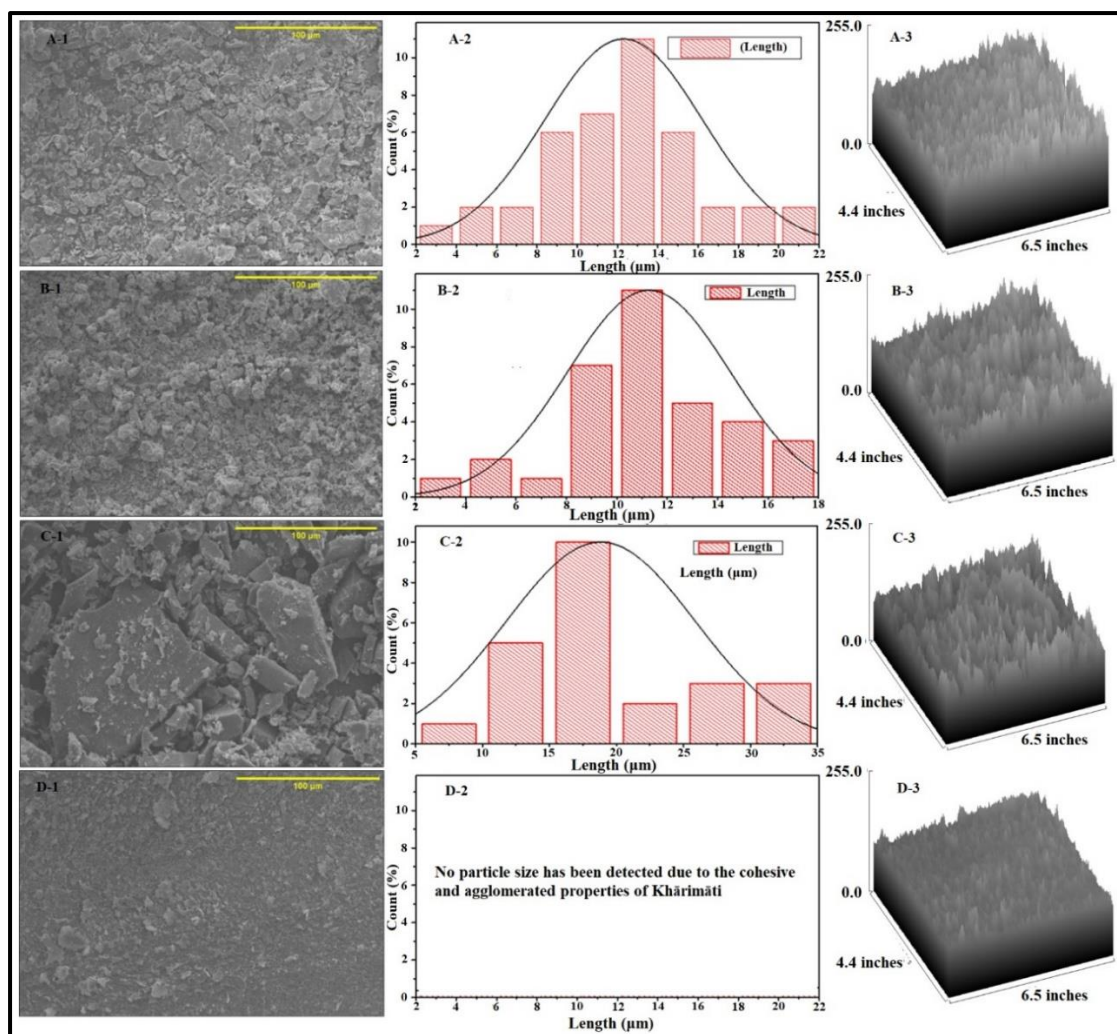


Figure. 3.3.1: SEM images of (A-1) *Hāitāl*, (B-1) *Hengul*, (C-1) *Nīl* and (D-1) *Khārimāti* at 100 μm scale; Histogram diagram of particle size distribution of (A-2) *Hāitāl*, (B-2) *Hengul*, (C-2) *Nīl* and (D-2) *Khārimāti*; surface plot of (A-3) *Hāitāl*, (B-3) *Hengul*, (C-3) *Nīl* and (D-3) *Khārimāti*.

The atomic percentage of different elemental composition in different pigment can be seen in the EDX analysis results presented in Figure. 3.3.2. From the EDX spectra shows the presence of 32.04:23.04 atomic percentage ratio of As to S in the sample of *Hāitāl* which is higher than the ideal atomic percentage ratio of 2:3 of the two elements in As_2S_3 . The atomic percentage of Si, O and C present in atomic percentages of 0.89%, 7.25% and 36.78% in the sample of *Hāitāl* suggest presence of considerable amounts of impurities containing these elements. This correlates with the moderate crystallinity of *Hāitāl* obtained from XRD. Similarly, EDX of *Hengul* (Figure. 3.3.2b) shows 11.77:35.75 atomic percentage ratio of Hg to S in the sample of *Hengul* which is lower than the ideal 1:1 atomic percentage ratio in HgS . Here, the presence of elements C, O in atomic

percentages 41.92 and 9.55, respectively, and also the presence of trace amount of Fe and As in atomic percentages of 0.03 and 0.98, respectively, again indicate presence of considerable impurities containing these elements in the sample of *Hengul*. The presence of the impurities is also reflected in the XRD data of *Hengul*. The atomic percentage of different elements present in *Nīl* is found from the EDX spectra (Figure. 3.3.2c) are C (53.28%), N (6.50%), O (15.30%), Fe (24.91%). The observed atomic ratios of C:N:O of 52.28:6.50:15.30 in the sample of *Nīl* is far from the ideal atomic ratios of C:N:O of 8:1:1 to match with the molecular formula of $C_{16}H_{10}N_2O_2$ of indigo. This suggests presence of impurities containing iron probably on the forms of iron cyanide or iron oxide in the *Nīl* sample. *Khārimāti* has shown the presence of C, O, Al and Si in the atomic percentages of 28.58, 59.35, 5.40 and 6.67 which commensurate with the clay containing aluminosilicate with metal carbonates and oxides.

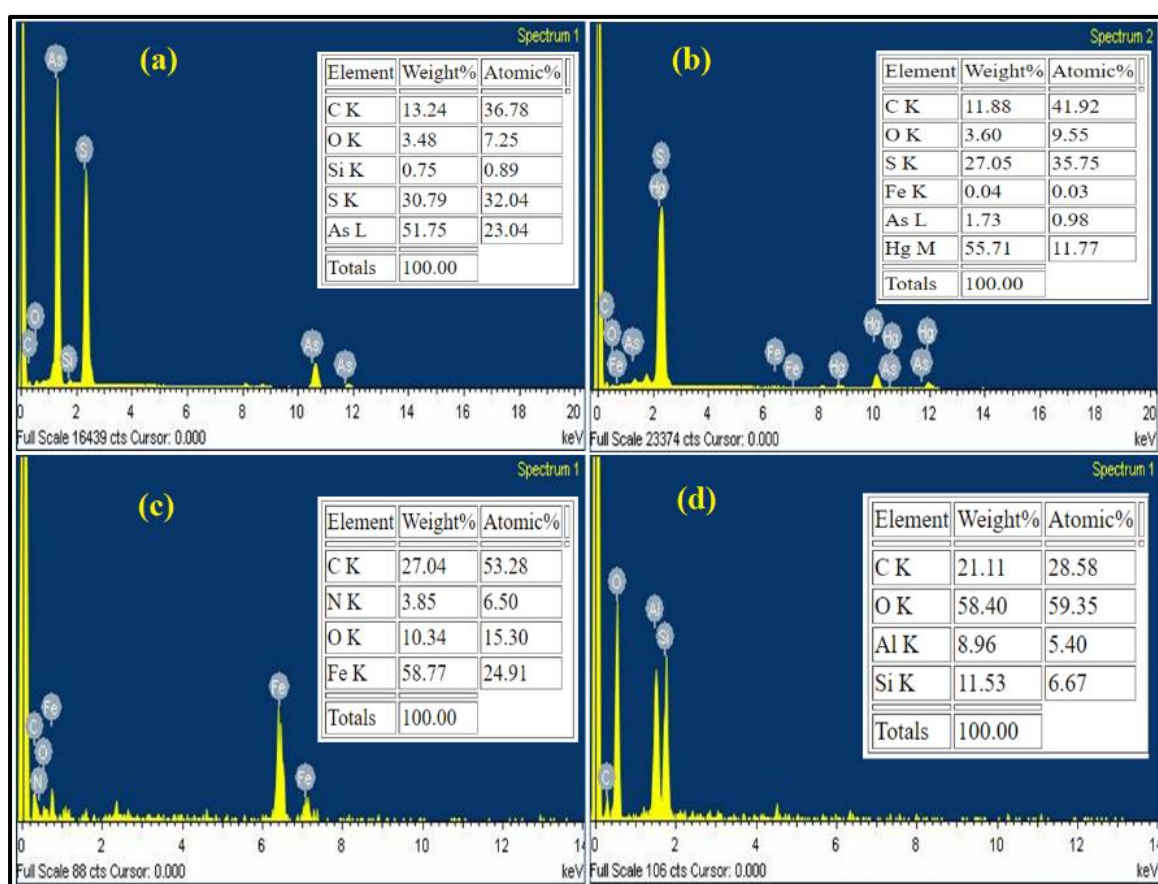


Figure. 3.3.2. EDX analysis of (a) *Hāitāl*, (b) *Hengul*, (c) *Nīl* and (d) *Khārimāti*.

3.3.1.2. FTIR Analysis

The FTIR spectra of *Hāitāl*, *Hengul*, *Nīl* and *Khārimāti* are shown in Figure. 3.3.3. There is hardly any FTIR spectra of the natural yellow orpiment or *Hāitāl* reported in the literature. The small peaks seen in the 1100-500 cm^{-1} range in the FTIR spectra of *Hāitāl* (Figure. 3.3.3A) indicate the presence of some arsenic containing compound [242]. The peak at 1098 cm^{-1} in Figure. 3.3.3A indicates the presence of strong S=O stretching frequency [243] while the peak at 650-950 cm^{-1} range indicate the presence of As-O stretching frequency possibly due to aerial oxidation of surface molecules of As_2S_3 [244,245] [242,246]. On the other hand, cinnabar of HgS is not expected to show any major characteristic IR absorption [40]. However, some absorption bands have been observed due to the presence of moisture and other impurities. The small peak at 1406 cm^{-1} in Figure. 3.3.3B indicate the presence strong S=O stretching frequency of some sulfate group associated with mercury containing compound [244,247] caused by ariel oxidation of HgS. Similarly, the peak at 1030 cm^{-1} in Figure. 3.3.3B indicates the presence of Si-O stretching frequency [248]. An absorption at 1639 cm^{-1} in Figure. 3.3.3B indicates the presence of calcite as impurity [248]. The FTIR spectra of *Nīl* or Indigo (Figure. 3.3.3C) have one sharp and broad peak in the 3100-3500 cm^{-1} range which indicates the presence of N-H stretching of 20 amines. Similarly, the peak at 1586 cm^{-1} indicates the presence of C=C stretching frequency. The peak at 1350-1000 cm^{-1} indicates the presence of C-N stretching of amines. Presence of some C-H stretching frequency of some aromatic compound is indicated by the presence of a peak at 900-700 cm^{-1} [249]. Two medium sharp peaks at 3688 and 3622 cm^{-1} seen in the FTIR spectra of *Khārimāti* (Figure. 3.3.3D) indicate the presence of alcoholic O-H stretching and the peak found in 1629 cm^{-1} may be attributed to the presence of medium physiosorbed H-O-H stretching frequency [250,251]. The peaks in the range of 1112 cm^{-1} to 779 cm^{-1} as shown in Figure. 3.3.3D may attributed to strong mono substituted Si-O stretching frequency [250,252].

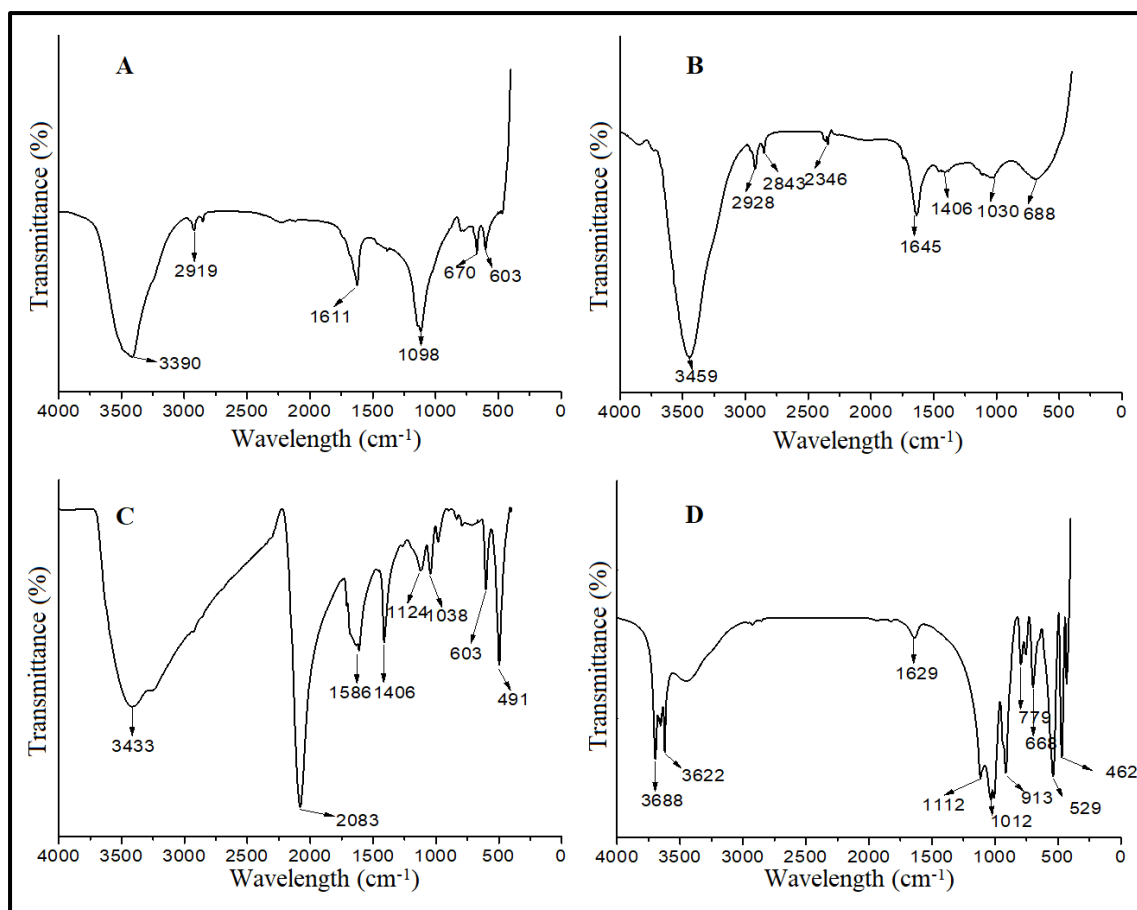


Figure. 3.3.3: FTIR spectra of (a) *Hāitāl*, (b) *Hengul*, (c) *Nīl* and (d) *Khārimāti*.

3.3.1.3. Raman analysis

Raman spectroscopy has been used to obtain information about the IR-inactive vibrational modes of the constituents of *Hāitāl*, *Hengul* and *Nīl* [56]. For all these samples, the excitation was at 514nm with same laser power of 10mW and different exposure time. Figure. 3.3.4A shows four strong Raman bands in the range of 400-100 cm^{-1} [253,254]. The peaks at 191 cm^{-1} and 145 cm^{-1} indicates the lattice vibrations of the compound and proves the presence of some arsenic containing sulphide compound (Figure. 3.3.4A) [253-255]. Some strong and broad peaks are observed in the range of 500-100 cm^{-1} in Figure. 3.3.4B. The peak at 337 cm^{-1} indicates the presence of Hg-S stretching frequency which clearly gives the evidence that mercuric sulphide, commonly known as Cinnabar is present [252,254,256]. On the other hand, the peak observed at 493 cm^{-1} indicates the presence of $\nu(\text{S-S})$, $\nu(\text{S-O-S})$ and $\nu(\text{Hg-O})$ stretching frequency [248,254,256,257]. In Figure. 3.3.4C, we have seen many characteristic peaks of indigo or *Nīl* within 1000-100 cm^{-1} . The position of the broad peak we see in the 949 cm^{-1} range refers to $\nu(\text{C-O-O})$. The Raman shift seen in the 727 cm^{-1} -534 cm^{-1} range indicates the

presence of aliphatic $\nu(\text{C-S})$ and $\nu(\text{C-Br})$, respectively [254]. Due to the presence of cohesive and agglomeration properties in *khārimāti*, Raman peaks could not be detected.

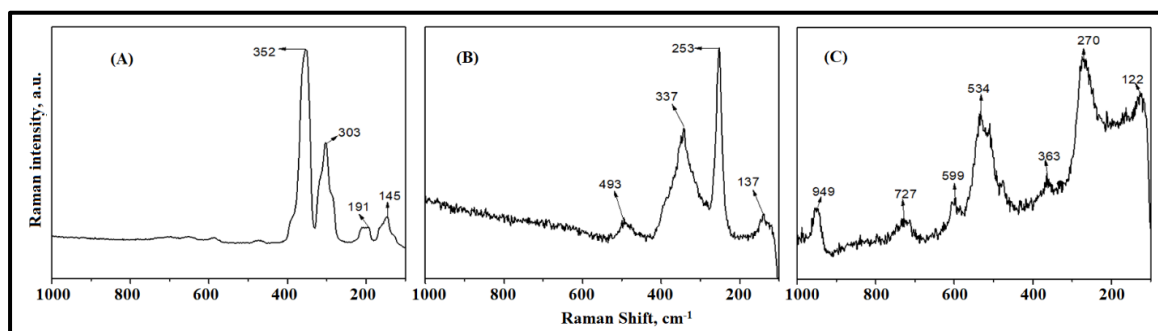


Figure. 3.3.4: Raman spectra for (A) *Hāitāl* (Excitation was at 514 nm exposure time = 1s and laser power = 10mW), (B) *Hengul* (Excitation was at 514 nm exposure time = 2s and laser power = 10mW) and (C) *Nīl* (Excitation was at 514 nm exposure time = 4s and laser power = 10mW).

3.3.1.4. XRD analysis

The XRD spectra of the pigments of *Hāitāl*, *Hengul* and *Nīl* and the p-XRD peak interpretation from Pcpdwin Software have been shown in Figure. 3.3.5. The moderate crystallinity of the three pigments, estimated to be 38%, 28% and 32%, respectively, may be attributed to impurities in the natural pigments (Figure. 3.3.5A-C). Two sharp peaks at 18.51° , 52.36° observed for *Hāitāl* (Figure. 3.3.5A, D) can be assigned to (020) and (051) reflections, respectively. The dense peak observed between 28.26° to 43.75° ranges correspond to the monoclinic crystal system of *Hāitāl* [258-260] [Figure. 3.3.5A, D]. The d-spacing of the highest peak is 4.79Å whereas for the smallest one is found to be 1.74Å . A comparison with JCPDS Card 00-044-1419 shows that the sample correspond to the As_2S_3 [258-260]. Similarly, we found two very sharp peaks at 26.46° and 31.43° for *Hengul* (Figure. 3.3.5B, E). These two peaks correspond to (101) and (012) reflection and 3.35Å and 2.86Å d-spacing. In addition to these, some comparatively sharp peaks were observed at 28.13° , 43.96° , 44.72° , 46.09° , 51.75° , 52.69° , 54.82° angle which correspond to (003), (110), (104), (111), (021), (113) and (015) reflection. A comparison with JCPDS card 00-080-2192, the sample was found to corresponded to the hexagonal crystal system of HgS , i.e., cinnabar [261,262]. Four major peaks were observed in the XRD spectra for *Nīl* as shown in Figure. 3.3.5C, F corresponding to the angles of 17.73° , 24.81° , 35.21° , 39.71° . These sharp peaks are associated with the (200), (220), (400) and

(420) reflections and 5.06 Å, 3.59 Å, 2.54 Å and 2.27 Å d-spacing. After comparing this data with the JCPDS card 00-051-0361 we found that the sample correspond to a cubic crystal of iron cyanide hydrate [263]. The remaining angles were associated with 1.84 Å (024), 1.69 Å (116), 1.60 Å (122), 1.41 Å (125) and 1.34 Å (208) d-spacing with reflections. After comparing these data with the JCPDS card 00-033-0664 we may say that the compound is also associated with rhombohedral crystal known as iron oxide (Fe_2O_3) which is commonly known as hematite mineral [264,265].

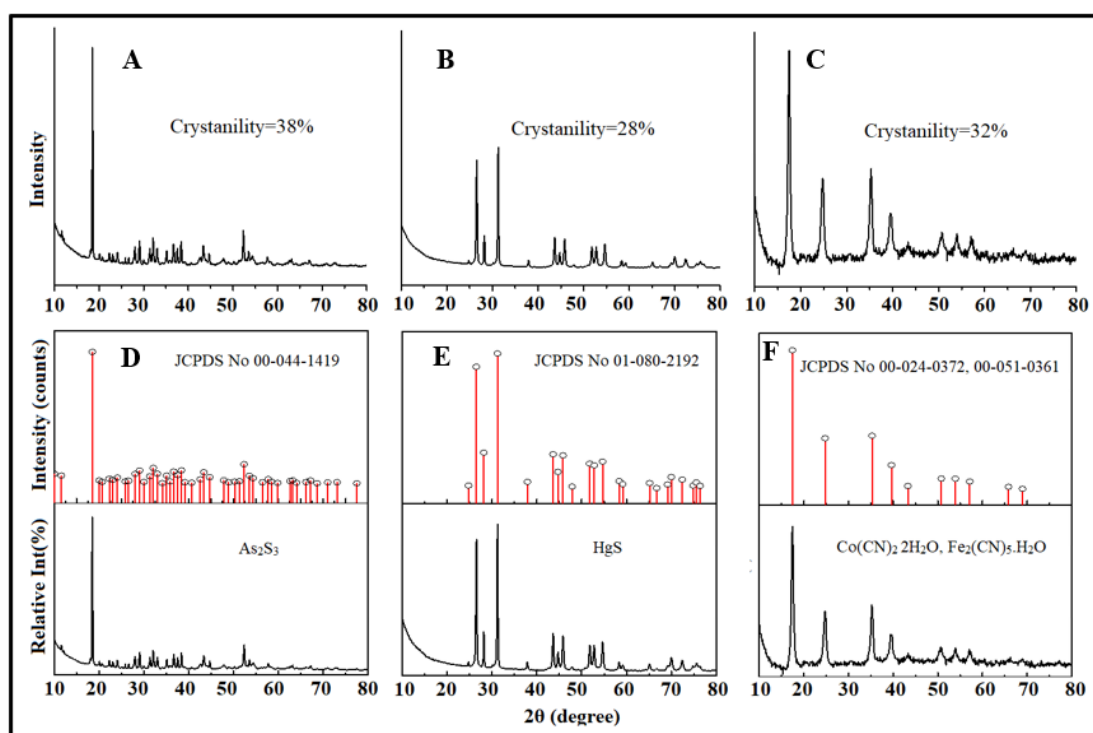


Figure. 3.3.5: p-XRD graphs of (A) *Hāitāl*, (B) *Hengul* and (C) *Nīl* and p-XRD peak interpretation from Pcpdwin Software of (D) *Hāitāl*, (E) *Hengul* and (F) *Nīl*.

3.3.1.5. Thermal analysis

The TG patterns of the pigments and the corresponding weight loss percentage can be seen in Figure. 3.3.6 and in Table 3.3.1, respectively. Interestingly, the pigment weight loss percentages for *Hāitāl* and *Hengul* are quite similar at 300-500 °C which indicates the decomposition of these two pigments is possible only at higher temperature range, i.e., the pigments can survive moderate temperature. We observed three main mass loss regions for *Nīl* corresponds to the ranges of 0-50 °C, 50-150°C and 200-400 °C. This indicates that this natural dye may degrade at normal temperature. Though the *Kharimāti* sample decomposes only at very high temperature and with a small weight loss

percentage up to 600 °C. The DTG curve shows that the maximum weight loss rate as well as the maximum reactivity temperature of thermal decomposition process in the samples (Figure. 3.3.6). The patterns indicate distinct peaks for *Hāitāl* and *Hengul* corresponding to the decompositions of Arsenic sulfide (As_2S_3) and Mercuric sulfide (HgS). The DTG pattern for samples of *Nīl* and *Kharimāti* are inconclusive. However, a sharp peak is observed at 48.68°C for *Nīl*, which indicates the dehydration of *Nīl* or Prussian blue sample.

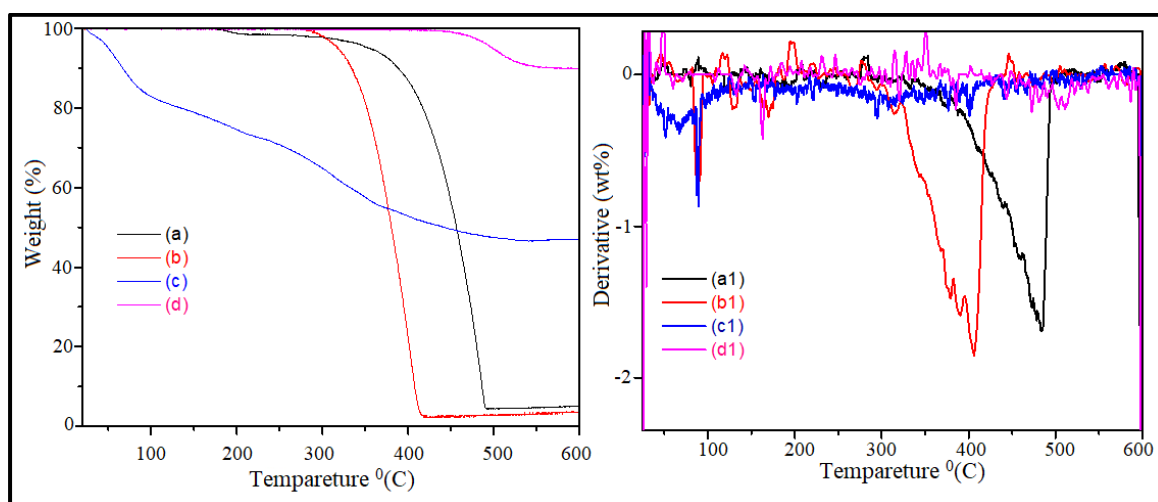


Figure. 3.3.6: TG and DTG patterns of (a, a1) *Hāitāl*, (b, b1) *Hengul*, (c, c1) *Nīl* and (d, d1) *Kharimāti*.

Table 3.3.1: Mass loss percentage of the pigments along with DTG peak temperature during thermal analysis.

Sample	Mass loss percentage in the temperature range (°C)					DTG peak temperature (°C)
	0-50	50-150	200-400	300-500	450-600	
<i>Hāitāl</i>	-	-	-	92.78	-	485.13
<i>Hengul</i>	-	-	-	94.13	-	406.44
<i>Nīl</i>	4.01	14.18	18.99	-	-	48.68, 90.52, 294.60
<i>Kharimāti</i>	-	-	-	-	7.48	512.10

3.3.1.6. Impurities in the pigments

The above physicochemical analyses suggest the samples of *Hāitāl*, *Hengul*, *Nīl* and *Kharimāti* available in locally as traditional dyes to contain mainly As_2O_3 , HgS , Prussian blue and aluminosilicate clay, respectively, with some impurities. Both *Hāitāl* and *Hengul* to contain oxide and carbonate impurities of the respective metals. The sample of *Hengul* contains traces of iron and arsenic impurities also. The sample of *Nīl* (Prussian blue) contains hematite iron impurity, probably added to increase its weight. The presence of some oxide or other mineral impurities is natural in the mineral pigments and is not expected to have any serious implication on the paints. However, the impurities and their levels may differ in the mineral pigment samples depending upon the source.

3.3.2. Analysis of paints of different shades prepared from the pigments

3.3.2.1. Zeta potential

The polarity changes and zeta potential of the pigments, prepared as per Table 2.1, were measured for dilute suspensions of the pigments using a Nanotrack wave machine. The zeta potentials of *Hengul* and *Hāitāl* and *Nīl* have been found to be 2.6, 2.0 and $-3.0\mu m$, respectively. Observed positive polarity values of *Hengul* and *Hāitāl* indicate positive surface charges as expected for mineral oxides and sulfides of the mineral pigments. On the other hand, an observed negative polarity of *Nīl* indicates a negative surface charge which may be due to the presence of iron cyanide impurity in *Nīl*. All the three pigments have low value of zeta potential which indicates the attracting forces exceeding the repulsive forces leading to agglomeration of the particles, decreasing the stability. The agglomeration and low stabilities of the pigments have been in fact observed with the pigments after if the paint mixture is kept for more than 2-3 hours. This may be the reason for which the paints once prepared is used up completely as quickly as possible.

3.3.2.2. Particle size analysis

We calculate the fineness of the final particle of all paints, prepared as per Table 2.1, with the help of Hagman scale. The fineness of *Hengul* and *Hāitāl* particles is 7 micron and 10 microns. Similarly, the fineness of *Nīl* is 4 micron and that of *Kharimāti* is 5 microns. The average particle size for composite brown, green, and black colors were measured to be 22, 32 and 31 microns, respectively, which are close to that of *Hāitāl*, an ingredient of the colors. It may be noted that the particle size of *Hāitāl* is large compared to the others despite a much greater effort was made for grinding it. The traditionally a much greater

effort is made for grinding *Hāitāl* as it is difficult to grind it to smaller size particles due to its flake-like shape. Interestingly, there is a saying among the traditional practitioners of *Hengul-Hāitāl* about *Hāitāl* that it is very difficult to grind *Hāitāl* the intensity of the color of this pigment continues to increase on grinding.

3.3.2.3. Hunter color analysis

The results of Hunter color lab analysis on paints of all compositions as described in Table 2.1 are shown in Table 3.3.2. Hunter color analysis was done also for compositions where the natural Bael gum was replaced with a commercial synthetic gum binder based on polysaccharides to examine the possibility of replacement of somewhat scarce and seasonal Bael gum with the commercial gum.

Table 3.3.2: Results of Hunter color analysis of the compositions as described in Table 2.1 except for the binder gum which here includes both Bael gum and a starch-based commercial gum with same proportions.

Sample color	L*		a*		b*		C*		h	
	Bael	Comm	Bael	Comm	Bael	Comm	Bael	Comm	Bael	Comm
Red		42.31	17.84	20.34	13.62	7.12	22.47	21.45	0.65	0.33
Yellow	79.91	69.33	3.94	6.29	55.27	49.30	55.42	49.70	1.50	1.44
Blue	54.41	35.58	-2.71	0.04	-4.04	-2.48	4.87	2.48	0.98	-1.55
White	51.72	69.33	4.44	6.29	14.08	49.30	14.76	49.70	1.24	1.44
Brown	64.69	48.15	19.45	5.70	37.54	8.96	42.20	10.62	1.09	1.00
Green	45.84	42.23	-12.30	-6.54	15.14	3.08	19.50	7.22	-0.89	-0.44
Black	54.94	35.58	0.53	0.04	-0.21	-2.48	0.57	2.48	-0.37	-1.55

Among the different shades prepared with Bael glue, only red and green paint samples, with L* less than 50, showed slight darkness property while all others showed lightness property with the maximum lightness for the yellow sample. The blue and green paint samples, with negative a* values, showed greenness property while all the other paint samples showed redness properties with the maximum redness for red and brown samples. The black and blue samples, with negative b* values, showed blueness property while all other samples showed yellowness property with the maximum yellowness for the yellow and the brown samples as expected. It was interesting to note that all paint samples were estimated to be bright (positive C*) with the blue and black with minimum

brightness. That the highest estimated brightness was obtained with the yellow followed by brown and then red paint samples is in commensurate with a very bright color observed with woodcarvings with the yellow, brown and red paints. The yellow sample also showed highest hue angle, h . There was hardly any change in the color properties of the red and yellow samples on changing the gum (Figure. 3.3.7). A small decrease in lightness of the white sample and an increase in the redness of the brown sample were observed on changing the gum from Bael to commercial starch-based gum. There was a marked increase in the yellowness and brightness of the white sample with some decrease in both brown samples with Bael gum and commercial gum. There was a notable decrease in the hue of the blue sample followed by black with the commercial gum. The observed variations in the color properties may be associated with some differences between the interactions of the components of the blue and the white paints samples with the two gums.

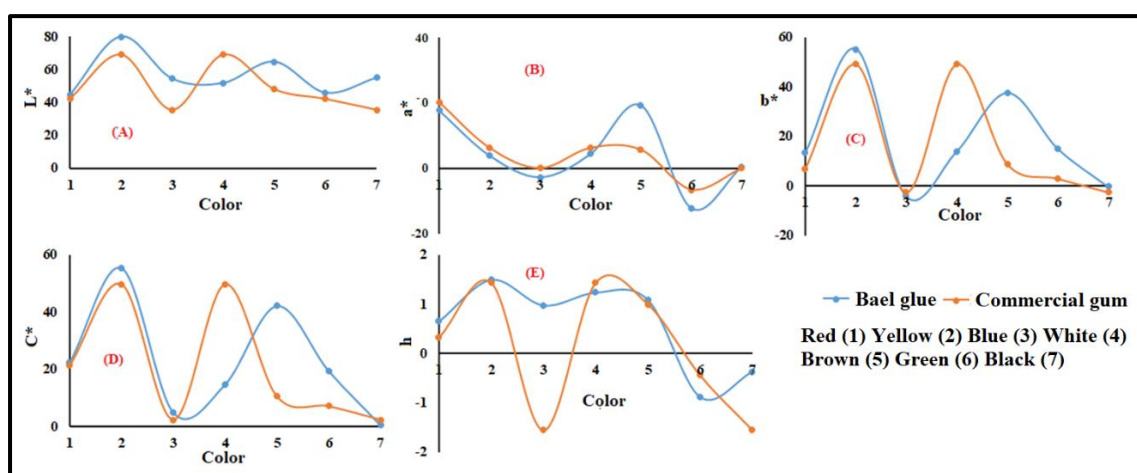


Figure. 3.3.7: Color characteristic parameters (color notations) obtained from Hunterlab analysis for various color shades prepared from the pigments.

3.3.2.4. Hiding power of the paint formulations

The hiding power of different color formulations prepared as per Table 2.1 have been measured as contrast ratio (CR), which is the ratio of light reflection from black to that from white after coating of respective colored paint on different colored panels (Figure. 3.3.8). The CR of the different color paints have been found to be 99.98 for red (*Hengul*), 92.85 for white (*Kharimāti*), 100 for blue (*Nīl*), 100 for yellow (*Hāitāl*), 100 for green (6:1 *Hāitāl* and *Nīl*) and 100 for brown (1:8 *Hāitāl* and *Hengul*). The results indicate that all the primary colors as well as the composite color formulations have very good hiding

power. However, the blue (Nīl) and the yellow have shown CR of 100. The hiding power of white has been found to be slightly lower. On the other hand, a CR of approximately 100 has been observed for all color formulations containing the mineral pigments of *Hāitāl* and *Hengul*.

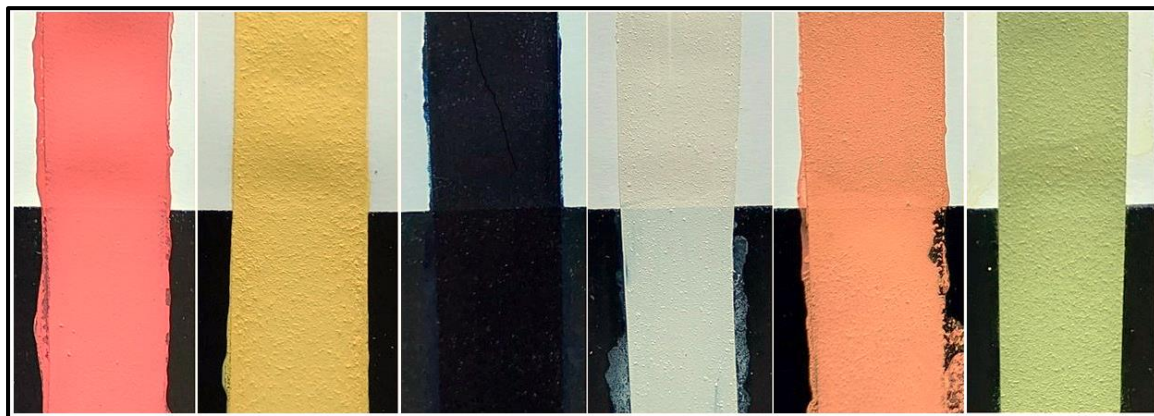


Figure. 3.3.8: Photographs of red, yellow, blue, white, brown and green colored panels prepared for contrast ratio measurement.

3.3.3. Traditional science in the painting tradition

The *Hengul-Hāitāl* painting tradition involved some interesting traditional knowledge, such as selecting primary color pigments that guard woodcarvings against termites and fungus and applying a thin coat of traditional varnish after painting to shield the dyes from natural erosive processes.

3.3.3.1. Selection of primary color pigments

Red, yellow, and blue or green are considered as three primary colors. Centuries ago, the artists of Assam knew how to prepare any other colors or shades, including black, by mixing these three pigments of three primary colors, namely red, yellow, and blue, in varying proportions. There is no record of use of any pigments of any other color, mineral or herbal.

3.3.3.2. Antifungal and insect-repellant component in paint formulations

Woodcarvings can be easily damaged by cellulose-eating fungi and termites which are abundant in hot and humid climate of Assam. The artists of the *Hengul-Hāitāl* painting tradition probably knew about antifungal and insect repellent properties of *Hengul* or

Hāitāl, and this might have been one of the reasons for choosing these two pigments [7]. These pigments were used throughout history in various artist techniques and very much loved for their color purity and intensity. However, using these pigments might impede the appearance of fungi or insects [7]. It is also interesting to note that the artists usually did not use *Nīl* alone for blue color and instead mixed a little of *Hāitāl* with *Nīl*, to protect the woodcarving from fungi and termites, which imparted a slight greenish tinge to the blue color. Figure. 3.3.9 shows how termites damaged portions of woodcarvings with white paint whereas the portions with paints containing either *Hengul* or *Hāitāl* or even black remain unaffected for much longer time. It is usually noticed that pure blue color was not applied on the woodcarvings which have been surviving for centuries (Figure. 3.3.9). A little of *Tutia* was also traditionally mixed with *Kharimāti* which was used for white color.

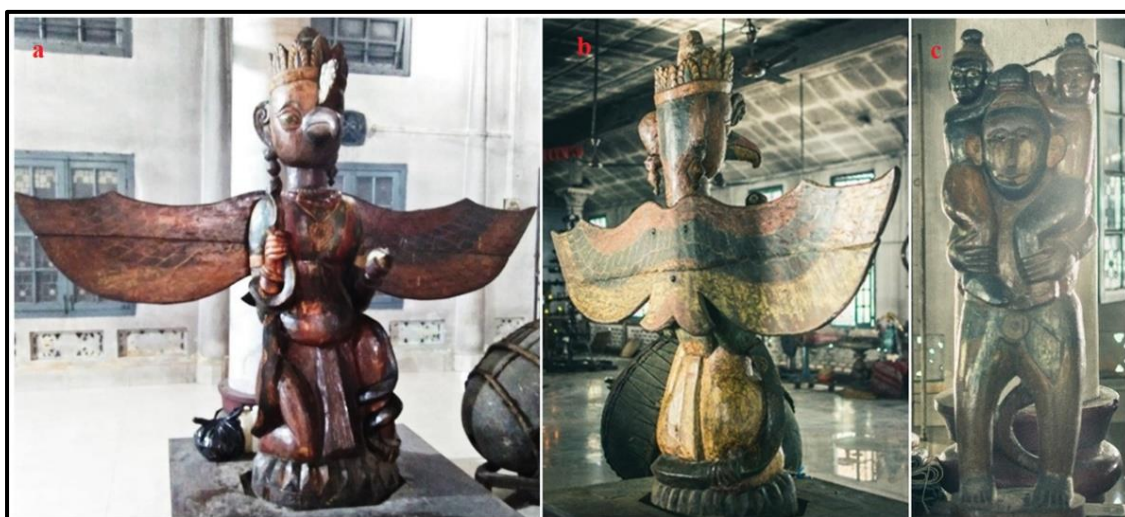


Figure. 3.3.9: Woodcarvings of 1916 AD at Bardowā Thān, Nagaon, Assam, (a,b,c) containing green color made by mixing *Nīl* with *Hāitāl* but without blue color of *Nīl* alone. The (a) left and the (b) middle pictures are of the same woodcarving before and after cleaning.

3.3.3.3. Avoiding natural erosion and contact by *Lā*-coating

Though *Hengul* and *Hāitāl* are traditionally used as *Sindur* by married Hindu woman, as make-up ingredient by *Kathakali* dancer in India, for lightening of dark skin, etc., contamination of antifungal and insect-repellant pigments may have some toxic effects on human health [238]. Users of utility wooden items painted with *Hengul-Hāitāl* naturally come into contact with the users. On the other hand, *Vaishnavite* woodcarvings are

usually placed open in Namghars where the devotees often touch them. The contamination of the pigments as well as natural erosion of the paints from the woodcarvings were avoided by applying a thin coating of wood sap on the woodcarvings after completion of the painting.

3.3.3.4. Selection of a non-staining natural gum

There are some more natural gums available in Assam, namely, gum of Outenga or elephant apple and the gum of fiddlehead fern in addition to the gum of stone apple or Bael gum. Bael gum is a very good adhesive and at the same time it does not leave any stain on the object. This gum is also available locally in all seasons of the year which are conducive for painting except the rainy season during which painting is usually not done.

3.3.3.5. Use of primer coating

It was traditional procedure to fill any gaps in the surface of woodcarving with a coat of Kharimāti primer followed by soft rubbing to smoothen it. The aluminosilicate Kharimāti primer coat also increases the hiding power of the paint. As Kharimāti does not have antifungal or insect-repellant properties, it was customary to mix a small quantity of Tutia with Kharimāti in order to make the primer antifungal and insect-repellant [7]. It may also be noted that a small quantity of Tutia was added to Kharimāti for preparing white paint.

3.3.3.6. Blending pigments with binders to create different shades

A recipe of preparation of *Hengul*, *Hāitāl*, Kharimāti and *Nīl* as per the traditional method is briefed here. About 30g of each of *Hengul* or *Hāitāl* is ground in a hard granite mortar manually into fine powder. About 50mL of water is added to the natural dye powder and ground again for about half an hour. Then the mixture is allowed to settle down for about 10 min. The highly insoluble powdered dye is settled down with scum appearing at the surface. The scum is removed by decanting to get cleaner powder. The pigment is ground again after replenishing the water. The process of removing scum is repeated until the scum appears on grinding and the particle size is reduced to approximately 5-10 and 27-32 μm . For *Kharimāti* and *Nīl*, the grinding is simple, and the scum removal only needs to be done once. About 40 fresh and matured wood apples were cut cross-sectionally into two halves with a knife and the glue was squeezed out from around the seeds and collected in a ceramic bowl. About 20 mL of distilled water is added to 80 mL of pure

glue obtained from Bael fruit and thoroughly mixed to get 100 mL of the natural glue, Bael gum. Various shades have been prepared by mixing the dyes in varying ratios together with a certain quantities of Bel gum as a natural binder (NB) and water as shown in Table 2.1.

3.3.4. Summary of the section

The present scientific study of the ingredients, the properties and application of traditional *Hengul-Hāitāl* paints has revealed some interesting traditional knowledge related to the pigments and their application. Mineral pigments of *Hengul* (mercuric sulfide, HgS), *Hāitāl* (arsenic sulfide, As₂S₃) and Kharimāti (calcium aluminum silicate clay) were used for red, yellow, and white, respectively. However, though a natural dye, Indigo, was traditionally used as blue color, it is now replaced by synthetic Prussian blue. The physicochemical analyses of the pigments have shown that while *Hengul* and *Hāitāl* samples showed some natural oxide and carbonate impurities. On the other hand, the sample of Nīl (Prussian blue)

was found to be adulterated with hematite. The sample of *Hāitāl* showed 38% crystallinity, which was higher than 28% observed for *Hengul*. The particles of *Hengul*, *Hāitāl* and Nīl, after grinding, have been found to be distinctly distributed while that of the particles of Kharimāti have been found to be spread smoothly. The average particle sizes of the pigments were between 4 to 10 μm. Measured low zeta potentials of the pigments indicated rapid agglomeration which was in fact observed in practice requiring complete use of the paints within 4-5 hours of preparation.

The use of three primary colors, viz., red, yellow, and blue in the tradition for preparing any desired shades is noteworthy. It was also interesting to note the selection of a non-staining robust natural gum, viz., Bael gum, to prepare the paints. However, there was hardly any change in the color properties of paint samples of different colors on replacing the Bael gum with a starch-based commercial gum. While all shades obtained from *Hengul*, *Hāitāl* and Nīl have shown very good hiding power, all shades containing *Hengul* and *Hāitāl* have shown high brightness. It is also interesting to note the use of either *Hengul* or *Hāitāl* or both for preparation of any of the shades except white probably to repel termites and fungi. It was also a practice to mix a little of antifungal and insecticide Tutia with Kharimāti for white color. Application of a primer coat of

Kharimāti mixed with Tutia is indicative of the traditional knowledge of use of primer as well as preservation of woodcarvings from fungi and insects. On the other hand, application of Lā coating finally is indicative of traditional knowledge of stopping natural erosion of the paints and avoiding toxic *Hāitāl* by devotees of idols and utility items by users upon touching. The unraveled traditional knowledge pertaining to glaze and durability applied in the preparation of woodcarvings and *Hengul- Hāitāl* painting tradition of Assam will be helpful in developing a customized method for restoration of worn-out woodcarvings for preservation in open ordinary environment in villages and Satras.

*A paper based on a part of this section has been accepted for publication in **Journal of Coating Technology and Research (2023)**

3.4. Section-4: Restoration of heritage woodcarving with Hengul-Hāitāl painting

In this section, a method based on the research findings of Section -3.3, has been proposed for restoration of worn-out heritage woodcarvings and heritage woodcarvings whose heritage look has been spoiled by painting with commercial paints, by repainting with original traditional *Hengul-Hāitāl* painting. The woodcarvings have been cleaned and mended including removal of commercial paints, if was applied on them, before painting or repainting with *Hengul-Hāitāl*. The proposed was aimed at to protect the woodcarvings from paste and fungus for centuries under ordinary rural set up of preservation at public places or places of worship in addition to reviving their original antique look, glare and appeal. Piloting of the proposed method has been performed at Batadrava Than in Nagaon, a Museum at Kaliabor College in Nagaon, Boralmora Satra in Tezpur and Auniati Satra in Majuli.

3.4.1. Proposed method of restoration

The method of restoration of partially damaged woodcarvings based on the findings of the above study of the ingredients, properties, and the traditional recipe of the *Hengul-Hāitāl* painting described in Section 3.3. Rainy season, July to September, should be avoided for the restoration for two reasons: firstly, for unavailability of Bael gum and secondly to avoid high humidity which makes drying difficult. The steps are described below:

- (a) **Cleaning of woodcarvings:** The woodcarving should be thoroughly cleaned through physical means removing dirt by brushing and rubbing with coarse cotton cloth using water and isopropyl alcohol. No further step is required if the woodcarving is not cracked, damaged by termite, or painted with synthetic paints destroying the original heritage look.
- (b) **Removal of synthetic paints:** Any synthetic paints, if applied on it, have also to be removed using knife and sandpaper. If an original *Hengul-Hāitāl* painting is found beneath the synthetic paints, then photographs of the original painting pattern need to be captured so that the final painting can be done in the same pattern.

- (c) **Mending:** Any crack or portions damaged by termite should to be cleaned and then filled with sawdust paste made with a polyvinyl adhesive (Fevicol) and Tutia. The filling should be dried completely before the nest step of restoration.
- (d) **Extraction of Bael gum:** Matured Bael fruits are cut across into two pieces and the gum is squeezed out along with the seeds using a small spatula. This is mixed with equal quantity of water and strained through a porous cloth.
- (e) **Application of primer coat of Kharimāti:** A thin primer coat of a paste of finely powdered Kharimāti, made with water, Bael gum and Tutia as per Table 2.1, is to be applied on the woodcarving and allowed to dry naturally.
- (f) **Application of Hengul-Hāitāl:** Paints of different required shades are to be made of finely ground pigments (5-25 μ m) in different proportions with water and Bael gum taking the examples in Table 1 as a guidance. It is very important to wear gloves and mask when handling *Hāitāl* and *Hengul* due to their possible toxicity [7]. The paints after preparation, should be applied using a brush as early as possible, to avoid agglomeration of the paint, in the same original pattern. A second coat or any decoration may be done after the first coat completely dries up. Mask and gloved must be used during grinding, handling, and application of *Hengul-Hāitāl*.
- (g) **Application of Lā:** Finally, a coat of Lā, dissolved in spirit (alcohol) is applied on completely dried painted woodcarvings softly with a small piece of cotton cloth. The Lā solution is prepared by dissolving 100g of solid Lā flakes in 250 ml spirit.

3.4.2. Results of restoration

Experimental restorations were carried out on some woodcarvings partially damaged by termites, coated with synthetic paints later damaging the heritage look, faded due to erosion and covered with dirt accumulated over centuries. The restorations were conducted in workshop mode involving some traditional artists who partially knew or have seen earlier the application of *Hengul-Hāitāl* as no artist with thorough knowledge of the tradition was available for the work. Among the woodcarvings chosen were two larger than life woodcarvings of Garud Pakhi, a mythological bird and two life size woodcarvings of Hanumān, a mythological character of Hinduism at Namghar of Bardowā Thān in Nagaon district of Assam (Figure. 3.4.1). Bardowā Thān was the birthplace of Srimanta Sankardev, a great Vaishnavite saint, social reformer, artist, poet and dramatist of medieval Assam. Then there were twenty-four pieces of woodcarvings,

including a life size Garud Pakhi and some more smaller woodcarvings of mythological characters and utility items at Boralimora Satra near Tezpur. This workshop was catalyzed by Indian National Science Academy (INSA) through a history of science research grant and generously sponsored by Tezpur University.

With the experience of the restoration work at Bardowā Thān in Nagaon, we have successfully piloted our restoration work with conventional *Hengul-Hāitāl* pigments at Kaliabor College Museum in Nagaon (Figure. 3.4.2), Borālimorā Satra in Tezpur (Figure. 3.4.3), and Auniāti Satra in Majuli (Figure. 3.4.4). These piloting were also carried out in a workshop mode, so that the participants also can give inputs for improvement of the method of restoration. The participants included traditional artists and new trainee with adequate orientation for traditional art. The scholar of Assamese manuscripts and traditional paintings, Dr Naren Kalita, was also associated with the workshops at Bardowa Than, Museum of Kaliabor College and Boralimora Satra. Using the proposed method of restoration based on the traditional painting, dozens of heritage woodcarvings have been restored during the workshops. These workshops were also supported by INSA and Tezpur University. The workshops at Bardowa Than, Museum of Kaliabor College and Auniati Satra also included conservation of *Sāncipāt* manuscripts.

3.4.2.1. Restoration of a Garud Pakhi woodcarving at Bardowā Than, Nagaon

Restoration of a life-size woodcarving of Garud Pakhi at Bardowā Than has been illustrated here as an example (Figure. 3.4.1). Interestingly, cleaning of this woodcarving revealed it was covered with at least two layers of enamel paints, but no specific pattern of colors was observed between these layers (Figure. 3.4.1a-d). Presence of an original layer of *Hengul-Hāitāl* paints was found beneath the layers of enamel paints (Figure. 3.4.1d). Attempts were made to note the patterns of the original *Hengul-Hāitāl* painting for using as a guidance for repainting with *Hengul-Hāitāl*. There was some more interesting finding during the cleaning. All of the mythical bird's exposed hands and legs' nails, except two, were made of ivory after the enamel paint on the nails was removed (Figure. 3.4.1e). One ivory nail from the first finger of the left hand was missing where a wooden nail has now been fixed. On the other hand, the big toe of the left leg was completely made of ivory. No *Hengul-Hāitāl* paint was noticed on the ivory nails and the big toe after cleaning and therefore only a Lā coating has been applied on them. After cleaning of the base, a text describing making of the woodcarving along with year became clear (Figure. 3.4.1h). The text engraved in old Assamese script reads as “The

Garud of Sri Bardowā Thān has been made by Dhbal Ātoi in Saka 1755 (1833 AD)". A mixture of sawdust, Favicol and a little Tutia was used as filler to mend the damaged portions and allowed to dry. The surface of the filling was then coated with a paste mixture of Kharimāti water and Bael gum. Cracks appear often in the Kharimāti coating after drying which is polished further with Kharimāti. After complete drying, the surface of Kharimāti is smoothened with a fine sandpaper. Complete drying of the mended portion is a must before painting.



Figure. 3.4.1: (a) A woodcarving of Garud Pakhi of height = 1.78m and width = 2.92m, of Bardowā Than at different stages of restoration: with enamel paint before restoration, (b-d) original *Hengul-Haitāl* paints seen after removal of multiple layers of enamel paint, (e) ivory nails, (f) description of the artist and year at the base, (g-h) mending with sawdust and Kharimāti, (i) primer coating with Kharimāti, (j) after application of *Hengul-Haitāl* and after (k) *Lā* coating.

A primer coating of a thin paste mixture of Kharimāti water and Bael gum was then applied with a brush on the woodcarving except the ivory nails and toe. After complete drying of the primer coat, *Hengul-Hāitāl* paints were applied on the woodcarving in double coat. The original pattern of *Hengul-Hāitāl* painting observed after removal of the enamel paints were adopted as far as possible for choosing the colors for painting and for decorations. Wherever the original patterns were not detectable, the patterns seen on another similar Garud Pakhi placed in the other side of the Namghar, which was too dirty due to deposition of lampblack and dirt over a century but not painted with enamel paints, was followed. Finally, after complete drying of the traditional *Hengul-Hāitāl* paints in a couple of days, a double coating of Lā was applied. The Lā solution, prepared in spirit (ethyl alcohol), was applied by smooth rubbing with a clean cotton cloth dipped in the Lā solution. The Lā coating dries up immediately as spirit is highly volatile.

3.4.2.2. Restoration of heritage woodcarving at Kaliabor College Museum, Nagaon

There were two partially damaged wooden palanquins (Dola) with beautifully crafted woodcarvings at the museum which were with the original *Hengul-Hāitāl* paints almost faded and covered with dirt [Figure. 3.4.2]. Both wood carvings have been cleaned, mended and repainted with *Hengul-Hāitāl* paints in the traditional way. Care was taken to retain the patterns of the original paintings during the repainting by taking photographs of the patterns after cleaning by applying the new paints in the same pattern.

3.4.2.3. Restoration of 24 heritage woodcarvings at Boralimora Satra, Tezpur

There were a large number of big and small heritage woodcarvings at Boralimora Satra, Tezpur, which were either partially damaged by white ants or covered with dirt. Out of them, twenty-four pieces of these woodcarvings including a large Garud Pakhi, ten pieces of mythological representations of ten reincarnations of God (Dashavatar), woodcarvings of Lord Krishna and two wooden manuscript boxes and some more utility items have been restored [Figure. 3.4.3]. The Garud Pakhi was highly damaged with the feathers detached and a big hollow from top to bottom leaving only the outer body, face and limbs intact. It was found covered with commercial paints. However, cleaning and removal of the commercial paints revealed evidence of original *Hengul-Hāitāl* paints except the head and the bottom. This suggested that white ants had eaten the inner body of the woodcarving leaving the *Hengul-Hāitāl*-coated outer body as expected from anti-insecticide property of *Hengul-*

Hāitāl paints. However, none of the other pieces of woodcarvings was painted with commercial paints and the *Hengul-Hāitāl* paints were revealed after removal of the dirt. Care was taken to retain the original pattern of the paintings during the repainting.



Figure. 3.4.2: (a) Restoration of Dola palanquins at the museum of Kaliabor College Museum, Nagaon, A century-old, worn-out Dola before restoration, and (b) its new appearance following restoration using the technique we suggest using the *Hengul-Hāitāl* painting tradition.

3.4.2.4. Restoration of a larger-than-life size woodcarving at Auniati Satra, Majuli

There was a huge woodcarving of Garud Pakhi at Auniati Satra with approximately 10 ft height and 14 ft width. It was found painted with commercial paint, but removal of the commercial paints revealed evidence of original *Hengul-Hāitāl* paints. There were some broken portions at one of the feathers. The broken feather was mended with a piece of wood and the filling and repainting was done following the traditional procedure.



Figure. 3.4.3: Restoration of various worn-out woodcarvings from a century ago at Borālimorā Satra, Tezpur, (a-c): Garud Pakhi, nine of ten incarnations (Dashavatar) of the God, and Lord Krishna; and (d-f): the same woodcarvings after restoration with *Hengul-Hāitāl* paint except one of the nine of the ten incarnations.



Figure. 3.4.4: (A) A larger than life woodcarving of Garud Pakhi at Auniati Satra with destroyed original look with modern synthetic paints over original *Hengul-Hāitāl* paints, and (B) the same Garud Pakhi after restoration.

3.4.2.5. Glossiness of the traditional paints

The average glossiness measured at 20°, 60° and 80° angles, of the cleaned Garud Pakhi before and after painting with different shades of *Hengul-Hāitāl* paints are shown in Figure. 3.4.5. The glossiness was too little before painting. The glossiness of the differently shaded parts of the Garud Pakhi were found to be high in the cases of brown, blue and green colors and moderate in the cases of white, yellow and red. Even the glossiness of the black color was greater than the glossiness before painting.

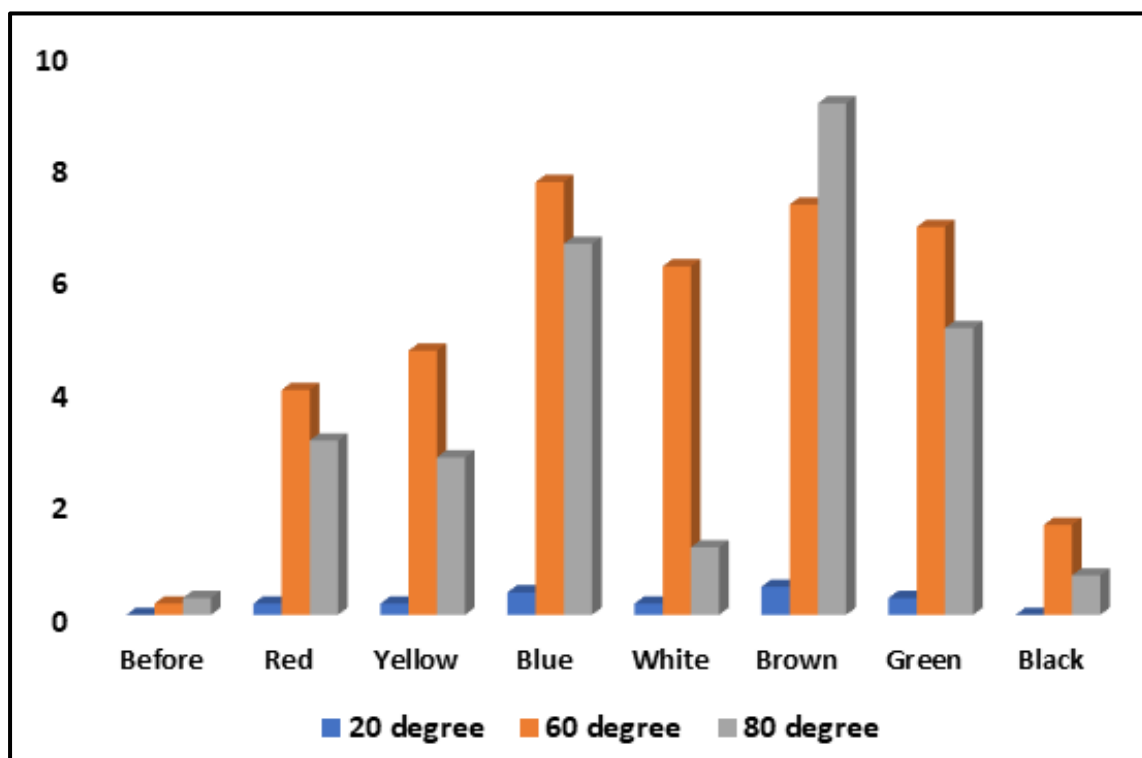


Figure. 3.4.5: Glossiness of cleaned Garud Pakhi woodcarving before and after painting with different *Hengul-Hāitāl* paints measured at 20, 60 and 80 degrees.

3.4.3. Social acceptability of the restoration method

The restoration of the woodcarvings carried out at Bardowa, and also the subsequent restoration works at other places, has received wide appreciation from local people to the Prime Minister of India and print and electronic media attraction including coverages in Indian national dailies [266]. Some of the artists trained in the workshops have carried out

similar restorations later at Bardowa Than independently. Some others have applied the traditional *Hengul-Hāitāl* paintings at two different places indicating revival of the dying tradition through our initiative. Another point to be noted here is that we wanted not to repaint another woodcarving of a Garud Pakhi at Bardowa as it looked quite good after cleaning barring some cracks and exposure of the wood at some areas. However, the local people did not allow that almost forced us to repaint that woodcarving also as the other one which had been already repainted was looking much better than that.

3.4.4. Summary of the section

A scientific traditional restoration method has been proposed for restoration of some old partially damaged woodcarvings due to natural weathering or woodcarvings which had lost the antique look due to application of enamel paints have shown good results receiving appreciation form local people. Revelation of ivory in nails and use of precious pigments indicates an economically strong patronage of the woodcarvings. The restoration has imparted new but traditional look with enhanced glossiness and thermal stability to the woodcarving enabling preservation of the woodcarvings at least for another century in the open public places like Namghars in an as is where is way. Thus, the present work brings to light a rich cultural heritage of making woodcarvings with an elegant painting tradition of medieval Assam involving interesting traditional science pertaining to glaze and durability.